Investigating the Resistance that arises in *Escherichia coli* towards the Furazolidone – Vancomycin Antibiotic Combination

Master of Science (Biological Sciences)

Massey University, Manawatū, New Zealand

Hannah Mary Wykes

2022

Abstract

Antibiotic resistance is a major threat to our current healthcare system. As bacterial resistance mechanisms continue to develop and spread, more and more antibiotics are becoming less and less effective, making an increasing number of bacterial infections difficult or even impossible to treat. Worryingly, bacterial antibiotic resistance is outpacing the rate of development of new antibiotics, making a return to the pre-antibiotic era a very real possibility. In particular, additional strategies are required to tackle gram-negative pathogens, the most pressing threat. One additional strategy is to utilise existing antibiotics in new combinations.

This thesis investigates the resistance development towards the furazolidone – vancomycin antibiotic combination in *Escherichia coli*. The synergistic FZ – VAN combination has been previously shown to be a promising potential combination against gram-negative pathogens, repurposing vancomycin, used against gram-positive pathogens, against gram-negative bacteria. By investigating the resistance development towards this combination, insight into the ease of resistance development and types of resistance development can be had, leading to increased understanding of the resistance mechanisms and potential use of this combination.

Resistance towards the FZ – VAN combination was selected for, and the isolated strains underwent comparative genome analysis, revealing the genomic changes behind their observed phenotypic resistance. Mutations affecting seven main genes were identified as potential causes of resistance, *ribE*, *ribB*, *ftsH*, *rpoC*, *opgG*, *wecC*, and *nlpI*.

In addition, the mechanism of resistance to FZ by the *ribB* and *ribE* riboflavin biosynthesis mutants was investigated. These mutations were found to result in a lower nitroreductase activity, predominantly affecting the key nitrofuran-activating nitroreductases NfsA and NfsB.

Acknowledgements

This journey to complete my thesis has been interesting, exciting, and challenging, and I would like to thank everyone that made it possible.

First and foremost, I would like to thank my supervisor Jasna Rakonjac for all your help, feedback, discussions, and guidance. It has been invaluable, especially when I got stuck trying to understand or interpret something.

Secondly, I would like to thank everyone in the Rakonjac lab for always being willing to help and for making the lab a fun and enjoyable place to be. I would especially like to thank Vuong for all his explanations and help, especially for bioinformatics, it would have taken me far longer to figure out and troubleshoot problems without your help so thank you. Also, I would like to thank Catrina for teaching me lab skills and helping me when I was first getting started in the lab. And Cathy and Rayen for always being willing to answer any questions I had.

I would also like to thank all the SNS staff (Ann, Paul, Cynthia, Debbie, Fiona) for all their help with everything.

Finally, I would also like to thank my parents for always supporting me with everything I do.

I would also like to acknowledge the Graduate Women Manawatū Charitable Trust, and the William Georgetti Scholarship for their financial support to help me complete my studies.

Table of Contents

List of Figures

List of Tables

List of Abbreviations

5’ UTR:	five prime untranslated region
AMP:	ampicillin
ATP:	adenosine triphosphate
AU:	absorbance units
BLAST:	basic local alignment search tool
CDC:	Centres for Disease Control and Prevention
CDS:	coding sequence
CFE:	cell-free extract
CFU:	colony forming units
CHL:	chloramphenicol
DMSO:	dimethyl sulfoxide
DNA:	deoxyribonucleic acid
ECA:	enterobacterial common antigen
FAD:	flavin adenine dinucleotide
FIC:	fractional inhibitory concentration
FICI:	fractional inhibitory concentration index
FLP:	flippase recombinase
FMN:	flavin mononucleotide
FRT:	FLP recombinase target
FZ:	furazolidone
IM:	inner membrane
IPTG:	isopropyl ß-D-1-thiogalactopyranoside
KAN:	kanamycin
LPS:	lipopolysaccharide
MIC:	minimum inhibitory concentration
NADH:	nicotinamide adenine dinucleotide
NADPH:	nicotinamide adenine dinucleotide phosphate
OD_{600}:	optical density at 600 nm
OM:	outer membrane
OPG:	osmoregulated periplasmic glucan
ORF:	open reading frame
PCR:	polymerase chain reaction
PG:	peptidoglycan
RNA:	ribonucleic acid
RNAP:	RNA polymerase
rpm:	revolutions per minute
VAN:	vancomycin
VRE:	vancomycin resistant enterococci
WHO:	World Health Organisation

1 Introduction

1.1 Antibiotic Resistance

Antibiotic resistance is a major global health concern. Since antibiotics were initially discovered, they have served as a major line of defence in combating bacterial infections. Without antibiotics, bacterial infections that are currently able to be treated would once again become deadly.

Antibiotic resistance is defined as when a bacterial infection is no longer treatable by a drug that was previously effective (European Centre for Disease Prevention and Control, 2008). This arises because of bacteria changing through developing or acquiring a resistance determinant that means the drug is no longer effective at killing the bacteria (World Health Organisation, 2020).

The consequences of losing antibiotics as a treatment option are frightening. Without effective antibiotics, we would return to a pre-antibiotic era in which infections that used to be easily treatable become life threatening. Antibiotic resistance would make administering antibiotics, either prophylactically to prevent infection, or in response to an established infection, effectively worthless, and drastically increase the risk of surgical procedures (O'Neill, 2014). For example, operations like joint replacements may become too risky to perform due to the threat of infection, leading to reduced quality of life for many people. Procedures where the immune system is suppressed, like during most cancer treatments, or during organ transplants, would be at heightened risk of life-threatening infection. The risk of childbirth would also increase, due to bacterial infection risks increasing, especially during caesarean sections (O'Neill, 2014).

1.1.1 How antibiotic resistance occurs

Antibiotic resistance is a naturally occurring phenomenon. This is because with every use of antibiotics, bacteria are forced to either adapt or die, meaning every use of antibiotics selects for resistance (European Centre for Disease Prevention and Control, 2008; World Health Organization, 2018). When treated with antibiotics, all the susceptible bacteria are killed or inhibited, leaving any resistant bacteria to grow and multiply, and this leads to an increased number of antibiotic resistant bacteria, as shown in Figure 1.

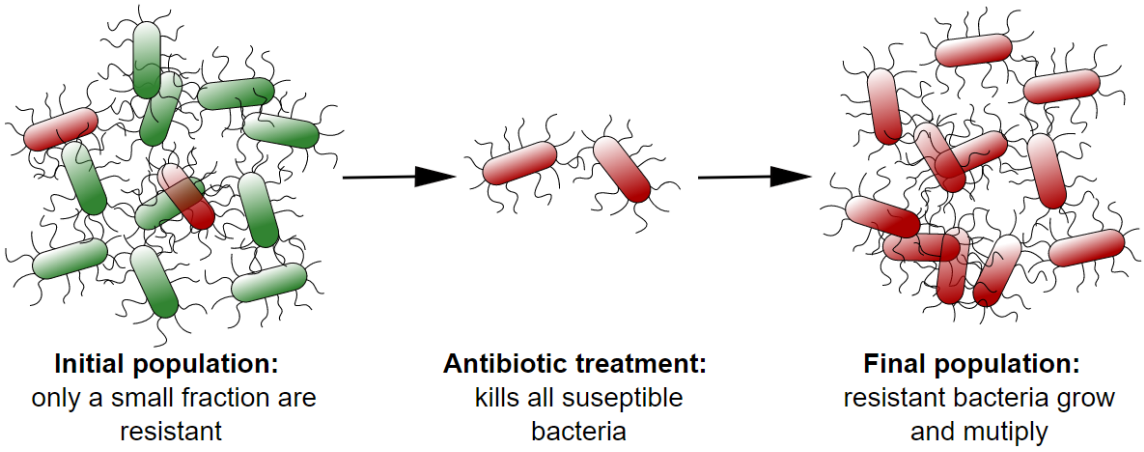

Figure 1: Antibiotic treatment selects for resistance

Antibiotic treatment selects for resistant bacteria by only killing/inhibiting susceptible bacteria and leads to a higher proportion of resistant bacteria after treatment.

The more exposure bacteria have to a specific antibiotic, the greater the selection pressure to develop resistance to it. The widespread overuse and misuse of antibiotics has been linked to increases in bacterial resistance development (Ventola, 2015; World Health Organization, 2018). Subsequently, antibiotic use should be restricted as much as possible, with unnecessary usage minimised to delay the occurrence and spread of bacterial antibiotic resistance, and so prolong the effective usage of existing antimicrobial treatments.

However, reducing antibiotic use is difficult due to the public perception of antibiotics and antibiotic resistance. Patient misunderstanding about the range of use and benefits granted from antibiotics leads to their over-prescription, especially for upper respiratory tract infections, where they have limited use (Huttner *et al.*, 2010). This is an issue, because while all use of antibiotics selects for antibiotic resistance, unnecessary antibiotic usage only exacerbates the problem. One solution for this is to better educate the public about the dangers of antibiotic resistance, and when it is appropriate to use antibiotics (Coxeter *et al.*, 2017), as well as increase the education around what antibiotic resistance is, as there has been shown to be a large amount of public misunderstanding surrounding this topic (Bakhit *et al.*, 2019).

1.1.2 The economic costs of antibiotic resistance

Another negative aspect of rising levels of antibiotic resistance is the associated increase in cost to the healthcare system. When patients acquire resistant infections, it leads to a higher healthcare cost as compared to patients that have non-resistant infections, and this cost is only expected to increase as antibiotic resistance becomes more widespread (O'Neill, 2014). This is because resistant infections lead to more prolonged infections, as well as the need for additional testing, and the requirement for more expensive medicines to try and treat the infection (World Health Organization, 2018).

1.2 Mechanisms and types of antibiotic resistance

Some general antibiotic resistance mechanisms include: limiting the drug uptake, inactivating the drug, modifying a drug target, active efflux of the drug, and interference with biochemical pathways (Reygaert, 2018). These mechanisms of resistance can be categorised as either acquired resistance, or natural resistance.

Natural resistance can be split into intrinsic resistance and inducible resistance. Intrinsic resistance is always expressed, while inducible resistance is only expressed after exposure to the antibiotic. Both intrinsic and inducible natural resistance arise from genes that are either always present or always absent in all strains of the bacterial species, that are not associated with previous exposure to antibiotics, and were not acquired through horizontal gene transfer (Cox & Wright, 2013; Reygaert, 2018). One example of this is in gram-negative (diderm) pathogens, which are, in contrast to gram-positive (monoderm) bacteria, intrinsically resistant to many antibiotics. This intrinsic resistance is due to the barrier function of the outer membrane and powerful efflux pumps that either prevent a drug from reaching its target or remove the drug from a gram-negative bacterial cell before it can reach its target (Cox & Wright, 2013).

Acquired resistance occurs either *via* a spontaneous mutation in the bacterial genome that is subsequently passed down vertically to the progeny through the bacterial generations, or alternatively through horizontal gene transfer, when bacteria acquire genetic material from an outside source. Horizontal gene transfer means that bacteria can pass around and express resistance determinants from other bacterial species or strains. This is problematic for the spread of antibiotic resistance, as it means not only can pathogenic bacteria pass around resistance genes between different species and

strains but can also acquire resistance genes from environmental or commensal bacteria (Sun *et al.*, 2019; von Wintersdorff *et al.*, 2016).

There are three types of horizontal gene transfer: conjugation, transformation, and transduction. Conjugation is the transfer of mobile genetic elements through a conjugative pilus structure that facilitates the direct transfer of DNA between two nearby bacteria, while transformation is the uptake of free environmental DNA. Transduction is the transfer of bacterial DNA between a bacteriophage-infected bacterium and a bacteriophage-susceptible bacterium (Huddleston, 2014; Thomas & Nielsen, 2005). Transduction occurs when a bacteriophage (a virus which infects bacteria) mistakenly packages bacterial DNA in addition to its own viral DNA during bacteriophage assembly, and then on subsequent infection of another bacterium, the bacterial DNA is injected into the recipient bacteria.

1.3 Antibiotic discovery

To make matters worse, the current rate of discovery of new antimicrobials is not fast enough to keep up with the increasing prevalence of antibiotic resistant pathogens.

1.3.1 History of antibiotic discovery

The first widespread antibiotic in use was penicillin, implemented in the 1940s, after Alexander Fleming's discovery in 1928 (Fleming, 1929). Following this, the so called "golden age" of antibiotic discovery occurred from the 1950s to the 1960s, when half of the different classes of antibiotics in use today were discovered (Davies, 2006) (Figure 2).

The introduction of a new antibiotic is accompanied by the discovery of pathogens resistant to the antibiotic. This is because the implementation of the antibiotic selects for resistance towards it. For example, resistance to penicillin was documented in 1940, before penicillin was widely used (Abraham & Chain, 1940). Studies of the microbial populations found in soil has revealed the presence of antibiotic resistance mechanisms is very widespread (D'Costa *et al.*, 2006). This is due to soil microbes being a large reservoir of both antibiotics and antibiotic resistance mechanisms as they are the origin of many clinically relevant antibiotics. However, despite antibiotic resistance

mechanisms being widespread throughout the environment, their presence in pathogenic bacteria was initially very rare, and the likelihood of resistance arising due to antibiotic usage was deemed unlikely at the time antibiotics were initially introduced (Davies, 2006). This has clearly proved to not be the case, with the implementation of widespread antibiotic use being heavily correlated to an increased prevalence in antibiotic resistant pathogens. This can be seen in the timeline of antibiotic discovery and resistance emergence shown in Figure 2.

Resistance Identified	Antibiotic Introduced
1910s	
	1910 – Salvarsan
1920s	
1930s	
	1936 – Sulfonamides
1940s	
1940 – Penicillins 1942 – Sulfonamides 1946 – Aminoglycosides	1941 – Polypeptides 1943 – Penicillins, Salicylates 1945 – Sulfones 1946 – Aminoglycosides 1948 – Tetracyclines, Bacitracin 1949 – Amphenicols
1950s	
1950 – Tetracyclines, Amphenicols 1955 – Macrolides	1952 – Macrolides, Pyridinamides 1953 – Tuberactinomycins, Nitrofurans 1958 – Glycopeptides 1959 – Polymycins
1960s	
1960 – Glycopeptides 1962 – Rifamycins 1968 – Quinolones	1960 – Azoles 1962 – Fusidic acid, Quinolones, Diaminopyrimidines, Ethambutol 1963 – Lincosamides, Ansamycins, Enniatins 1964 – Cycloserines, Cephalosporins 1965 – Thioamides 1969 – Phenazines
1970s	
	1971 – Phosphonates
1980s	
1987 – Third generation cephalosporins	1985 – Carbapenems, Mupirocin 1986 – Monobactams
1990s	
1998 – Carbapenems	
2000s	
2001 – Oxazolidinonoes 2005 – Lipopeptides, PDR *Acinetobacter* and *Pseudomonas* 2009 – PDR *Enterobacteraceae*	2000 – Oxazolidinonoes 2003 – Lipopeptides 2007 – Pleuromutilins
2010s	
	2011 – Lipiarmycins 2012 – Diaylquinolones
2020s	

Figure 2: Timeline of introduction of antibiotic classes and observed resistance

(Centers for Disease Control and Prevention, 2013; Hutchings et al., 2019). PDR: pandrug-resistant.

1.3.2 Current rate of discovery of new antibiotics

Once a new drug is on the market, the aim is to maximise sales to reimburse the cost of drug development. Antibiotics do not follow this pattern, as during their initial profit earning stage, their usage is being minimised as much as possible.

After the initial "golden age" period, the discovery of new antibiotics slowed dramatically. One reason for this is that antibiotic discovery is not profitable in the same way as the development of other drug types. Normally, a new drug offers a significant improvement over existing drugs on the market, and so becomes the main line of treatment, and generates profits that exceed the cost of the drug's development (O'Neill, 2015). However, antibiotics do not work like this. New antibiotics are reserved for use only in cases where the patient has an infection resistant to existing antibiotics. So, the new antibiotic only offers a benefit in the case of resistant infections, and existing, mainstream, cheaper antibiotics remain the main line of treatment. In addition, use of the new antibiotic would be restricted to minimise resistance to the new antibiotic. So, by the time the new antibiotic becomes the main line of treatment it is probably near the end, or at the end, of its patent, meaning generating enough sales to cover the cost of the drug development is difficult, except in cases where there is a specific need (O'Neill, 2015). Only when resistance to an existing class of antibiotics has become widespread is the development of a new antibiotic class financially viable, however because the pipeline of antibiotic development is so long, this means investment into new antibiotics is not occurring until there is an urgent need for them, and at this point it is too late.

1.3.3 Alternative approaches

The current rate of development of new antibiotic treatments is not keeping up with the speed at which antibiotic resistance is occurring. What this means is that alternative approaches are required to complement the development of new drugs, such as bringing together existing antibiotics into new combinatory treatments, or repurposing drugs approved for different diseases.

Drug repurposing involves using existing drugs not originally designed as antibiotics to treat bacterial infections. Often these drugs would be required in doses far too high for safe patient toxicity levels if used as a monotherapy treatment against bacterial

infections. However, combinations of these drugs, especially synergistic combinations, which lower the concentrations required to be effective, can open a range of drugs not previously viable to counteract bacterial infections (Gómara & Ramón-García, 2019; Sun *et al.*, 2016; Zheng *et al.*, 2018). Drug combinations will be discussed in detail in section 1.5. Drug repurposing also has the advantage of the drug already being clinically approved, so the safety profiles and pharmacological data for the drug are already present (Gómara & Ramón-García, 2019).

1.4 The bacteria with high levels of antibiotic resistance

The WHO (World Health Organisation) has a Priority Pathogens List, which outlines which microorganisms pose the greatest risks, and therefore which should be targeted most urgently in research into new antimicrobials. All the bacteria in the highest "Critical" category are gram-negative pathogens, and encompass carbapenem-resistant *Acinetobacter*, carbapenem-resistant *Pseudomonas aeruginosa*, and ESBL-producing carbapenem-resistant *Enterobacteriaceae* (World Health Organisation, 2017). Therefore, treatments that target these gram-negative bacterial pathogens are those that should be the most urgently investigated. The full list is shown in Figure 3.

WHO Priority Pathogens List for R&D of New Antibiotics

Priority 1: CRITICAL

1. *Acinetobacter baumannii*, carbapenem-resistant

2. *Pseudomonas aeruginosa*, carbapenem-resistant

3. *Enterobacteriaceae*, carbapenem-resistant, ESBL-producing

Priority 2: HIGH

1. *Enterococcus faecium*, vancomycin-resistant

2. *Staphylococcus aureus*, methicillin-resistant, vancomycin-intermediate and resistant

3. *Helicobacter pylori*, clarithromycin-resistant

4. *Campylobacter* spp., fluoroquinolone-resistant

5. *Salmonellae*, fluoroquinolone-resistant

6. *Neisseria gonorrhoeae*, cephalosporin-resistant, fluoroquinolone-resistant

Priority 3: MEDIUM

1. *Streptococcus pneumoniae*, penicillin-non-susceptible

2. *Haemophilus influenzae*, ampicillin-resistant

3. *Shigella* spp., fluoroquinolone-resistant

Figure 3: WHO Priority Pathogen List

(World Health Organisation, 2017)

1.4.1 Gram-negative pathogens

Bacteria can be split into two main groups, gram-negative and gram-positive, and this is determined by their cell envelope (cell wall) characteristics. Gram-negative bacteria have a much thinner (<10 nm) and less tightly cross-linked layer of peptidoglycan in comparison to gram-positive bacteria. Gram-negative bacteria also have an additional membrane layer, the outer membrane, beyond the peptidoglycan, that is not present in gram-positive bacteria. The composition of the outer membrane is different from that of the inner membrane; it has an outer layer of lipopolysaccharide (LPS), as shown in Figure 4. The differences in cell envelope between gram-negative and gram-positive

bacteria mean that each has different properties, especially with regards to external stresses, such as heat, ultraviolet radiation, and antibiotics (Mai-Prochnow *et al.*, 2016).

Therefore, most antibiotics are more effective against either gram-positive or gram-negative bacteria. Because gram-negative bacteria have an additional outer membrane, this protects them from many antibiotics that are effective against gram-positive bacteria, because the outer membrane prevents the antibiotics from gaining access to the cell. So, for example, antibiotics that target peptidoglycan synthesis are more effective on gram-positive pathogens, because the peptidoglycan layer is accessible, whereas in gram-negative pathogens, the drug would first have to get through the outer membrane layer.

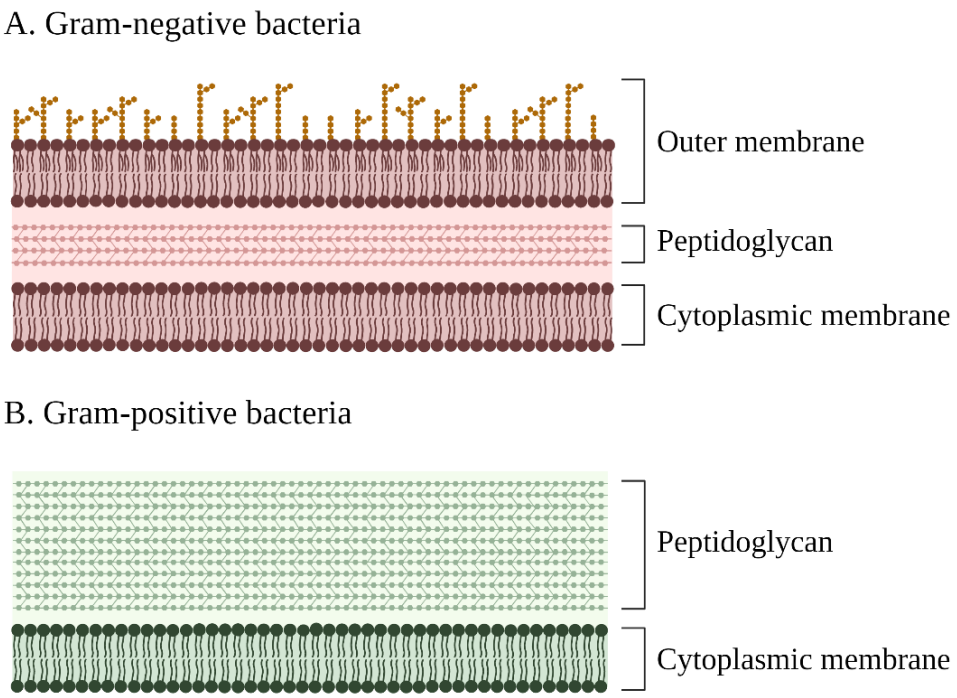

Figure 4: Gram-negative and gram-positive bacterial cell walls

(A) Gram-negative bacterial cell walls have an outer membrane and a thinner layer of peptidoglycan compared to (B) gram-positive bacterial cell walls. Created with Biorender.com

1.5 Drug interactions

When two or more drugs are used together, they can interact in a few different ways. The combined effect can be greater than the sum of the component drugs added together, creating a synergistic interaction. Conversely, the combined effected may be less than the sum of the component drugs added together, leading to an antagonistic interaction. Or the combined effect may simply be the same as the sum of the components added together, which is an additive interaction. An example of these interactions is shown in Figure 5.

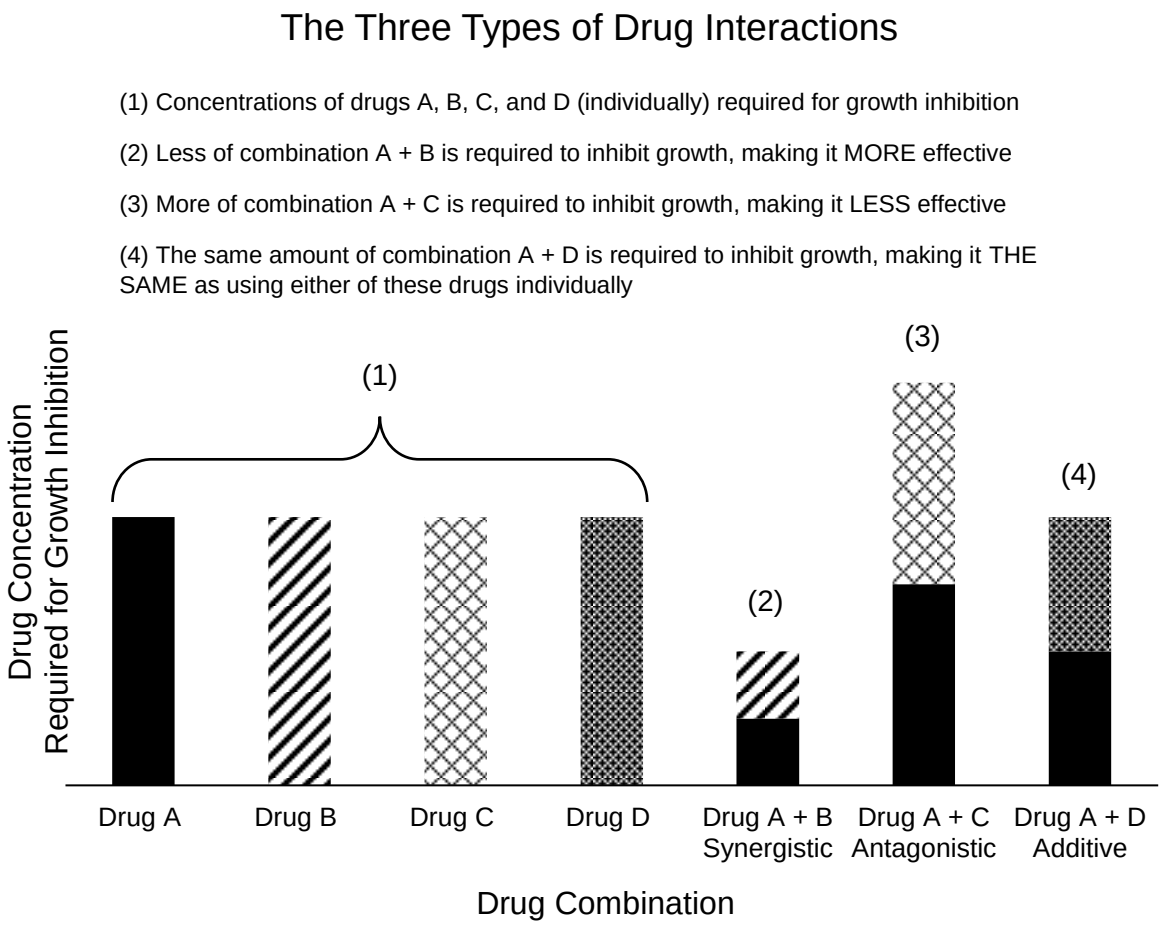

Figure 5: Drug interactions

Column heights show the concentration of drugs/drug combination required to be effective. Drug A + B is synergistic, as less of this combination is required to be effective, when compared to the drugs alone. Drug A + C is antagonistic, as more of this drug combination is required to be effective, when compared to the drugs alone. Drug A + D is additive, as the same amount of this drug combination is required to be effective, when compared to the drugs alone.

An example of a synergistic interaction between antibiotics is between trimethoprim and sulfamethoxazole. This combination is synergistic due to each antibiotic enhancing the effect of the other as both antibiotics act on the same tetrahydrofolate biosynthesis pathway (Minato *et al.*, 2018). A typical example of an antagonistic interaction is between bactericidal and bacteriostatic drugs. This is because bactericidal drugs, which kill bacteria, are normally only effective against actively growing cells, so when combined with bacteriostatic drugs, which slow bacterial growth, the bactericidal drug is no longer as effective, creating an antagonistic interaction (Ocampo *et al.*, 2014).

1.5.1 Characterising drug interactions

Determining the interaction between two drugs is commonly done through a checkerboard assay, performed using a microtiter plate. The microtiter plate can be thought of as a grid, with each well containing liquid media with varying concentrations of each drug. Along the x-axis of the plate, the concentration of "drug A" decreases, while the concentration of "drug B" decreases along the y-axis, as shown in Figure 6. All the wells are then inoculated, and the wells that grow indicate the interaction present between the two drugs.

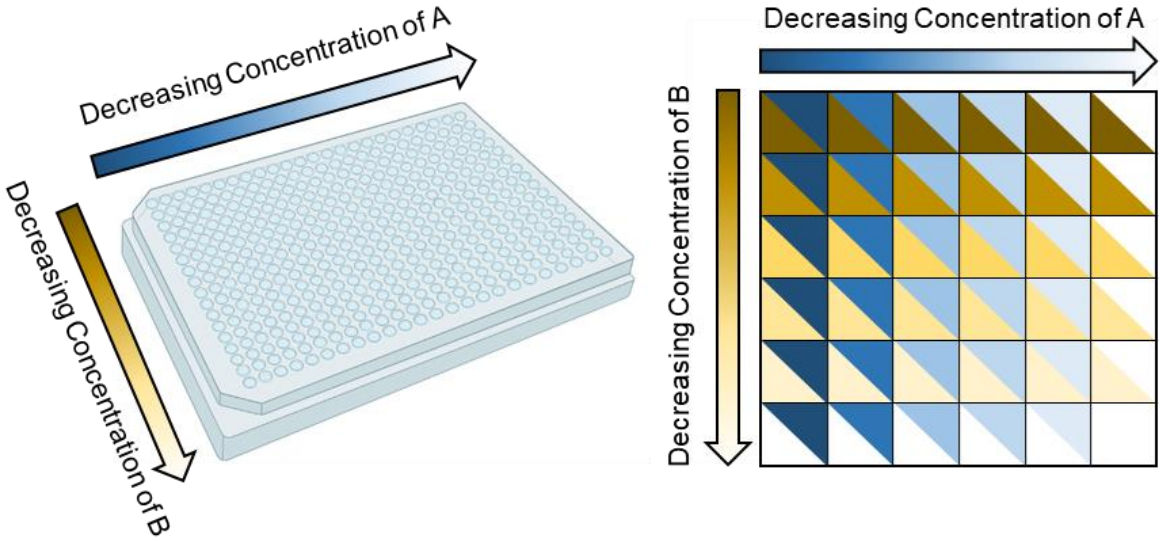

Figure 6: Checkerboard assay

Each well of the plate has a different combination of concentrations of the two drugs, with the concentration of Drug A decreasing along the x-axis of the plate and the concentration of Drug B decreasing along the y-axis of the plate. Image created using Biorender.com

The fractional inhibitory concentration index, or FICI, is using to characterise the interaction between two drugs. The FICI is the result of adding the individual FIC (fractional inhibitory concentration) values for each drug. FIC values are concentration ratios, with the drug concentration used in the combination comprising the numerator, and the MIC of the drug alone forming the denominator.

$$\mathrm{FIC}_{\text{drug A}} = \frac{\mathrm{MIC}_{\text{drug A}}(\text{combination})}{\mathrm{MIC}_{\text{drug A}}(\text{alone})}$$

Where $\mathrm{MIC}_{(\text{drug A})}$ is the minimum inhibitory concentration for drug A. Therefore, the FICI is calculated as shown below.

$$\mathrm{FICI} = \mathrm{FIC}_{\text{drug A}} + \mathrm{FIC}_{\text{drug B}}$$

$$\mathrm{FICI} = \frac{\mathrm{MIC}_{\text{drug A}}(\text{combination})}{\mathrm{MIC}_{\text{drug A}}(\text{alone})} + \frac{\mathrm{MIC}_{\text{drug B}}(\text{combination})}{\mathrm{MIC}_{\text{drug B}}(\text{alone})}$$

A perfectly additive interaction, where the combination is equal to the sum of the individual drugs, is indicated by a FICI value of 1. If the combination is less effective than the combined individual drug components, the FICI value would be greater than 1, and this would be an antagonistic interaction. Conversely, if the combination is more effective than the combined individual drug components, then the FICI value would be less than 1, and this would be a synergistic interaction. However, FICI values are treated using more conservative interpretation criteria. This is to account for the +/- one concentration range error present in MIC experiments. The interpretation criteria used is that an FICI value of less than 0.5 is indicative of a synergistic interaction, while an FICI value greater than 4 is indicative of an antagonistic interaction. Any FICI values between 0.5 and 4 represent an additive interaction (Odds, 2003).

Drug interactions can also be visualised through graphs known as isobolograms, as illustrated in Figure 7. The isobolograms work by plotting the FIC values for each drug against each other. On the graph, there is a line that represents additivity (FICI, or the

sum of the FIC values, is equal to 1). If the sum of the FIC values/the FICI is greater than one, indicating antagonism, the point will lie above the additivity line, and form a convex curve. If the FICI is less than one, that point would lie below the additivity line, and form a concave curve.

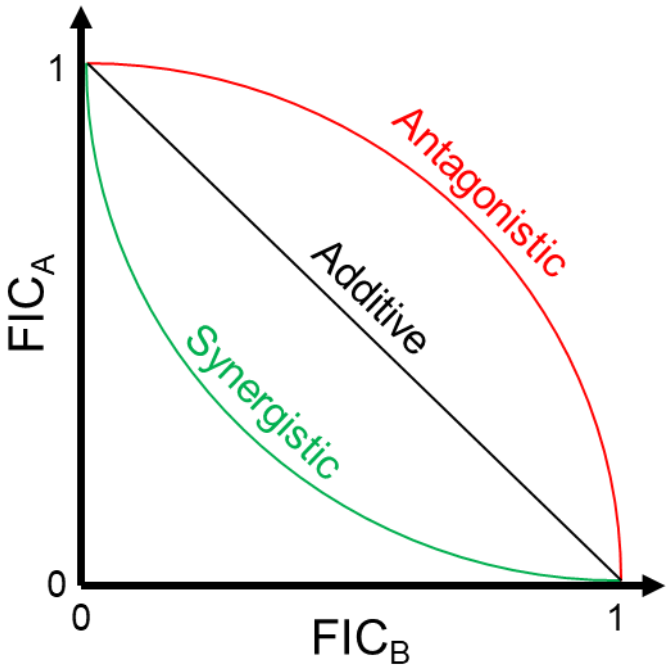

Figure 7: Isobologram showing drug interaction curves

Additive interactions form a straight line, while antagonistic interactions form a convex curve and synergistic interactions form a concave curve.

1.5.2 How drug combinations affect antibiotic resistance

Drug combination therapies have been shown to have advantages such as increased efficacy, reduced toxicity, and decreased development of resistance when compared to monotherapies (Foucquier & Guedj, 2015; Gómara & Ramón-García, 2019) and have been utilised for a range of different diseases, for example in the treatment of AIDS (Palella Jr *et al.*, 1998), tuberculosis (Houghton *et al.*, 1950; Kerantzas *et al.*, 2017), and cancer (Leary *et al.*, 2018; Mokhtari *et al.*, 2017). Combination therapies have also shown success as a strategy to help counteract antibiotic resistance, for example

Augmentin®, which combines the beta-lactam antibiotic amoxicillin with the beta-lactamase inhibitor clavulanate (White *et al.*, 2004).

Drug combinations also come with challenges, including potential undesirable drug-drug interactions, or different tissue distribution and pharmacokinetic properties of the drugs that prevent co-bioavailability (Gómara & Ramón-García, 2019).

Using a combination of drugs can be beneficial for slowing resistance development. To develop resistance to a drug combination that consists of a pair of drugs which each have a different mechanism of action, mutations that grant resistance to each drug individually must both occur. This means the likelihood of developing resistance is much less. For example, if the chance of a spontaneous mutation is 10^{-8} mutations per genome replication, then the chance of two spontaneous mutations occurring becomes $10^{-8} \times 10^{-8} = 10^{-16}$. This shows the chance of developing resistance when a drug combination is used is significantly reduced. However, if resistance to a combination could occur through a single mutation that grants resistance to both drugs, then this would not be the case, and this reduced resistance would not be an advantage of that particular combination (Pirrone *et al.*, 2011).

The type of interaction between drugs influences resistance development, as well as the presence or absence of collateral sensitivity or cross-resistance (where acquiring a mutation that grants resistance to one drug increases or decreases sensitivity to another, respectively).

In clinical use, synergistic combinations are favoured due to the ability to have reduced drug concentrations used. This is advantageous because of the reduced toxicity and side effects towards the patient from the antibiotics. On the other hand, antagonistic combinations would require higher concentrations of each drug component to be effective, and this comes with a higher toxicity risk and increased side effects. However, in terms of selection for resistance, the choice between synergistic and antagonistic combinations is a lot less clear.

Synergistic interactions, where a combination is more effective than the sum of the individual drug components, have conflicting effects when it comes to selecting for resistance. On one hand, synergistic drug combinations are more effective at clearing infections, and a faster clearance of infection means bacteria have less time to develop resistance to the combination (Torella *et al.*, 2010). However, a synergistic interaction

between drugs has been shown to create a higher selection pressure for resistance. This has been attributed to a single drug resistance mutation having a higher selective advantage in a synergistic drug environment, because not only would the mutation grant resistance to one of the drugs, but it would also reduce the effect of the other drug, as the synergistic effect is no longer present (Hegreness *et al.*, 2008; Michel *et al.*, 2008; Torella *et al.*, 2010).

Antagonistic interactions, where the combination has a lesser effect than the individual drug components, have been shown to select against resistance. This has been specifically shown in so-called suppressive drug interactions, where the combined effect is less than the effect of either drug on its own (Chait *et al.*, 2007). This was rationalised through resistance mutations being unfavourable to the overall survival of bacteria when exposed to the suppressive combination of antibacterial drugs. Specifically, while the mutation would grant resistance to one of the drugs in the combination, it would also remove the suppressive effect on the other, leading to the mutated strain being selected against as compared to the wild-type strain (Chait *et al.*, 2007).

Collateral sensitivity, where acquiring a mutation to one drug increases sensitivity to another, has implications for selecting against resistance. Collateral sensitivity cycling, where drugs with favourable collateral sensitivity are implemented in a cyclical fashion, has been shown to select against resistance development (Imamovic & Sommer, 2013). Cross-resistance, where a mutation that grants resistance to one drug also increases tolerance to another drug, is obviously not a favourable clinical option, as one mutation could increase the minimum inhibitory concentration of both drugs in the combination.

1.6 Furazolidone

1.6.1 History and structure of furazolidone

Furazolidone is one of the 5-nitrofuran antibiotics. The nitrofuran structure consists of a furan ring, with a nitro group (Figure 8).

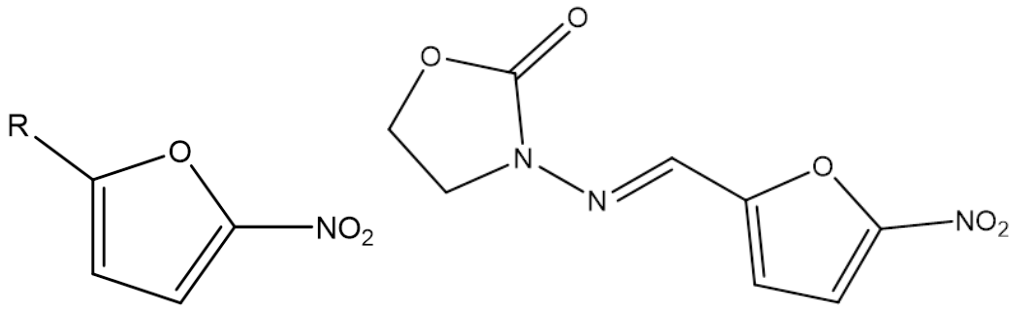

Figure 8: Structure of furazolidone (FZ)

General nitrofuran structure (left). Furazolidone structure (right). CAS RN: 67-45-8.

Nitrofurans were first discovered and implemented as antibiotics in the 1940s – 1950s and are a broad-spectrum class of antibiotics, effective against both gram-negative and gram-positive pathogens (Chamberlain, 1976). Nitrofurans were used widely in veterinary medicine, until the identification of residues in animal tissues resulted in nitrofurans being banned for use in food animals, due to fears around carcinogenicity of these residues towards humans (McCracken & Kennedy, 2007). These residues remain even after cooking of the animal products (Cooper & Kennedy, 2007) and studies in mice and rats revealed the toxicity and carcinogenic properties of nitrofurans towards these species (Kari *et al.*, 1989).

The nitrofuran furazolidone is used to treat both bacterial as well as protozoal enteritis and diarrhoea, including *Helicobacter pylori* infections (Zhuge *et al.*, 2018).

1.6.2 Furazolidone mechanism of action

Nitrofurans are prodrugs, meaning that they themselves are not toxic to bacteria, but rather must first be activated by bacterial nitroreductase enzymes, creating intermediates which are toxic to bacteria and it is these compounds that are responsible for the

antibacterial activity of nitrofurans (McCalla, 1979). In *Escherichia coli*, reduction of nitrofurans by nitroreductase enzymes has been shown to form hydroxylamine and nitroso derivatives (Race *et al.*, 2005). There are a wide range of reported targets of nitrofurans, including DNA, ribosomes, RNA, and proteins (Bertenyi & Lambert, 1996; McCalla, 1979; Ona *et al.*, 2009). However, which molecules are targeted through direct interaction with activated nitrofuran intermediates, and which are downstream consequences through interaction of the activated intermediates with essential targets is unknown (Le & Rakonjac, 2021).

There are two different kinds of type I oxygen insensitive bacterial nitroreductases in *E. coli*, NfsA and NfsB. NfsA is the major nitroreductase, and NfsB is the minor. These enzymes have low sequence similarity, yet their reaction modes are similar, with both enzymes catalysing the reduction of nitrofurans through a ping pong Bi-Bi mechanism (Zenno, Koike, Kumar, *et al.*, 1996; Zenno, Koike, Tanokura, *et al.*, 1996). A 2-electron reduction converts the nitrofuran to a nitroso derivative, and a further 2-electron reduction forms a hydroxylamine derivative (Race *et al.*, 2005). NfsA uses NADPH as a reducing equivalent, while NfsB can use either NADPH or NADH as sources of reducing equivalents. FMN (flavin mononucleotide) is required as a cofactor for NfsA, and NfsB can use either FMN or FAD (flavin adenine dinucleotide) (Zenno, Koike, Kumar, *et al.*, 1996).

There are also oxygen-sensitive nitroreductases, or type II nitroreductases. The first step of this mechanism reduces nitrofurans to nitro anion free radicals using a 1-electron reduction, and this reaction is oxygen sensitive because in the presence of oxygen, the nitro anion free radical formed in the first step is oxidised back to the nitrofuran, along with the formation of superoxide (Peterson *et al.*, 1979). The oxygen-sensitive nitroreductase AhpF has been identified in *E. coli*, through selecting for resistance in *ΔnfsA ΔnfsB* mutants (Le *et al.*, 2019).

The reaction mechanisms for type I and type II reduction of nitrofurans are shown in Figure 9.

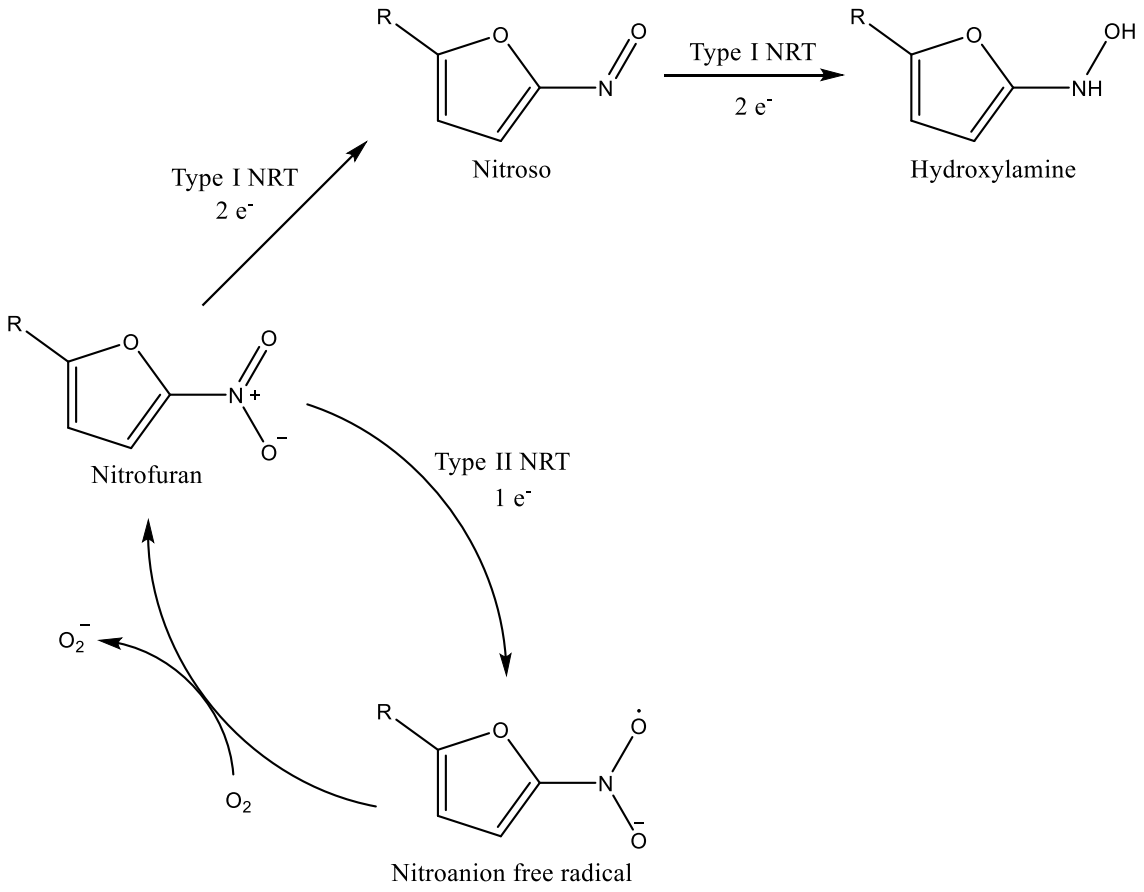

Figure 9: Mechanism of NTR (nitroreductase) enzymes reduction of nitrofurans

Type I (oxygen insensitive) and type II (oxygen sensitive) nitroreductases have different reaction mechanisms for reducing nitrofurans.

1.6.3 Nitrofuran resistance

Resistance to nitrofurans arises through bacterial mutations that affect the enzymes responsible for activating the nitrofuran prodrugs. Without enzymatic activation, nitrofurans do not exhibit bactericidal activity, rendering bacteria with mutations in these enzymes resistant to nitrofurans. Because the primary nitroreductases responsible for activating nitrofurans are the oxygen insensitive NfsA and NfsB, the most common resistance mechanism is through mutations in the *nsfA nfsB* genes (Whiteway *et al.*, 1998). A one step mutation in *nfsA* grants a three-fold increase in MIC, while a second mutational step, in *nfsB*, grants a ten-fold increase in MIC as compared to the wild-type parent (McCalla *et al.*, 1978). Mutation in *nfsB* alone does not change susceptibility, hence the MIC is unchanged from that of the wild-type parent (McCalla *et al.*, 1978), showing NfsA is the major nitroreductase responsible for activating nitrofurans.

1.7 Vancomycin

1.7.1 Vancomycin background, structure, and history

Originally derived from the soil bacterium *Amycolatopsis orientalis*, vancomycin is a glycopeptide antibiotic used to treat gram-positive bacterial infections. These include methicillin-resistant *Staphylococcus aureus* (MRSA), *Clostridiodes difficile*, streptococci, enterococci, and methicillin-susceptible *Staphylococcus aureus* (MSSA) (Patel, 2021). The chemical structure of vancomycin is shown below in Figure 10.

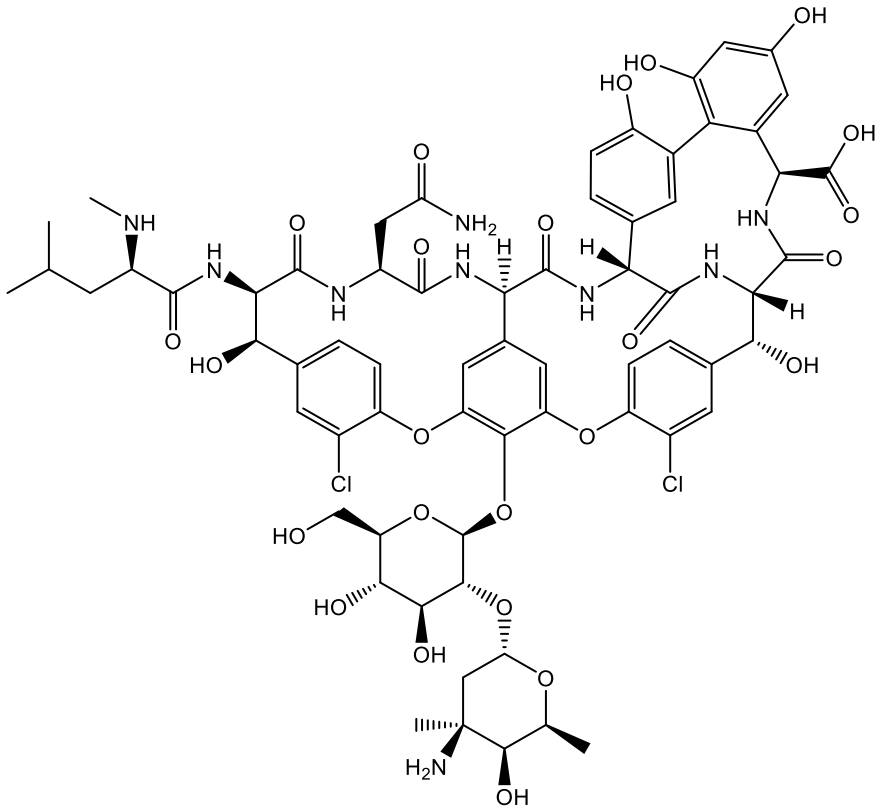

Figure 10: Vancomycin structure

CAS RN: 1404-90-6

Vancomycin is FDA approved for use both intravenously and orally, however it has poor oral bioavailability, so other than for intestinal infections, it is administered intravenously (Patel, 2021). Negative effects of intravenous vancomycin use include nephrotoxicity, hypotension, and hypersensitivity reactions (Patel, 2021).

Vancomycin was first discovered in 1952 and was approved by the FDA in 1958. Widespread use of vancomycin was initially limited due to the arrival of methicillin and cephalothin, with vancomycin being reserved for patients with β-lactam allergies or resistant infections (Levine, 2006). Vancomycin use began increasing during the 1980s, due to both a rise in MRSA, and a rise in pseudomembranous enterocolitis, which is mainly caused by *Clostridiodes difficile*, but also *S. aureus*. This widespread use, however, led to a rise in vancomycin resistant enterococci (VRE) (Levine, 2006).

1.7.2 Vancomycin mechanism of action

Vancomycin targets the cell wall of bacteria through inhibition of peptidoglycan synthesis (Jordan, 1961; Reynolds, 1961). Peptidoglycan consists of a carbohydrate backbone of alternating N-acetylmuramic acid (NAM) and N-acetylglucosamine (NAG) residues, cross-linked through short peptides attached to the NAM residues, creating a highly cross-linked structure that imparts rigidity to the cell wall. Vancomycin works through inhibition of both the polymerisation and cross-linking reactions (Reynolds, 1989). It does this by binding to the N-terminal D-alanyl D-alanine (D-Ala-D-Ala) residues of the peptidoglycan precursor required for polymer cross-linking (Nieto & Perkins, 1971; Perkins, 1969) (Figure 11). Vancomycin interacts with D-Ala-D-Ala through hydrogen bonding, forming a stable complex which directly prevents cross-linking by obscuring the necessary D-Ala-D-Ala residues. Furthermore, vancomycin disrupts chain extension of the backbone glycan polymers due to steric hinderance from vancomycin binding to the D-Ala-D-Ala residues of wall intermediates (Figure 11). Inhibition of cross-linking leads to weakening of the cell wall, resulting in its rupture and leakage of cellular contents, causing bacterial cell death (Patel, 2021).

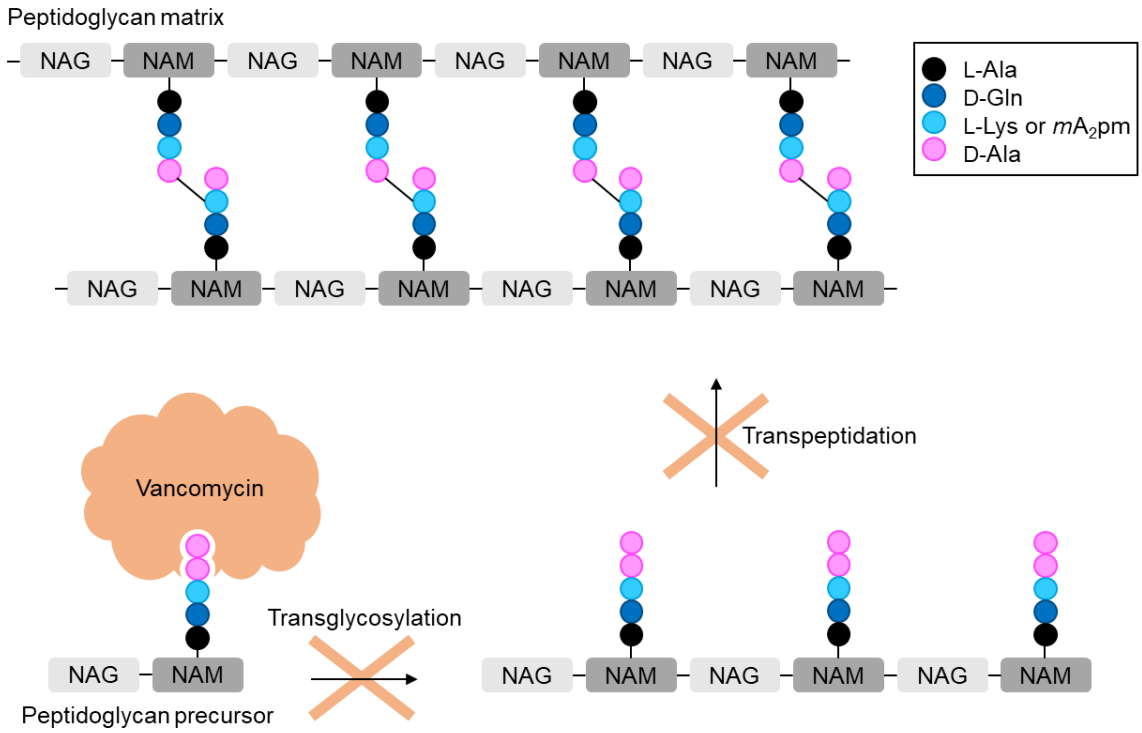

Figure 11: Vancomycin mechanism of action

The peptidoglycan synthesis transglycosylation and transpeptidation reactions, responsible for chain extension and cross-linking, respectively, are shown. Vancomycin binds to the D-Ala-D-Ala residues, preventing both transglycosylation and transpeptidation. (Kouidmi *et al.*, 2014; Vollmer *et al.*, 2008).

1.7.3 Vancomycin resistance

Vancomycin resistant enterococci (VRE) have six different forms of documented resistance, designated VanA, B, C, D, E, and G.

VanA, VanB and VanD resistance types involve the synthesis of D-alanyl-D-lactate instead of D-alanyl-D-alanine, which results in high-level vancomycin resistance, lowering the vancomycin binding affinity to the dipeptide by more than 1000-fold (Reynolds & Courvalin, 2005). These resistance mechanisms not only involve the synthesis of D-alanyl-D-lactate, but also the degradation of already synthesised D-alanyl-D-alanine through a VanX dipeptidase (Reynolds *et al.*, 1994). Another enzyme, VanY, prevents the translocation of D-Ala-D-Ala-containing precursors to the cell surface (Arthur *et al.*, 1994). VanX and VanY can also be together in the same strain.

VanC, VanE and VanG resistance types involve low level resistance, due to the synthesis of D-alanyl-D-serine instead of D-alanyl-D-alanine, which results in a six-fold lower binding affinity of vancomycin. VanC type resistance is found in intrinsically glycopeptide-resistant Enterococci, while VanE and VanG type resistance occurs when *Enterococcus faecalis* acquires the resistance genes encoding these proteins (Reynolds & Courvalin, 2005).

Often, the genes responsible for vancomycin resistance are located on mobile genetic elements, enabling their spread to other organisms.

Gram-negative bacteria are tolerant to high concentrations of vancomycin due to the presence of an outer membrane. The lipopolysaccharide layer of the outer membrane does not allow diffusion of hydrophobic or hydrophilic molecules unless their size permits diffusion through the outer membrane pore-like channels called porins. Due to the large size of VAN (>1400 Da), it cannot cross the outer membrane through porins. Therefore, any alterations to the outer membrane that make it more or less difficult for vancomycin to pass through will affect susceptibility to vancomycin. For example, increased levels of phosphatidic acid have been shown to increase the already extremely high resistance of *E. coli* and other gram-negative bacteria to vancomycin by further restricting access of vancomycin through the outer membrane (Sutterlin *et al.*, 2014).

1.8 FZ – VAN synergistic antibiotic combination

Synergy has been shown to exist between vancomycin and nitrofurans, specifically nitrofurantoin, in *E. coli* (Zhou *et al.*, 2015). This suggests that very small amounts of VAN can enter gram-negative bacteria, which would usually be insignificant, however when combined with nitrofurans, this can create a synergistic inhibitory effect (Zhou *et al.*, 2015). The SOS response has been linked to the mechanism of synergy between FZ and VAN, as deletion of *recA*, encoding the RecA DNA recombination/repair protein, was found to convert the interaction between FZ and VAN from a synergistic to an additive interaction (Olivera, 2021). It was proposed that the mechanism of synergy is due to VAN inhibition of the SOS response, increasing the DNA damaging effects of FZ.

1.9 Why investigating resistance is important

Investigating the resistance that can develop to a drug is an important research tool to combat increasing spread of antibiotic resistance. Investigating resistance can lead to the discovery of a drug's mechanisms of action, which in turn identifies bacterial drug targets that can be exploited in further drug development. In addition, identifying bacterial mechanisms of resistance can lead to the development of antibiotic adjuvants designed to target this resistance, and render the bacteria susceptible to original drug once again. In addition, investigating the resistance towards a drug is a crucial tool in assessing the clinical viability of that drug.

1.10 Project aims

This project aimed to investigate the resistance development to the synergistic antibiotic combination of furazolidone (FZ) and vancomycin (VAN) in gram-negative bacteria, using *Escherichia coli* as a model organism.

The first aim was to identify potential resistance mechanisms that evolve when *E. coli* is subjected to the FZ – VAN combination. This aim was broken down into the following objectives:

A) Assessing the FZ – VAN combination in the parental strain,

B) Selecting resistant mutants to the FZ – VAN combination,

C) Characterising isolated resistant mutants both phenotypically and using comparative genome analysis to identify any mutated genes.

A subsequent aim was to confirm the mechanism of resistance of the riboflavin biosynthesis pathway mutants isolated in the first aim.

2 Materials and Methods

2.1 Bacterial strains and growth conditions

E. coli strains and plasmids are listed below in Table 1.

Unless otherwise specified, *E. coli* strains were grown at 37°C at 200 rpm. Media used was either 2× YT media (BD Difco™) or CAMH (cation-adjusted Mueller Hinton media) (BD BBL™), and agar plates were made at 1% (agar from Pure Science).

Table 1: Bacterial Strains and plasmids used in this study

***E. coli* K12 Laboratory Strains**	**Genotype/Description**	**Source**
BW25113	*rrnB3 ΔlacZ4787 hsdR514 Δ(araBAD)567 Δ(rhaBAD)568 rph-1*	(Baba *et al.*, 2006)
JW3009	*recA1 endA1 gyrA96 thi-1 hsdR17 (r_K^- m_K^+) supE44 relA1* + pCA24N::*ribB*	(Kitagawa *et al.*, 2005)
JW0405	*recA1 endA1 gyrA96 thi-1 hsdR17 (r_K^- m_K^+) supE44 relA1* + pCA24N::*ribE*	(Kitagawa *et al.*, 2005)
JW0567	*recA1 endA1 gyrA96 thi-1 hsdR17 (r_K^- m_K^+) supE44 relA1* + pCA24N::*nfsB*	(Kitagawa *et al.*, 2005)
K2653	BW25113 with spontaneous insertion in *gtrB*	This study
K2654	K2653, no additional mutations identified	This study
K2655	K2653, nonsense mutation in *nlpI*	This study
K2656	K2653, unsequenced	This study
K2657	K2653, frameshift in *opgG*	This study
K2658	K2653, missense in *rpoC*	This study
K2659	K2653, frameshift in *ftsH*	This study
K2660	K2653, missense in *ftsH* + *insH1* inserted in *waaR*	This study
K2661	K2653, frameshift in *wecC*	This study
K2662 (B1)*	K2653, point mutation in 5’ UTR of *ribB*	This study
K2663 (E1)*	K2653, in-frame insertion in *ribE*	This study
K2664	K2653, frameshift in *ftsH*	This study
K2665 (E2)*	K2653, in-frame deletion in *ribE* + missense in *fabH*	This study

K2666 (E3)*	K2653, in-frame deletion in *ribE* + missense in *yjhQ*	This study
K2667 (E4)*	K2653, in-frame deletion in *ribE*	This study
K2668 (E5)*	K2653, in-frame deletion in *ribE* + missense in *ycjM*	This study
K2669 (B2)*	K2653, *insA* inserted in *ribB* promoter	This study
K2670 (B3)*	K2653, *insH1* inserted in *ribB* promoter	This study
K2671 (B4)*	K2653, point mutation in 5' UTR of *ribB*	This study
K2672	K2653, unsequenced	This study
K2673	K2653, in-frame deletion in *lpp*	This study
K2642 (PS + *ribE*)	K2653 + pCA24N::*ribE*	This study
K2643 (E1 + *ribE*)	K2663 + pCA24N::*ribE*	This study
K2644 (E2 + *ribE*)	K2665 + pCA24N::*ribE*	This study
K2645 (E3 + *ribE*)	K2666 + pCA24N::*ribE*	This study
K2646 (E4 + *ribE*)	K2667 + pCA24N::*ribE*	This study
K2647 (E5 + *ribE*)	K2668 + pCA24N::*ribE*	This study
K2648 (PS + *ribB*)	K2653 + pCA24N::*ribB*	This study
K2649 (B1 + *ribB*)	K2662 + pCA24N::*ribB*	This study
K2650 (B2 + *ribB*)	K2669 + pCA24N::*ribB*	This study
K2651 (B3 + *ribB*)	K2670 + pCA24N::*ribB*	This study
K2652 (B4 + *ribB*)	K2671 + pCA24N::*ribB*	This study
K2709 (PS knockout)	K2653 Δ*nfsA* Δ*nfsB*	This study
K2710 (E1 knockout)	K2663 Δ*nfsA* Δ*nfsB*	This study
K2711 (E4 knockout)	K2667 Δ*nfsA* Δ*nfsB*	This study
K2712 (B2 knockout)	K2669 Δ*nfsA* Δ*nfsB*	This study
K2713 (B3 knockout)	K2670 Δ*nfsA* Δ*nfsB*	This study
K2718 (PS + *nfsB*)	K2653 + pCA24N::*nfsB*	This study
K2719 (E1 + *nfsB*)	K2663 + pCA24N::*nfsB*	This study
K2720 (E4 + *nfsB*)	K2667 + pCA24N::*nfsB*	This study
K2721 (B2 + *nfsB*)	K2669 + pCA24N::*nfsB*	This study
K2722 (B3 + *nfsB*)	K2670 + pCA24N::*nfsB*	This study

*(The *ribB* and *ribE* mutants will be referred to by their B/E numbers)

Plasmids	Description	Source
pCP20	AMP^r, CHL^r, FLP^+, λ $cI857^+$, λ p_R Rep^{ts}	(Cherepanov & Wackernagel, 1995)
pCA24N::*ribB*	CHL^r; *lacI*^{q}, pCA24N $P_{T5\text{-}lac}$::*ribB*	(Kitagawa *et al.*, 2005)
pCA24N::*ribE*	CHL^r; *lacI*^{q}, pCA24N $P_{T5\text{-}lac}$::*ribE*	(Kitagawa *et al.*, 2005)
pCA24N::*nfsB*	CHL^r; *lacI*^{q}, pCA24N $P_{T5\text{-}lac}$::*nfsB*	(Kitagawa *et al.*, 2005)

2.2 Antibiotics

Antibiotics were purchased from Goldbio, and stocks made up in either water (ampicillin AMP, kanamycin KAN, vancomycin VAN), or DMSO (chloramphenicol CHL, furazolidone FZ).

2.3 Antimicrobial susceptibility assays

The antimicrobial susceptibility of the *E. coli* strains was determined using both broth microdilution and agar methods and expressed as minimum inhibitory concentration (MIC). Determination of MIC in both liquid and solid media was conducted according to CLSI (Clinical & Laboratory Standards Institute) guidelines as previously described (Cockerill *et al.*, 2012). Where the antibiotic stocks were prepared in DMSO (CHL and FZ), all media was normalised to 1% DMSO.

In strains transformed with pCA24N and its derivatives, which contain the *cat* marker (CHL^r), media contained CHL at 30 μg/mL for selection. When required, the expression of specific *E. coli* genes cloned into this vector were induced by adding IPTG (isopropyl ß-D-1-thiogalactopyranoside) to a final concentration of 0.1 mM.

Riboflavin (Sigma Aldrich) was added to the liquid media as required, at a final concentration of 1 mM.

Dose-response curves were plotted using the values of the OD_{600} (optical density at 600 nm) reading at 18 hours using a Multiskan^{TM} GO Microplate Spectrophotometer.

2.4 Checkerboard assays

Checkerboard assays were conducted to determine the interaction between the antibiotics in the *E. coli* strains. These assays were conducted in 384 multi-well plates. Two-fold serial dilutions of each antibiotic (FZ and VAN) were prepared at a concentration 4-fold higher than the final concentration, with 12.5 μL of each antibiotic added to each well. Bacteria were added (25 μL of 1×10^6 CFU/mL) to give a final concentration of 5×10^5 CFU/mL, for a total volume of 50 μL in each well. Media in all wells contained 1% DMSO. Each antibiotic concentration was prepared in triplicate as technical replicates. The checkerboard assays were incubated at 37°C for 18 hours, and growth was measured spectrophotometrically (Multiskan™ GO Microplate Spectrophotometer). MIC was determined as the concentration at which the OD_{600} was decreased by 90% or more, in comparison to the no-antibiotic control, as previously described (Zimmerman *et al.*, 2020). Growth/inhibition for the checkerboard assays was also confirmed visually.

2.5 Isolating Resistant Mutants

Spontaneous resistance-causing mutations in the *E. coli* overnight cultures were selected for on antibiotic agar plates. *E. coli* strain K2653 was used as the parental strain for the selection of the FZ/VAN resistant mutants (and the VAN resistant mutant).

The selection plates contained CAMH agar and antibiotic(s), depending on the selection type. For selection of mutants growing on the FZ/VAN combination, plates contained 256 μg/mL VAN and 2 μg/mL FZ, whereas for resistance to VAN, plates contained only this antibiotic at 1024 μg/mL. Twenty selection plates were used for both the FZ/VAN combination and VAN alone. Twenty independent parallel overnight cultures were prepared, and 100 μL of each were added to a tube containing 2.5 mL of molten 0.5% CAMH agar (at ~47°C), vortexed, and poured onto the selection plates and tilted to spread the molten agar evenly. Plates were incubated at 37°C for 48 hrs. Colonies formed on the selection plates were passaged onto fresh CAMH agar plates and incubated at 37°C to give single colonies. More than one colony was selected from plates if the colonies had visual differences. There is the risk of isolating identical mutations if multiple colonies are selected from a single plate, but no colonies originating from the same plate had identical mutations, likely due to the choice of

different colony morphologies. Isolated colonies were tested for increased resistance to FZ and VAN in CAMH broth to characterise the resistance phenotypically.

2.6 Comparative genome analysis

Genomic DNA of the isolated FZ-VAN resistant mutants, the isolated VAN resistant mutant, and the parental strain were extracted using the DNeasy UltraClean Microbial Kit (Qiagen) according to the manufacturer's instructions. The DNA samples were submitted for whole genome sequencing to Massey Genome Service (New Zealand Genomics Ltd., Massey University, Palmerston North, New Zealand). Libraries were prepared using the Illumina DNA Prep kit and run on one Illumina MiSeq™ 2× 250-base paired-end run, version 2 chemistry.

The raw reads were trimmed to an error probability of 0.001 (Phred score of 30), and any short reads of less than 25 bases were removed using SolexaQA++ v3.1.7.1 (Cox *et al.*, 2010). The trimmed reads were then aligned to the reference strain genome *E. coli* BW25113 (accession number CP009273.1) (Grenier *et al.*, 2014) using bowtie2 v2.4.2 (Langmead & Salzberg, 2012) in very sensitive mode. SAMtools v1.14 (Li *et al.*, 2009) was then used to convert the resultant sam files into bam files, followed by calling the variants with freebayes v1.3.1 (Garrison & Marth, 2012), with ploidy set to 1. The variants were then annotated using Snpeff v4.4.20(1) (Cingolani *et al.*, 2012).

Structural variations in the genomes were identified by extracting the unmapped reads using SAMtools v1.14 (Li *et al.*, 2009), and these unmapped reads were then assembled into contigs using SPAdes v3.13.0 (Bankevich *et al.*, 2012), set at "careful". The generated contigs were then compared to the reference *E. coli* BW25113 genome (accession number CP009273.1) (Grenier *et al.*, 2014) using NCBI nucleotide BLAST 2.12.0+ (Altschul *et al.*, 1997) to determine the location of the structural variations.

2.7 Growth rate assays

Growth rate experiments were conducted in either flat-bottom 384-well (Corning) or flat-bottom 96-well (Jet Biofil) plates. 50 µL final volume was used in each well for 384-well plates, 200 µL final volume for 96-well plates. Each well had 5×10^5 CFU/mL of *E. coli*. CAMH media for growth of strains containing pCA24N-derived plasmids contained 30 µg/mL CHL and was normalised to 1% DMSO. When required, expression of proteins from the pCA24N recombinant plasmids was induced with 0.1 mM IPTG (isopropyl ß-D-1-thiogalactopyranoside). Riboflavin was added as required, at a final concentration of 1 mM. All growth rate assays were incubated at 37°C, and OD_{600} was measured every hour for either 24 or 48 hrs using Multiskan^{TM} GO Microplate Spectrophotometer.

2.8 Transformation

Chemically competent cells were prepared as follows from the *ribB* and *ribE* mutants as well as the parental strain. An overnight culture was diluted 1:100 into 25 mL of 2× YT broth (BD Difco^{TM}) and grown up at 37°C with shaking to OD_{600} between 0.15 – 0.2. The cultures were cooled on ice for 20 mins, then centrifuged for 10 min (4°C at 4,000 × g) and the supernatant poured and aspirated off. The pellet was resuspended in 5 mL of cold 0.1 M $CaCl_2$, centrifuged for 5 min (4°C at 4,000 × g) and the supernatant poured and aspirated off. The pellet was then resuspended in 500 µL of cold 10% glycerol (v/v), 0.1 M $CaCl_2$, and competent cells were stored at -80°C.

Plasmids pCA24N::*ribB*, pCA24N::*ribE* and pCA24N::*nfsB* were purified from strains JW3009, JW0405, and JW0567, respectively (Kitagawa *et al.*, 2005), using the Monarch plasmid miniprep kit #T10105 according to the manufacturer's instructions.

The *ribB* and *ribE* mutants and their parental strain were transformed as follows. 1 µL of extracted plasmid DNA was mixed into 50 µL of chemically competent cells and incubated on ice for 30 mins, followed by heat shock in a 42°C water bath for 45 sec. The tubes were then put on ice for 2 min, and 450 µL SOC media added, and the tubes incubated with shaking at 37°C for 45 mins.

Drops (25 μL) of concentrated transformation and 10-fold serial dilutions (10^1, 10^2, 10^3, 10^4) were spread on 2× YT agar plates containing CHL at 30 μg/mL and incubated at 37°C to get single colonies.

2.9 P1 transduction

The Δ*nfsA* Δ*nfsB* double knockout strains were constructed *via* P1 transduction using the corresponding single-gene deletions from Keio collection strains (Baba *et al.*, 2006) as donors. Deleted genes in these Keio strains are replaced by a kanamycin cassette flanked by FLP recombinase recognition target (FRT) sequences. These single-gene knockouts were transduced into recipient *E. coli* strains through P1 transduction as previously described (Thomason & Constantino, 2007). To summarise, first a P1 stock lysate was made, then the P1 donor transducing lysates were constructed by allowing the P1 phage stock to replicate within the donor strains, which contained the desired gene knockout (Δ*nfsA* or Δ*nfsB*) replaced by a kanamycin cassette. The P1 donor transducing lysate was then used to transfer the desired gene knockout Δ*nfsA::KAN*^{R} into the recipient strain, where successful transduction of the deleted gene was selected for using kanamycin. Following this, FLP-mediated recombination was used to remove the FRT-flanked KAN^r cassette as described previously (Datsenko & Wanner, 2000), creating Δ*nfsA* knockout strains. The Δ*nfsB::KAN*^{R} allele was then transduced into the Δ*nfsA* knockout strains, followed by FLP-mediated recombination to remove the FRT-flanked KAN^r cassette, resulting in Δ*nfsA* Δ*nfsB* double knockout strains.

2.10 PCR confirmation of gene knockouts

PCR was used to confirm the *nfsA nfsB* gene knockouts. One bacterial colony was mixed with 1 mL of water and boiled for 10 minutes, then centrifuged at 1,000 × g for 5 minutes. Supernatent (5 μL) containing released DNA was used as a template in the PCR reaction, along with 10 μL PrimeSTAR GXL buffer, 200 μM each dNTP, 0.2 μM forward primer, 0.2 μM reverse primer and 0.5 μM of PrimeSTAR GXL DNA Polymerase, in a total reaction volume of 50 μL. The PCR reaction conditions were 35 cycles of 98°C for 10 seconds, 53°C for 30 seconds, 72°C for 2 minutes. The PCR

reactions were analysed using DNA gel electrophoresis and visualised using ethidium bromide stain. Primers used were

nfsA forward primer (5'-TGTTTTGCTCATGCTTCCC-3'),

nfsA reverse primer (5'-TTTGTAGTGAATAGAAGACGCC-3'),

nfsB forward primer (5'-AATACCCGCTAAATCTTCAACC-3') and

nfsB reverse primer (5'-CGATCAAAAAAGAGTGCGTCC-3').

2.11 Nitroreductase assays

Nitroreductase assays were conducted on selected *ribB* and *ribE* mutants, the parental strain, and the corresponding *ribB* and *ribE* complemented strains. Each strain was analysed in three independent assays. Overnight cultures were diluted into 25 mL of CAMH broth and grown into exponential phase (OD_{600} ~0.5) at 37°C. For strains containing a pCA24N plasmid, 30 μg/mL CHL and 0.1 mM IPTG was added. The exponential phase cultures were then centrifuged for 10 min at 4,000 × g, and the pellets frozen at -20°C until use.

The pellets were washed with 10 mL of chilled 50 mM Tris-HCl (pH 7.4), and centrifuged for 10 min (4,000 × g, 4°C), before resuspension in 3.5 mL of chilled 50 mM Tris-HCl (pH 7.4). The OD_{600} of each strain was then measured using a Multiskan^{TM} GO Microplate Spectrophotometer, and 3 mL of each culture adjusted to a titre of 1×10^9 CFU/mL through dilution with 50 mM Tris-HCl. Cell density was determined using $\frac{CFU}{mL} = OD_{600} \times 4 \times 10^8$, which was the formula for cell density determined from *E. coli* concentrations measured by this spectrophotometer. The concentrated cells were then sonicated twice using the microtip of a Virsonic 600 ultrasonic cell disruptor, with each session lasting 2 minutes, with alternate 2 seconds on, two seconds off, at an amplitude of 15, followed by centrifugation at 14,000 × g for 30 minutes. The resulting supernatent was cell-free extract of soluble *E. coli* proteins used for nitroreductase assays.

All nitroreductase assays were performed on a 96-well plate and each reaction was performed in triplicate. Each well contained a reaction mixture of final volume 200 μL (50 mM Tris-HCl (pH 7.4), 0.1 mM NADH (Goldbio) or NADPH (Roche), 0.1 mM FZ,

and 50 μL of cell-free extract). Wells without the cell-free extract were used as negative controls. The plate was incubated at 25°C, and the absorbance was measured every minute for 12 hrs at both 340 and 400 nm. The 96-well plate containing the incomplete reaction mix (FZ in Tris buffer) was incubated at 25°C for ~2 hrs prior to the addition of NADH/NADPH and cell extract.

3 Investigating the resistance that arises in *E. coli* towards the FZ – VAN antibiotic combination

3.1 Introduction

The antibiotic combination of furazolidone and vancomycin has been previously investigated and found to display synergy in *E. coli* (Olivera, Le, *et al.*, 2021). Synergistic interactions are important clinically as they lower the dosage required to be effective, leading to reduced side-effects and lower toxicity, while also opening the range of drug options available by including drugs that cannot be used as effective treatment alone. The FZ – VAN combination is promising as it has the potential to repurpose vancomycin, an antibiotic used for the treatment of gram-positive infections, into a treatment option for gram-negative infections.

Investigating the genetic basis of resistance can give insight into the mechanism of action of a drug/drug combination, which can reveal bacterial targets for further drug development. In addition to revealing targets for direct inhibition, understanding mechanisms of resistance can lead to the design of antibiotic-adjuvanting molecules targeting specifically these resistance mechanisms, to render the bacteria susceptible to the drug once more. In addition, the ease bacterial resistance arises can be used to assess the viability of using the drug/combination in practice.

This chapter describes the selection for mutants resistant to the FZ – VAN antibiotic combination, as well as the subsequent phenotypic and genotypic characterisation of these mutant strains to gain further understanding of the mutations that occurred.

3.2 Results

3.2.1 FZ – VAN combination in the parental strain

The parental strain used for all experiments was strain K2653. Vancomycin and furazolidone, individually and combined, were investigated in the parental strain to establish a baseline for these antibiotics in the parental strain. The MICs (minimum inhibitory concentrations) for FZ were found to be 0.5 μg/mL on CAMH agar, and 2 μg/mL in CAMH broth. The VAN MICs were 256 μg/mL in both CAMH agar and in CAMH broth.

A checkerboard assay showed that the FZ – VAN combination was synergistic in the parental strain, as has been previously reported (Olivera, Le, *et al.*, 2021; Zhou *et al.*, 2015). The checkerboard assay was conducted on a 384-well plate, with the concentration of VAN varying along the y-axis, and the concentration of FZ varying along the x-axis. This creates different combinations of drug concentrations, and the patterns of bacterial growth observed are then used to determine the drug interaction in the strain. The FZ – VAN combination was found to be synergistic as the FICI (fractional inhibitory concentration index) was 0.25, which is below 0.5, indicating synergy (Odds, 2003). For a combination where there was no bacterial growth, the FICI is calculated by adding the FIC (fractional inhibitory concentration) for the VAN component and the FIC for the FZ component together. The FIC is calculated as the ratio of the concentration of the drug in the well containing both antibiotics over the MIC for that drug when used alone. Plotting the FICs for each drug against each other gives an isobologram, and the parental strain isobologram is shown below, with the FICI values for each point shown (Figure 12). The concave shape of the curve shows the synergistic relationship between FZ and VAN in the parental strain.

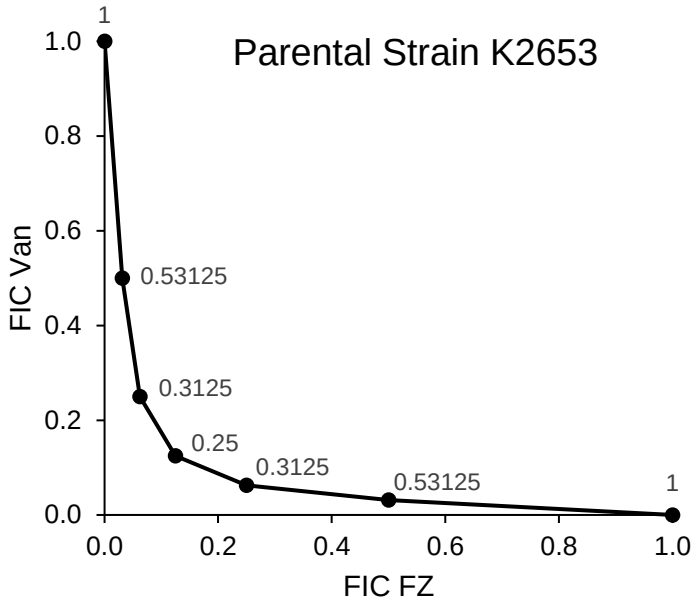

Figure 12: Isobologram showing the interaction between FZ and VAN in the parental strain (K2653)

The concave curve shows the synergistic interaction. The FICI values for each point are shown.

3.2.2 Selection for resistant mutants

The aim of selection was to isolate colonies at concentrations where the parental cells are killed. These colonies arose from cells that acquired spontaneous mutations that resulted in increased resistance to the FZ-VAN combination.

Selection for resistant mutants was done by mixing 100 µL of the parental strain K2653 overnight culture with 2.5 mL of molten 0.5% agar and pouring this on top of the antibiotic plates. The MICs for this method were first established to determine the concentrations to be used. The MIC for FZ alone was 8 µg/mL and for VAN alone was 1024 µg/mL. The combination plates were then constructed from fractions of these MICs, and it was found that one quarter (2 µg/mL FZ + 256 µg/mL VAN) was the minimum inhibitory concentration. This was the plate concentration used to select for mutants to the combination. VAN plates (1024 µg/mL) were used to select for VAN mutants. No FZ mutants were selected for due to nitrofuran resistance already being well characterised in *E. coli* (Le *et al.*, 2019; McCalla *et al.*, 1978; Vervoort *et al.*, 2014; Whiteway *et al.*, 1998). Twenty independent parallel *E. coli* K2653 overnight cultures plated on twenty separate agar plates were used to select for any spontaneous mutations that resulted in resistance.

After 48 hrs incubation, nine out of the twenty combination plates had at least one colony, and one of the twenty vancomycin plates had a colony as shown in Table 2. Plate 1 had significantly more colonies than the other plates, however as there was a small number of plates used, variation in the number of mutants is expected.

From these plates, colonies were isolated for further testing to confirm their resistance phenotype. More than one colony was isolated from two of the plates, because there were multiple different colony morphologies. (Isolating more than one colony from a single plate runs the risk of isolating the same mutation multiple times, however none of the sequenced colonies from the same plate had identical mutations, as determined by genome sequence analyses).

The single colony found on plate 8 did not grow when passaged to a fresh plate, so this colony was not used. Two different morphologies from one of the isolated colonies from plate 1 (big and small) maintained these morphological differences upon passaging to a new plate, so these were tested independently.

Table 2: Isolation of colonies from inhibitory concentration FZ + VAN and VAN plates

Plate (FZ + VAN)	**No. of colonies**	**No. of colonies isolated from plate**
1	19	10
2	1	1
3	1	1
4	2	1
5	1	1
6	2	2
7	1	1
8	2	1
9	1	1
Plate (VAN)	**No. of colonies**	**No. of colonies isolated from plate**
1	1	1

3.2.3 Phenotypic characterisation of resistant mutants

Checkerboard assays were conducted on each isolated strain to determine the FZ and VAN MICs as well as the interaction between FZ and VAN. Results are summarised in Table 3.

Table 3: MIC and FICI values for isolated strains

	FZ MIC* (µg/mL)	VAN MIC* (µg/mL)	FICI*
K2653 (Parental strain)	2	256	0.250
K2654	2	256	0.375
K2655	1	512	**0.531**
K2656	2	512	0.500
K2657	2	**1024**	0.375
K2658	2	512	0.500
K2659	1	**1024**	**1.000**
K2660	1	**1024**	**0.516**
K2661	2	512	0.375
K2662 (B1)**	4	256	**0.750**
K2663 (E1)**	4	512	**0.625**
K2664	**0.5**	**1024**	**0.625**
K2665 (E2)**	**8**	512	**0.750**
K2666 (E3)**	**8**	256	**0.750**
K2667 (E4)**	**8**	512	**0.625**
K2668 (E5)**	**8**	512	**0.625**
K2669 (B2)**	**8**	256	**0.750**
K2670 (B3)**	**8**	512	0.500
K2671 (B4)**	4	512	**0.563**
K2672	2	256	0.375
K2673***	2	**1024**	0.250

*MIC values that changed four-fold are indicated in bold. FICI values that are additive (greater than 0.5) are also indicated in bold.

**_ribB_ and _ribE_ mutant strains are referred to by their B/E numbers

***mutant isolated from VAN only plate

MIC or FICI in 15 of the 20 tested isolated strains changed substantially, with either a four-four change in MIC, or changing from a synergistic to an additive interaction between FZ and VAN, or both. Of particular interest was strain K2664, which displayed a collateral sensitivity phenotype, with a four-fold decrease in FZ MIC, and a four-fold increase in VAN MIC, and loss of FZ-VAN synergy.

3.2.4 Sequencing

It was decided to send 18 strains for whole genome sequencing, as well as the parental strain. Strains K2672 and K2656 were not sequenced. K2672 was found to have a changed MIC, when initially tested it showed resistance and had small colonies, but then the colony morphology reverted to the parental strain appearance, as did the MICs, so potential contamination by the parental strain, or a mutation reverting the initial mutation occurred, and so this mutant was not selected for sequencing. K2656 was also not selected for sequencing because both K2656 and K2657 were derived from the same original isolated colony (K2656 had bigger colonies, K2657 had smaller colonies and so they were tested independently). K2657 had a more interesting resistance phenotype (four-fold increase in VAN MIC) and so was selected for sequencing.

3.2.5 Genes of Interest found

Whole genome sequencing was performed on the 18 chosen isolated strains and the parental strain, then comparative genome analysis was used to analyse the sequenced mutants. This involved mapping the sequencing reads to the BW25113 reference genome to identify any mutations. In addition, unmapped reads were assembled into contigs to identify any structural variations. The contigs were run through the NCBI nucleotide BLAST platform to identify their genomic location. The mutations found are shown in Table 4.

Table 4: Summary of mutations found in the isolated strains

Strain	Gene	Description
K2653 (PS)*	*gtrB***	*insA i*nsertion**
K2654	-	No mutations identified
K2655	*nlpI*	Stop gained
K2657	*opgG*	Frameshift
K2658	*rpoC*	Missense
K2659	*ftsH*	Frameshift
K2660	*ftsH*	Missense
	waaR	*insH1* insertion
K2661	*wecC*	Frameshift
K2662 (B1)	*ribB*	Point mutation in 5' UTR
K2663 (E1)	*ribE*	In-frame insertion
K2664	*ftsH*	Frameshift
K2665 (E2)	*ribE*	In-frame deletion
	fabH	Missense
K2666 (E3)	*ribE*	In-frame deletion
	yjhQ	Missense
K2667 (E4)	*ribE*	In-frame deletion
K2668 (E5)	*ribE*	In-frame deletion
	ycjM	Missense
K2669 (B2)	*ribB*	*insA* inserted in promoter
K2670 (B3)	*ribB*	*insH1* inserted in promoter
K2671 (B4)	*ribB*	Point mutation in 5' UTR
K2673	*lpp*	63bp in-frame deletion

*PS: parental strain

**the *gtrB* mutation was present in the parental strain and all progeny strains, and differs from the BW25113 reference genome

3.2.6 Mutations in the parental strain

Phase variation due to reversible inversion was identified between the *stfE* and *ycfK* gene loci as has been previously reported (Goldberg *et al.*, 2014). In addition, an insert in the *gtrB* gene, which encodes bactoprenol glucosyl transferase was identified in the parental strain used for mutant selection, as compared to the BW25113 reference genome. This *gtrB* mutation was also present in all other sequenced strains, which were all derived from this parental strain. As such the parental strain for this experiment was not identical to BW25113 as expected, due to this mutation.

Table 5: Parental strain *gtrB* mutation

Strain	MICs	FICI	Mutation position	Mutation type
K2653 (PS)	2 μg/mL FZ 256 μg/mL VAN	0.25	2461967	*insA* insertion

3.2.7 Riboflavin biosynthesis pathway mutations, *ribB* and *ribE*

Riboflavin, or vitamin B_2, is a precursor for flavin mononucleotide (FMN) and flavin adenine dinucleotide (FAD). Many proteins contain FMN or FAD as essential coenzymes, and these proteins are known as flavoproteins. Flavoproteins have a wide array of different functions including a variety of redox reactions involved in the metabolism of proteins, carbohydrates, lipids, and ketone bodies (Averianova *et al.*, 2020).

E. coli lacks the ability to import flavins (Hemberger *et al.*, 2011; Vogl *et al.*, 2007), therefore the riboflavin biosynthesis pathway is essential in *E. coli* as the only source of flavins. Both RibB and RibE are essential enzymes in the riboflavin biosynthesis pathway. RibB catalyses the synthesis of 1-deoxy-L-glycero-tetrulose 4-phosphate, while RibE catalyses the formation of 6,7-dimethyl-8-(1-D-ribityl)lumazine in the next step in the pathway. The riboflavin biosynthesis pathway is shown in Figure 13.

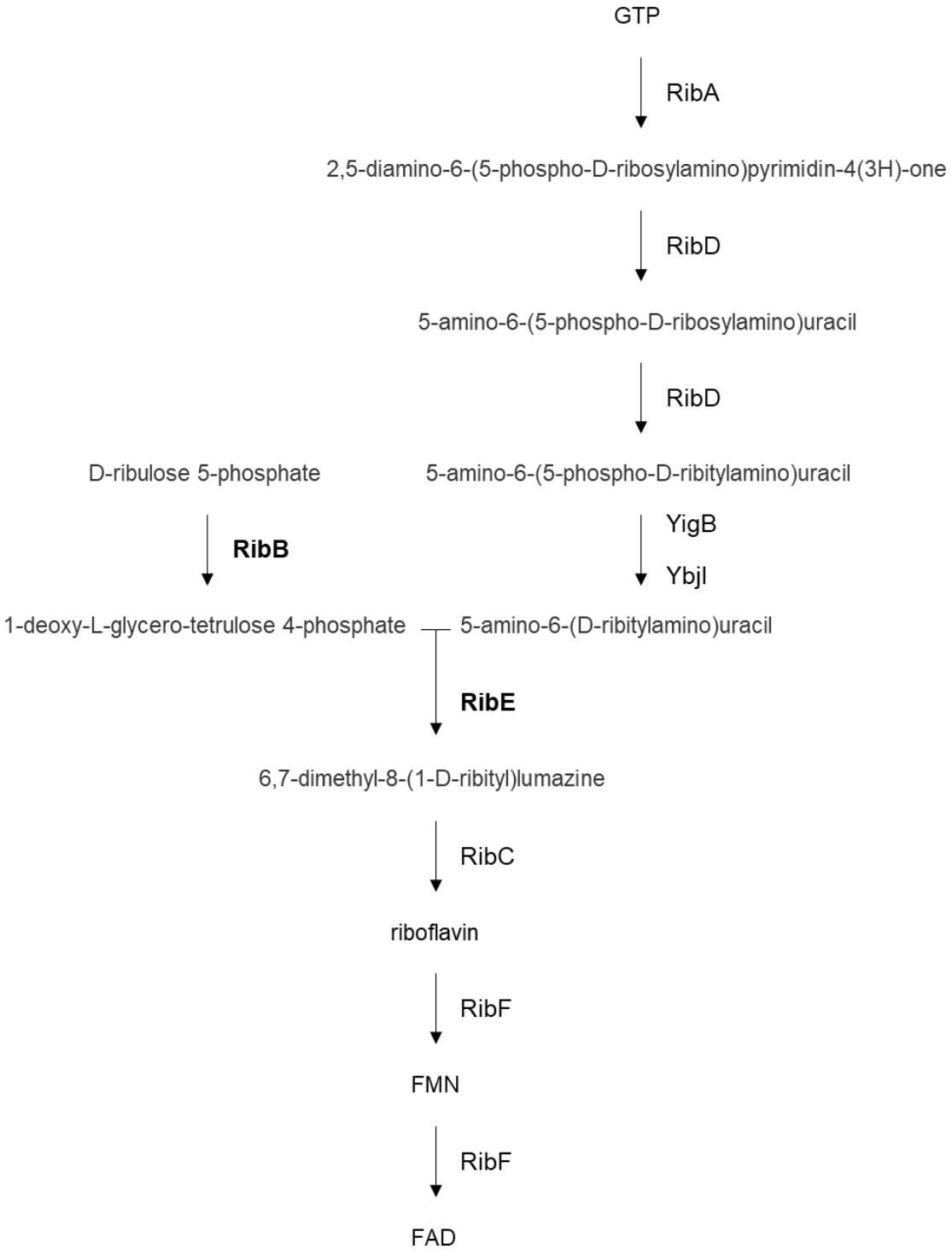

Figure 13: Riboflavin biosynthesis pathway

Schematic of the riboflavin biosynthesis pathway in *E. coli* showing compound names and the enzymes responsible. RibB and RibE are indicated in bold.

Four of the isolated strains had mutations associated with the *ribB* gene (Figure 14). These were strains K2662, K2669, K2670 and K2671, which were given the shorthand B1, B2, B3, and B4, respectively. B1 and B4 had single nucleotide point mutations upstream of the open reading frame (ORF) in the mRNA 5' UTR (untranslated region) and both strains had a two-fold increase in FZ MIC. B2 and B3 both had insertions upstream of *ribB* transcription start, within the promotor sequence, and both had a four-fold increase in FZ MIC. All four *ribB* mutants had an increase in FICI; B1, B2 and B4 to the point of changing from a synergistic to an additive interaction between FZ and VAN (FICI greater than 0.5). B3 and B4 had a two-fold increase in VAN MIC.

Table 6: *ribB* mutants

Strain	MIC changes	FICI	Mutation position	Mutation type	Mutation
B1	2-fold increase FZ no change VAN	**0.75**	3177902	Point mutation in 5' UTR	C → A
B2	**4-fold increase FZ** no change VAN	**0.75**	3178086	*insA* inserted in promoter	
B3	**4-fold increase FZ** 2-fold increase VAN	0.5	3178092	*insH1* inserted in promoter	
B4	2-fold increase FZ 2-fold increase VAN	**0.563**	3178074	Point mutation in 5' UTR	A → C

Interestingly, all the *ribB* mutations occurred upstream of the CDS (coding sequence), as shown in Figure 14. The B1 and B4 substitutions occurred in the 5'UTR. The 5'UTR of *ribB* has been previously shown to form an FMN riboswitch. Binding of FMN to the FMN-binding aptamer creates a stem-loop structure that acts as a transcription terminator as well as a mechanism for sequestering the ribosome binding site, controlling expression of *ribB* at both the transcriptional and translational level (Pedrolli *et al.*, 2015). It is possible that the B1 and B4 mutations in the 5'UTR may affect the folding of the regulatory stem-loop structure. Both B2 and B3 had large insertion sequences in the promoter region, disrupting the -35 and -10 boxes that bind the sigma factor and RNA polymerase, respectively.

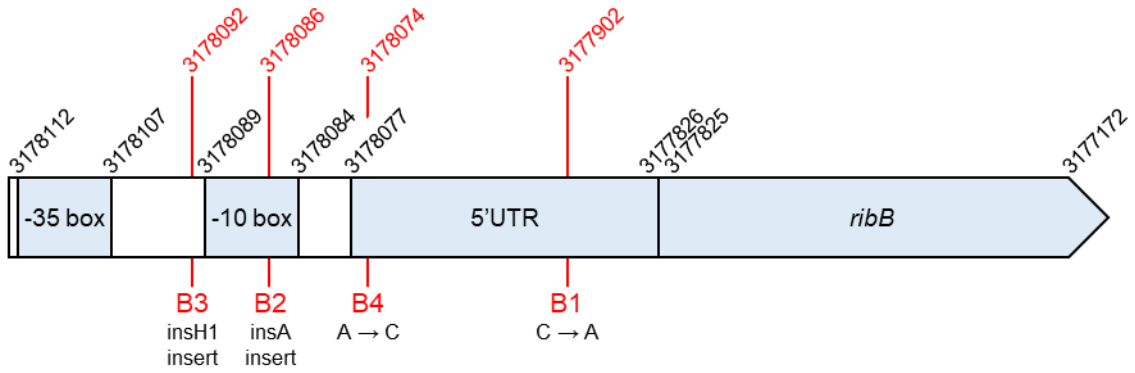

Figure 14: Position of *ribB* mutations

The position of the mutations in strains B1, B2, B3, and B4 are shown. The genome positions are in accordance with the BW25113 reference genome. Diagram not to scale.

Five of the isolated strains had mutations in the *ribE* gene, interestingly all in the same position. It is worth noting all the *ribE* mutants were isolated from different plates, indicating these mutations occurred independently. Strain K2663 (E1) had an in-frame insertion mutation, while strains K2665 (E2), K2666 (E3), K2667 (E4) and K2668 (E5) all had an identical in-frame deletion mutation. All mutants had an increase in FZ MIC, E1 a two-fold increase, whilst E2, E3, E4 and E5 all had a 4-fold increase. All *ribE* mutants had an increase in FICI to greater than 0.5, resulting in conversion from synergistic to additive interactions between FZ and VAN. E1, E2, E4, and E5 also had a two-fold increase in the VAN MIC.

E2, E3, E4 and E5 had identical deletion mutations in *ribE*, however E2, E3, and E5 had additional mutations. These are shown in brackets in Table 7 below. All three of these additional mutations were missense, involving the substitution of one base. One was in the *fabH* gene, another was in the *yjhQ* gene, and the third was in the *ycjM* gene. As all three of these mutants had the same 4-fold increase in furazolidone MIC as the mutant with only the *ribE* deletion mutation, it seems unlikely that these additional mutations were contributing to the furazolidone resistance.

Table 7: *ribE* mutants

Strain	MIC changes	FICI	Mutation position	Mutation type	Mutation
E1	2-fold increase FZ 2-fold increase VAN	**0.625**	430486	In-frame insertion	TGCTGGCACCAAAG → TGCTGGCACCAAAG CTGGCACCAAAG
E2	**4-fold increase FZ** 2-fold increase VAN	**0.75**	430486 (1144409)	In-frame deletion (Missense in *fabH*)	TGCTGGCACCAAAG → TG (G → T)
E3	**4-fold increase FZ** no change VAN	**0.75**	430486 (4523535)	In-frame deletion (Missense in *yjhQ*)	TGCTGGCACCAAAG → TG (C → T)
E4	**4-fold increase FZ** 2-fold increase VAN	**0.625**	430486	In-frame deletion	TGCTGGCACCAAAG → TG
E5	**4-fold increase FZ** 2-fold increase VAN	**0.625**	430486 (1364641)	In-frame deletion (Missense in *ycjM*)	TGCTGGCACCAAAG → TG (C → A)

Mutations in *ribE* have already been associated with resistance to nitrofurans, specifically nitrofurantoin (Vervoort *et al.*, 2014). The *ribE* mutation reported by Vervoort and colleagues was a 12 bp in-frame deletion resulting in the removal of amino acids 131-134 (TKAG), located in the active site of RibE. This mutation resulted in at least a two-fold increase in nitrofurantoin MIC, as well as causing slower growth of this strain.

The deletion in strains E2, E3, E4 and E5 was a 12 bp in-frame deletion of amino acids 129-132 (AGTK) in the active site of RibE and includes two of the same amino acid residues as the mutation reported by Vervoort and colleagues. The insertion mutation in strain E1 is a 12 bp insertion that results in duplication of amino acids 129-132. The deletion strains in this study displayed an increased FZ MIC as well as a slower growth, very similar to the previously reported results. The amino acid sequence of RibE is shown in Figure 15.

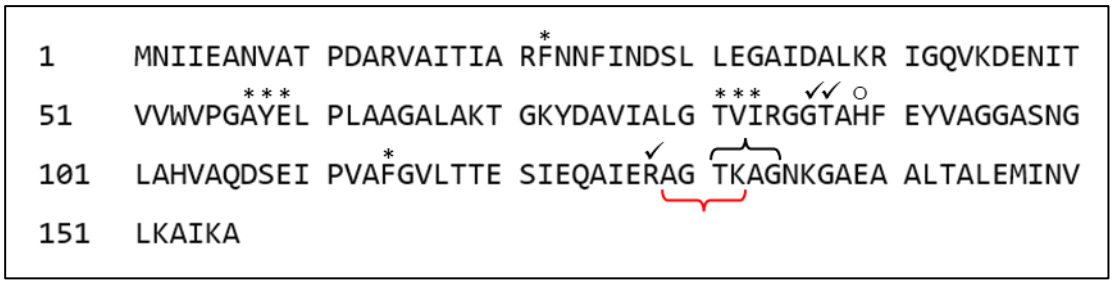

Figure 15: Amino acid sequence of RibE

The four residues deleted in the mutation found by Vervoort and colleagues are shown in black, the four residues either deleted or duplicated in mutants identified in this thesis are shown in red (Vervoort *et al.*, 2014). Indicated residues are involved in *binding to 5-amino-6-(D-ribitylamino)uracil, ✓binding to 1-deoxy-L-glycero-tetrulose 4-phosphate, °proton donor (Consortium, 2020).

3.2.8 Regulatory protease FtsH

The *ftsH* gene encodes an essential inner-membrane AAA ATPase and protease, FtsH, which is involved in protein turnover (Ogura & Wilkinson, 2001; Tomoyasu *et al.*, 1993). FtsH eliminates proteins in two different contexts; misfolded proteins are eliminated due to their incorrect structure, while correctly folded proteins are eliminated in order to regulate the amount of those proteins in the cell (Ito & Akiyama, 2005). The ATPase domain of FtsH unfolds protein substrates and transfers them into the protease domain, where they are broken into pieces. The ATPase activity of FtsH is required to unfold the substrate proteins in order to present the unfolded protein to the protease domain, where hydrolysis of the polypeptide chain can occur. FtsH can also dislodge protein substrates from the cytoplasmic membrane.

The *ftsH* gene is essential, meaning it is required for bacterial survival, due to its role in maintaining the proper LPS/phospholipids ratio by degrading LpxC, a deacetylase that catalyses the first committed step in the biosynthesis of LPS (Ogura *et al.*, 1999). The LPS and phospholipid biosynthesis pathways are connected because they both share the same precursor molecule, R-3-hydroxymyristoyl-ACP, which can act as the initial acyl donor for lipid A/LPS biosynthesis or can be elongated and act as an acyl donor in the formation of membrane phospholipids (Magnuson *et al.*, 1993; Ogura *et al.*, 1999). The LpxC deacetylase is short-lived, with a half-life of about 4 minutes, due to FtsH-catalysed degradation. If FtsH is dysfunctional, then the LpxC activity leads to a lethal overaccumulation of LPS. However, a suppressor mutation that upregulates the *fabZ*

gene, which encodes *R*-3-hydroxy-acyl-ACP dehydrase, enables the survival of *E. coli ftsH* null mutants (Ogura *et al.*, 1999). Upregulated FabZ channels more R-3-hydroxymyristoyl-ACP into the phospholipid biosynthesis pathway, preventing lethal overaccumulation of LPS.

Mutations in the *ftsH* gene were found in three of the mutants isolated in this thesis (Figure 16), and correlated to a collateral sensitivity phenotype, in which resistance to VAN increased 4-fold in all three mutants, while all three mutants displayed higher sensitivity to FZ (2 or 4-fold decrease in FZ MIC), and all displayed an additive interaction between FZ and VAN, showing the synergy between these two antibiotics was also affected. Because FtsH is essential, and no suppressor mutations were detected in the *fabZ* gene, it can be concluded that FtsH should retain some functionality in all the mutants. Strain K2659 has a frameshift mutation halfway along the gene, so it seems unlikely it has retained any function. It is possible an additional suppressor mutation was missed it this strain, this would need to be investigated further.

One of the mutants (K2660) also had an *insH1* insertion in the *waaR* gene. The *waaR* gene encodes an α-1,2 glucosyltransferase that is involved in the synthesis of the R-core of lipopolysaccharide (Shibayama *et al.*, 1999). As strain K2660 displays the same collateral sensitivity phenotype as the other two *ftsH* mutants, it seems likely the *ftsH* mutation is solely responsible for the resistance phenotype observed, whereas the *waaR* mutation could be compensatory given its role in LPS synthesis.

Table 8: *ftsH* mutants

Strain	MIC changes	FICI	Mutation position	Mutation type	Mutation
K2659	2-fold decrease FZ **4-fold increase VAN**	**1**	3319613	frameshift	CACCGACG AACAT → CT
K2660*	2-fold decrease FZ **4-fold increase VAN**	**0.516**	3318752	missense	G → A
K2664	**4-fold decrease FZ** **4-fold increase VAN**	**0.625**	3318881	frameshift	CAC → CC

*K2660 also has *insH1* inserted into the *waaR* gene

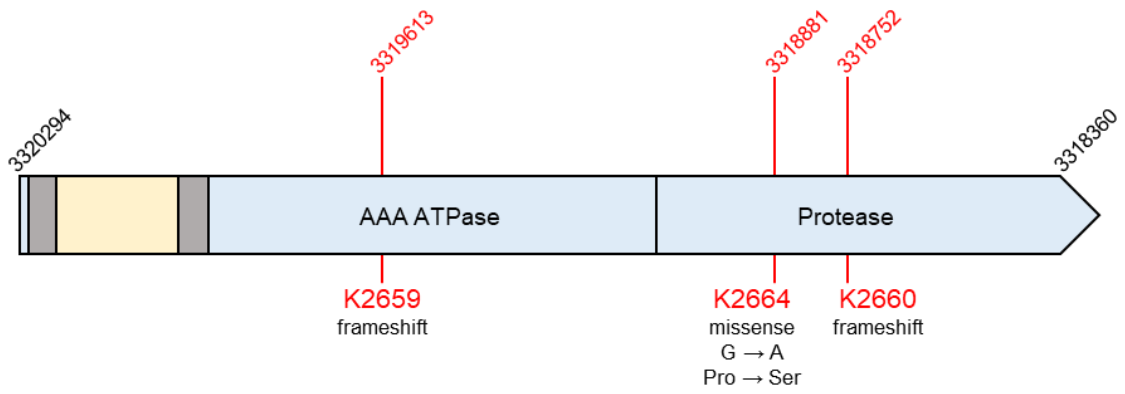

Figure 16: Position of *ftsH* mutations

The position of the mutations in strains K2659, K2660 and K2664 are shown within the CDS (coding sequence) of *ftsH*. The CDS regions are colour coded (blue: cytoplasm, grey: transmembrane, yellow: periplasm) according to the corresponding cellular location of the protein, and the AAA ATPase and protease regions are also shown (Ito & Akiyama, 2005). The genome positions are in accordance with the BW25113 reference genome. Diagram not to scale.

3.2.9 OPGs

Osmoregulated periplasmic glucans (OPGs) are located in the periplasm of many species of gram-negative bacteria. OPGs are highly branched oligosaccharides that consist of a glucose backbone substituted with other types of molecules. For example, in *E. coli* the glucose backbone is substituted by phosphoglycerol, phosphoethanolamine and succinyl residues (Bohin & Lacroix, 2006; Bontemps-Gallo *et al.*, 2013; Kennedy *et al.*, 1976).

One function of OPGs is in osmoprotection. OPGs are osmotically regulated in *E. coli* and are most prevalent in low-osmolarity media (Lacroix *et al.*, 1991; Rumley *et al.*, 1992). In addition to osmoprotection, OPGs also have functions relating to cell division, structure, and cell signalling (Fiedler & Rotering, 1988; Kennedy, 1982; Murakami *et al.*, 2021).

The *opgGH* operon in *E. coli* encodes OpgG and OpgH, which are osmoregulated periplasmic glucans biosynthesis proteins G and H, respectively. These proteins are responsible for the polymerisation of the glucose backbone of OPGs, and both proteins are required (Lacroix *et al.*, 1991; Loubens *et al.*, 1993). In addition, *opgB* is required

for the substitution of phosphoglycerol residues (Jackson *et al.*, 1984; Lanfroy & Bohin, 1993), and *opgC* for substitution of succinyl residues (Lacroix *et al.*, 1999).

One mutant was found to have a frameshift mutation in the *opgG* gene, shown in Figure 17. This mutant had no change in FZ MIC, and a four-fold increase in VAN MIC as compared to the parental strain (Table 9). The interaction between FZ and VAN remained synergistic in this strain.

Table 9: *opgG* mutant

Strain	MIC changes	FICI	Mutation position	Mutation type	Mutation
K2657	No change FZ **4-fold increase VAN**	0.375	1105354	frameshift	CAAAGAGT → CAAAAGAGT

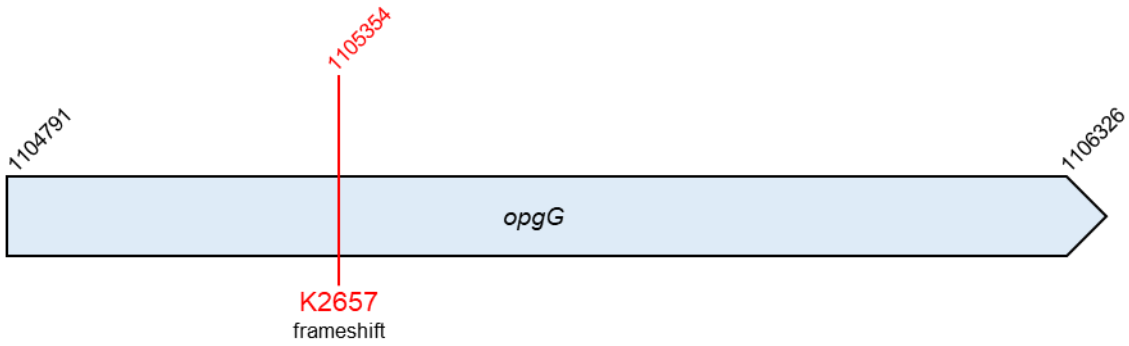

Figure 17: Position of strain K2657 frameshift mutation in *opgG* CDS

The genome positions are in accordance with the BW25113 reference genome. Diagram not to scale.

Murakami and colleagues have previously investigated knockouts within the *opgGH* operon, and found that single deletion of either *opgG* or *opgH*, as well as double deletion, increases *E. coli* virulence against silkworms, as well as resistance to silkworm antimicrobial peptides, vancomycin, levofloxacin, and tetracycline (Murakami *et al.*, 2021). This strongly suggests that the frameshift mutation found in *opgG* in strain K2657 is responsible for the observed VAN resistance.

In addition, Murakami and colleagues investigated the mechanism behind the resistance. Colonic acid production has previously been shown to increase due to inactivation of *opgH* (Ebel *et al.*, 1997) and in the *opgGH* knockout. Colonic acid is involved in resistance of *E. coli* to antibiotics and is a survival mechanism for hostile environments (Laubacher & Ades, 2008; Sailer *et al.*, 2003). The *opgGH* knockout was also found to have altered expression of the *evgS/evgA* two-component system, which is also involved in antibiotic resistance (Itou *et al.*, 2009). In addition, the *envZ/ompR* two-component system that senses osmolarity and temperature, and controls the ratio of larger vs. smaller porins, OmpF and OmpC, interacts genetically with *opgGH* (Fiedler & Rotering, 1988).

These three potential mechanisms were investigated by Murakami and colleagues. However, the virulence and resistance of the *opgGH* knockout were unaffected in a colonic acid-negative background, an *envZ/ompR*-null background, and an *evgS*-null background. Therefore, the mechanism by which the *opgGH* knockout causes vancomycin resistance and increased virulence against silkworms remained unresolved (Murakami *et al.*, 2021).

3.2.10 RNA polymerase subunits

The *E. coli* RNA polymerase (RNAP) holoenzyme is a multisubunit protein complex, with a core enzyme responsible for catalysing transcription of bacterial DNA into RNA. This core enzyme is composed of five subunits, two α subunits, as well as the β, β', and ω subunits. The holoenzyme (active form) of RNAP is formed when the core enzyme binds to a sigma factor, which is responsible for binding promotors and initiating transcription (Sutherland *et al.*, 2018).

The β' subunit of RNAP is encoded by *rpoC*, an essential gene (Baba *et al.*, 2006; Ovchinnikov *et al.*, 1982).

Strain K2658 was found to have a missense mutation in the *rpoC* gene (Figure 18). This strain had minor phenotypic changes, with only a two-fold increase in VAN, and no change in FZ MIC (Table 10). The FICI did increase to 0.5, but this is still classed as a synergistic interaction between FZ and VAN.

Table 10: *rpoC* mutant

Strain	MIC changes	FICI	Mutation position	Mutation type	Mutation
K2658	No change FZ 2-fold increase VAN	0.5	4178876	Missense	A → G

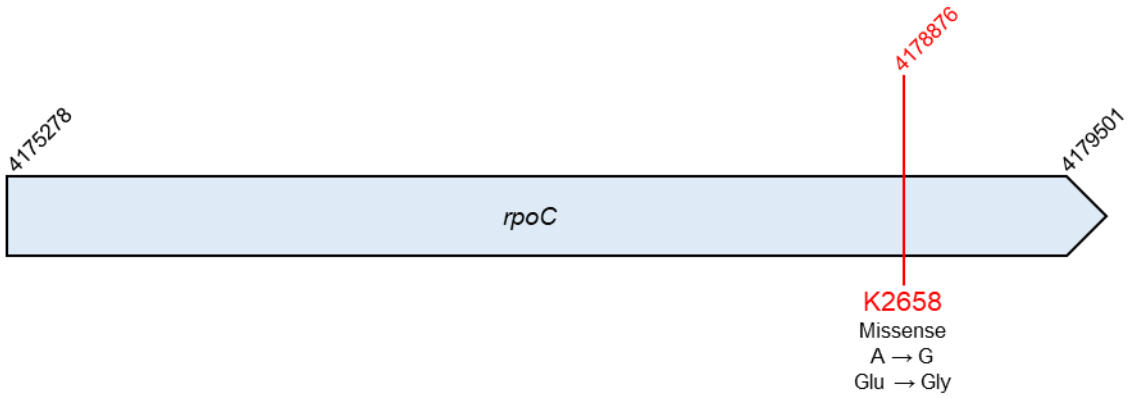

Figure 18: Position of strain K2658 missense mutation in *rpoC* CDS

The genome positions are in accordance with the BW25113 reference genome. Diagram not to scale.

3.2.11 ECA biosynthesis

Enterobacterial common antigen, or ECA, is a carbohydrate antigen (which causes immune activation and production of cognate antibodies), conserved among *Enterobacterales*. ECA is present in three different forms; i) linked to LPS (ECA_{LPS}), ii) linked to diacylglycerol through phosphodiester linkage (ECA_{PG}), and iii) cyclic, found in the periplasm (ECA_{CYC}) (Kuhn *et al.*, 1988; Rai *et al.*, 2020).

ECA plays a role in the pathogenicity of *Enterobacterales* and its biosynthesis pathway interacts with those of the O-antigen and peptidoglycan (Rai *et al.*, 2020). Cyclic ECA plays a role in maintaining the outer membrane permeability barrier (Mitchell *et al.*, 2018). Genes responsible for ECA biosynthesis are located in the *wec* operon.

Strain K2661 was found to have a frameshift mutation in the *wecC* gene (Figure 19), which encodes UDP-N-acetyl-D-mannosamine dehydrogenase, one of the enzymes responsible for the synthesis of ECA (Meier-Dieter *et al.*, 1990). This strain had no

change in FZ MIC, a two-fold increase in VAN MIC, and has retained a FZ – VAN interaction that was synergistic, as shown by the FICI value of 0.375 (Table 11). Overall, strain K2661 had no major phenotypic changes.

Table 11: *wecC* mutant

Strain	MIC changes	FICI	Mutation position	Mutation type	Mutation
K2661	No change FZ 2-fold increase VAN	0.375	3964946	Frameshift	GAAAAAAGGC → GAAAAAGGC

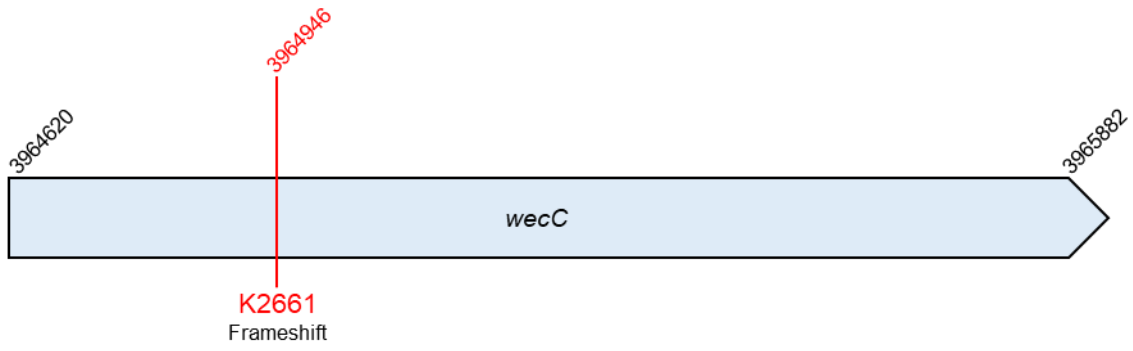

Figure 19: Position of strain K2661 frameshift mutation in *wecC* CDS

The genome positions are in accordance with the BW25113 reference genome. Diagram not to scale.

There has been a previous link found between *wecC* mutations and vancomycin resistance in *E. coli*. Jiang and colleagues found that deletion of the *wecC* gene partially restored resistance to VAN in *tol-pal* strains (Jiang *et al.*, 2020). The *tol-pal* strains had a compromised outer membrane, which made them more susceptible to VAN in comparison to the wild-type parent. It was concluded that loss of function in the biosynthesis of ECA restored the OM barrier function in strains lacking the Tol-Pal complex.

Given that the *wecC* frameshift was the only mutation identified in the K2661 strain, the outer membrane was not leaky. Therefore, restoring outer membrane function cannot

be said to be the mechanism of increasing VAN resistance, as the outer membrane function was intact to begin with. Also, in the study by Jiang *et al.* (2020), *wecC* mutation restored the resistance back to wild type, whereas for the mutation isolated in this thesis the MIC increased to a level higher than the wild type.

3.2.12 Lipoprotein NlpI

Bacterial lipoproteins are membrane proteins comprising polypeptide and covalently attached lipid. Bacterial lipoprotein synthesis involves exporting the prolipoproteins through the cytoplasmic membrane, which is where the proteins undergo lipid-modification (Zückert, 2014), followed by retention in this membrane or trafficking to the outer membrane. Lipoproteins are involved in a variety of different roles and functions (Kovacs-Simon *et al.*, 2011; Zückert, 2014) including envelope stability, in the synthesis of peptidoglycan (Egan *et al.*, 2014), cell division, conjugation, signal transduction, sporulation, nutrient acquisition, as well as in the transport and folding of proteins. In addition, lipoproteins are also involved in pathogenicity, being involved in invasion, adhesion, immune evasion, and colonisation.

Bacterial lipoprotein NlpI is involved in cell division (Ohara *et al.*, 1999; Tao *et al.*, 2015). NlpI has also been linked to the ability to adhere to and invade intestinal epithelial cells (Barnich *et al.*, 2004). Overexpression of *nlpI* has been linked to a reduction in the amount of bacterial extracellular DNA in *E. coli*, which is a structural component of biofilms (Sanchez-Torres *et al.*, 2010). NlpI also plays a role in peptidoglycan biosynthesis (Banzhaf *et al.*, 2020). In addition, a hypervesiculation phenotype is associated with deletion of *nlpI* in *E. coli* (Schwechheimer *et al.*, 2015). The increased production of outer membrane vesicles in this deletion mutant was also associated with a reduction in the number of outer membrane – peptidoglycan covalent crosslinks. It was also found that NlpI regulates PBP4 (penicillin-binding protein 4) and peptidoglycan endopeptidase MepS (Schwechheimer *et al.*, 2015; Singh *et al.*, 2015).

Strain K2655 was found to have a nonsense mutation in the *nlpI* gene, as shown in Figure 20. This strain had a two-fold decrease in FZ MIC, and a two-fold increase in VAN MIC and had a loss of synergy between FZ and VAN, shown by the FICI value of 0.531, as shown in Table 12.

Table 12: *nlpI* mutant

Strain	MIC changes	FICI	Mutation position	Mutation type	Mutation
K2655	2-fold decrease FZ 2-fold increase VAN	**0.531**	3302181	Stop gained	G → A

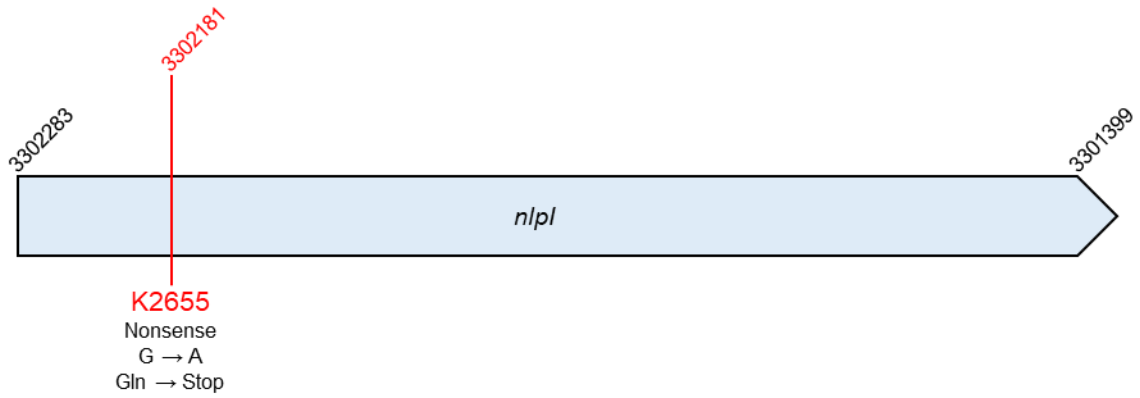

Figure 20: Position of strain K2655 nonsense mutation in *nlpI* CDS

The genome positions are in accordance with the BW25113 reference genome. Diagram not to scale.

3.2.13 Lipoprotein Lpp

Lpp is an α-helical lipoprotein and is the most abundant protein in *E. coli*, with over one million copies per cell. Lpp is responsible for attaching the outer membrane (OM) to the peptidoglycan (PG). The N-terminus of Lpp is anchored in the periplasm-facing phospholipid leaflet of the OM, while the C-terminus is attached to the PG. Lpp affects cell envelope mechanical stiffness by covalently connecting the OM to the PG, and by controlling the width of the periplasmic space (Asmar *et al.*, 2017; Mathelié-Guinlet *et al.*, 2020).

The OM-PG link, as well as the length of Lpp, is important for the transmission of stress signals from the outer membrane to the IM (inner membrane) (Mathelié-Guinlet *et al.*, 2020).

Unlike all other strains which were isolated from the FZ-VAN combination plates, K2673 was the only strain isolated from a VAN plate (and was the only resistant colony that formed on the VAN plates).

As shown in Table 13, K2673 had a 63 bp in-frame deletion in the *lpp* gene and demonstrated a 4-fold increase in VAN MIC, no change in FZ MIC, with FZ and VAN remaining synergistic.

Table 13: *lpp* mutant

Strain	MIC changes	FICI	Mutation position	Mutation type
K2673	No change FZ **4-fold increase VAN**	0.25	1751783-1751845	63bp in-frame deletion

It has been reported that increasing the length of Lpp makes *E. coli* more susceptible to VAN (Mathelié-Guinlet *et al.*, 2020). This is in agreement with observations made in this thesis, where a decrease in the length of Lpp leads to increased resistance to VAN.

3.2.14 Cell envelope associated mutations

Many of the mutations identified in this chapter were associated with the cell envelope of *E. coli*, namely those affecting lipoproteins (*nlpI* and *lpp*), OPG biosynthesis (*opgG*), ECA biosynthesis (*wecC*), and membrane bound FtsH (*ftsH*) (Figure 21). Interestingly all these mutations were associated with an increase in VAN MIC, perhaps unsurprising given that VAN targets the cell wall of bacteria and that its entry into the periplasm is limited by the LPS leaflet of the outer membrane.

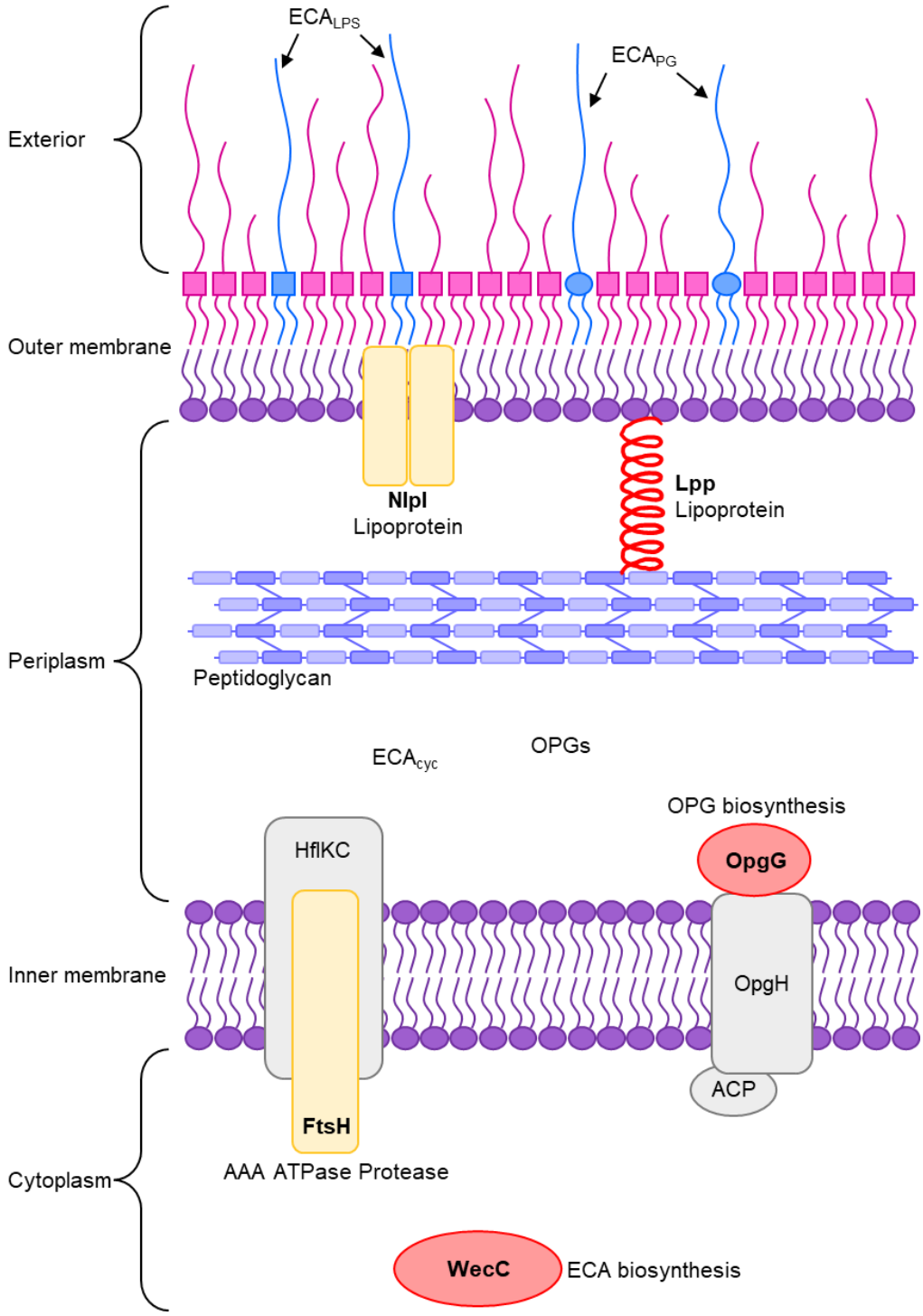

Figure 21: Mutations associated with the cell envelope

Selected proteins identified in this chapter (indicated in bold) associated with the cell envelope, and proteins they complex to, are shown. Mutations affecting proteins shown in red were linked to higher VAN MIC. Mutations affecting proteins shown in yellow were linked to collateral sensitivity (higher VAN MIC and lower FZ MIC). ECA: enterobacterial common antigen, ECA_{cyc}: cyclic ECA, ECA_{PG}: ECA attached to diacylgycerol through phosphodiester linkage, ECA_{LPS}: ECA attached to LPS. OPGs: osmoregulated periplasmic glucans. (Banzhaf *et al.*, 2020; Bontemps-Gallo *et al.*, 2013; Ito & Akiyama, 2005; Mathelié-Guinlet *et al.*, 2020; Rai *et al.*, 2020)

3.3 Discussion

Investigating and understanding bacterial mechanisms of resistance is crucial in the struggle to develop new antimicrobial treatments. Improved understanding of resistance mechanisms can potentially provide information on crucial pathways and processes or bacterial resistance mechanisms that can be targeted in future antibacterial drug development efforts.

A range of different mutations were identified in the selection for FZ – VAN resistant mutants. A few of the identified genes appeared more than once, increasing the likelihood that they are important in the resistance mechanisms.

Interestingly, many of the mutations identified occurred in essential genes. Thirteen mutant strains had changes in the essential genes *ribB*, *ribE*, *ftsH*, and *rpoC*. Mutations in essential genes are often not very favourable as they may affect a function of the gene, impacting an essential process within the cell. Mutating a non-essential gene to gain resistance is a lot more likely to occur, as the gene does not have to remain functional. With essential genes however, a mutation must alter the gene function to grant resistance, but still retain enough functionality for the cell to remain viable, or must acquire a suppressor mutation, which counteracts the lethal effects of the original mutation. The high proportion of essential gene mutations indicates that resistance does not easily arise to the FZ – VAN combination, a promising finding for its potential as a treatment option for gram-negative bacterial infections.

The genes identified in this chapter can be linked to the observed resistance identified with varying degrees of certainty, depending on whether mutations in a gene appeared multiple times, increasing the chance that the gene is responsible for resistance, or whether there has been previously observed resistance associated with that gene.

Knockout of the *opgG* gene has been associated with increased resistance to VAN, acting through an unknown mechanism (Murakami *et al.*, 2021). This means it is very likely that the frameshift *opgG* mutation identified in strain K2657 is responsible for the four-fold increase in VAN MIC that was observed.

Mutations in the *ribE* gene have already been linked to nitrofuran resistance (Vervoort *et al.*, 2014). The previously identified in-frame deletion overlaps with the in-frame deletion found in strains E2, E3, E4 and E5 by two amino acids, and the insertion

mutation in strain E1 is also in this area of the gene. Because the same area of the gene has been affected, it is likely that similar loss of functions occurred, and therefore that these *ribE* mutations are responsible for the increase in FZ resistance.

The *ribB* gene is a likely candidate for FZ resistance, as it is part of the riboflavin biosynthesis pathway, which has already been implicated in increasing FZ resistance through previously identified mutations in *ribE* (Vervoort *et al.*, 2014). Because both RibE and RibB act in the same biosynthesis pathway, it is also likely that both cause FZ resistance through their impact on this pathway. In addition, mutations upstream of *ribB* occurred in four separate mutants, B1, B2, B3 and B4, resulting in either a large four-fold increase in FZ MIC, a loss of synergy between FZ and VAN, or both. The presence of multiple mutations associated with the *ribB* gene increases the likelihood it is responsible for the observed increase in FZ resistance.

The *ftsH* gene mutations occurred on three separate occasions. All three of the FtsH mutants had a four-fold increase in VAN resistance, and a loss of synergy between FZ and VAN. In addition, all three mutants displayed a collateral sensitivity phenotype, where the MICs to FZ were lowered, either 2-fold or 4-fold. Because FtsH is a protease responsible for regulating the amounts of many different proteins, predicting how a partial loss of function of FtsH results in a collateral sensitivity phenotype is difficult. It is easier to explain the effect of these mutations on susceptibility to VAN, because FtsH is responsible for maintaining the ratio of LPS and phospholipids in the outer membrane of *E. coli*. It is possible that the *ftsH* mutations affected the outer membrane permeability, which might be linked to the observed increase in VAN MIC.

The *lpp* gene was associated with increasing VAN resistance, as VAN MIC increased 4-fold in strain K2673, which had a 63-bp deletion in the *lpp* gene. In addition, changing the length of Lpp has been previously associated with changing VAN susceptibility. Specifically, increasing the length of Lpp, or complete removal of Lpp, was shown to result in greater sensitivity to VAN (Mathelié-Guinlet *et al.*, 2020).

Mutation in the *nlpI* gene was associated with resistance to the FZ – VAN combination. Strain K2655, which had a nonsense mutation in *nlpI*, displayed a loss of synergy between FZ and VAN, in addition to a 2-fold increase in VAN MIC, and a 2-fold decrease in FZ MIC. The nonsense mutation, located at codon 35, very likely causes a loss of function of NlpI.

Multiple different phenotypes have been reported for the *nlpI* knockout mutant of *E. coli*, including a hypervesiculation colony phenotype (Schwechheimer *et al.*, 2015). The increased production of outer membrane vesicles in this deletion mutant was also reported, and it was associated with a reduction in the number of outer membrane – peptidoglycan covalent crosslinks. The mechanism of vancomycin lethality is through peptidoglycan, so it is possible that the *nlpI* mutation affecting the outer membrane is responsible for somewhat decreased access to the VAN target, resulting in the two-fold increase in the MIC. There has been an additional reported link between NlpI and VAN resistance. In a Δ*yhcB* mutant, which has loss of envelope stability, increased cell permeability and dysregulated control of cell size, knockout of *nlpI* was associated with restoring VAN resistance (Goodall *et al.*, 2021).

wecC is a gene candidate for increased VAN resistance. While strain K2661 had no major phenotypic changes, there was a two-fold increase in the MIC of VAN. In addition, there has been previous research that linked deletion of *wecC* to restored wild-type resistance to VAN in compromised outer membrane *tol-pal* strains which were more susceptible to VAN than a wild-type parent (Jiang *et al.*, 2020). The outer membrane is assumed to be normal in strain K2661 given that the *tol-pal* system is not mutated.

Mutation of the *rpoC* gene was linked to increased VAN resistance. Strain K2658 had a 2-fold increase in VAN MIC. *rpoC* is an essential gene that encodes one of the core subunits of RNA polymerase (RNAP), the enzyme responsible for transcription. It is possible that the missense mutation in *rpoC* in K2658 resulted in the increase in VAN resistance. Mutations in *rpoC* have been previously associated with VAN resistance in *Staphylococcus aureus* (Matsuo *et al.*, 2015).

In all cases, further experiments are required, including complementation and knockout mutations (where possible), to determine whether the loss of function or other change in function of a particular gene is responsible for the observed resistance. Furthermore, extended investigation into the resistance mechanisms is warranted to gain understanding of how specific gene mutations result in resistance.

4 Investigating the link between mutations in the riboflavin biosynthesis pathway and furazolidone resistance

4.1 Introduction

Riboflavin, also known as vitamin B_2, is a precursor for FMN and FAD. FMN and FAD are essential coenzymes used in a variety of redox reactions involved in the metabolism of proteins, carbohydrates, lipids, and ketone bodies (Averianova *et al.*, 2020). In *E. coli*, the ability to synthesise flavins is essential because *E. coli* does not import flavins (Hemberger *et al.*, 2011; Vogl *et al.*, 2007), instead relying on the correct functioning of the riboflavin biosynthesis pathway, shown in Figure 13, as the sole source of flavins.

Of the *E. coli* mutants selected for increased resistance to the FZ-VAN combination, those containing mutations in the riboflavin biosynthesis genes were the most numerous and were therefore selected for further investigation. These were the strains with mutations in either the *ribB* or *ribE* genes that demonstrated up to a 4-fold increased resistance to FZ.

The B1, B2, B3 and B4 strains had mutations in the *ribB* gene. B1 and B4 had a 2-fold increase in FZ MIC as compared to the parental strain and both had one-base substitution mutations in the 5' UTR. B2 and B3 both had a 4-fold increase in FZ MIC, and both had an insertion sequence in the promoter region. The E1, E2, E3, E4 and E5 strains had mutations in the *ribE* gene. E1 had a 2-fold increase in FZ MIC as compared to the parental strain and had an in-frame insertion in *ribE*. E2, E3, E4 and E5 had an identical in-frame deletion mutation in *ribE*, and all had a 4-fold increase in FZ MIC. (E2, E3 and E5 had additional one-base missense mutations in additional genes as compared to the parental strain).

Mutations in *ribE* have been previously associated with resistance to nitrofurans, specifically nitrofurantoin (Vervoort *et al.*, 2014), however mutations in *ribB* have not been previously associated with nitrofuran resistance. Confirming that mutations in *ribB* are linked to increased nitrofuran resistance would allow for *ribB* to be including in genomic screening processes to predict antibiotic susceptibility and would allow for better resistance identification and improved selection of antibiotics for treatment.

The *ribB* and *ribE* mutants were further investigated experimentally. This involved characterising the growth rates to assess the effect of the mutations on the fitness of the mutant strains, as well as dose-response curves to FZ. Secondly, the *ribB/ribE* mutants were tested to confirm that the effect of the identified mutations on FZ MIC was due to

the loss of function of the mutated genes, rather than indirect effect on other genes. This was done through complementation with plasmid-expressed wild-type *ribB* or *ribE*.

Finally, the mechanism of resistance was investigated in selected *ribB* and *ribE* mutants. The prediction behind the FZ resistance mechanism is that the mutations in *ribB*/*ribE* lead to less functionality of these enzymes, resulting in an impact to the riboflavin biosynthesis pathway, and so less FMN and FAD being produced. Because FMN and FAD are essential cofactors required for the functioning of the NfsA and NfsB nitroreductases, it is predicted that these nitroreductases will have reduced activity. Reduced activity of the nitroreductases was hypothesised to lead to increased FZ resistance, because FZ is a pro-drug which must be activated by nitroreductases (Vervoort *et al.*, 2014).

Nitroreductase assays were conducted on the selected mutants and their associated complemented strains to confirm that complementation restored nitroreductase activity. The selected mutants were also supplemented with riboflavin, which is downstream of the reactions catalysed by RibB and RibE in the riboflavin biosynthesis pathway, to check if this reverted the effects of the mutations. Double knockout mutants of the oxygen insensitive nitroreductases NfsA and NfsB were constructed to check if the resistance mechanism was acting solely through affecting the activity of these nitroreductases. Finally, overexpression of the FZ-activating nitroreductase NfsB in the selected mutant strains was conducted, to examine the effect of additional NfsB in the mutant vs. parental strains on FZ resistance.

4.2 Results

4.2.1 Growth rates and FZ dose-response curves

It was observed that some of the *ribB* and *ribE* mutants took noticeably longer to grow to full-density cultures than the parental strain. This is to be expected, as both *ribB* and *ribE* are essential genes, and mutations in essential genes are more likely to result in fitness costs. The growth curves over 48 hrs for these strains are shown in Figure 22.

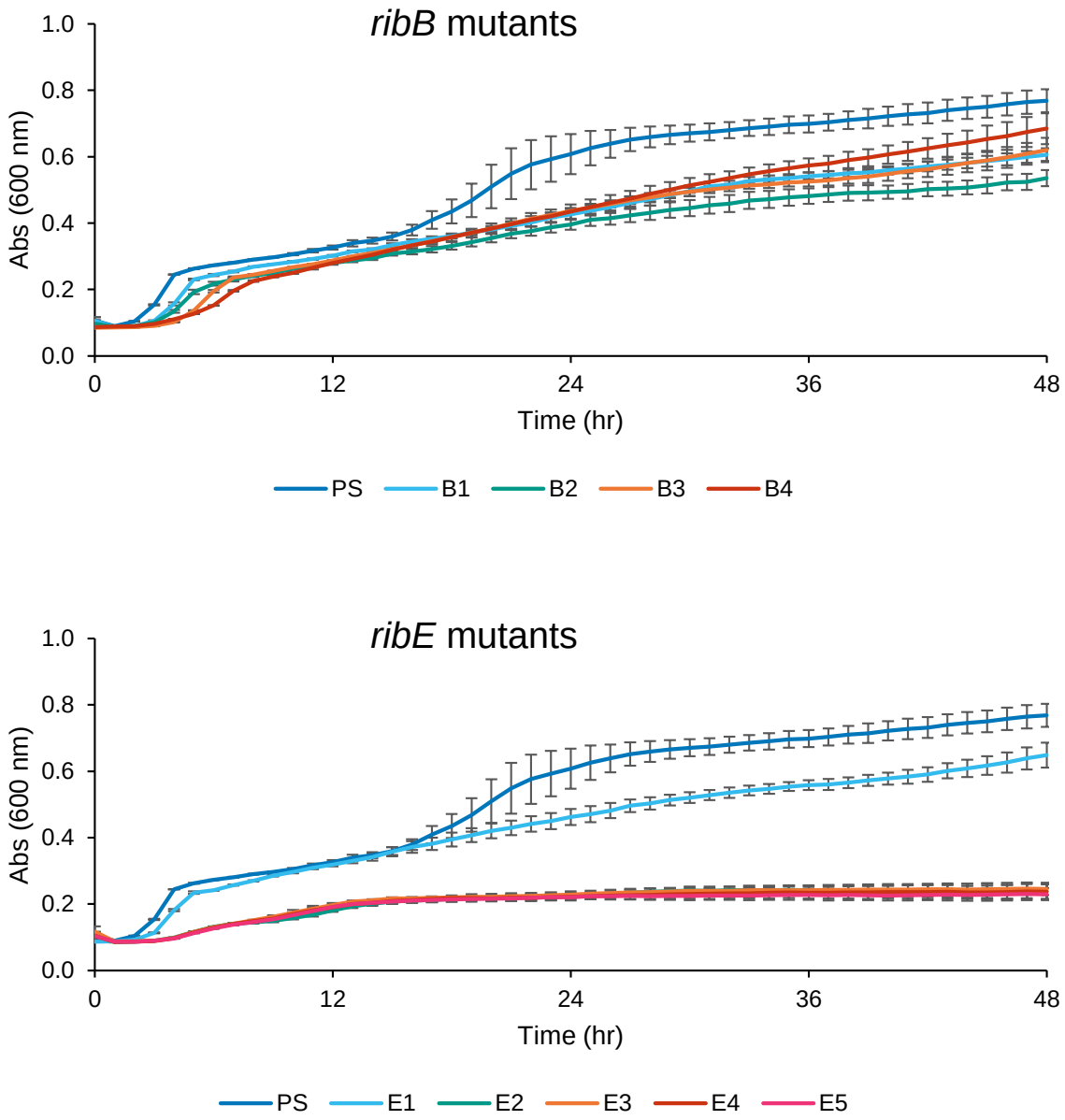

Figure 22: Growth curves for the *ribB* and *ribE* mutants

Absorbance at 600 nm was measured every hour for 48 hrs. Data shown is the mean ± standard error of the mean for three technical replicates.

All strains grew slower than the parental strain and could not reach the densities of the parental strain in the stationary phase. Growth was especially stunted in the *ribE* deletion mutants (E2, E3, E4, E5), which entered the stationary phase at a density of only approximately 0.2 OD_{600}.

In addition, the FZ dose-response curves for these strains were determined (Figure 23). Interestingly, the mutants that showed very poor growth as compared to the parental strain (strains E2, E3, E4, and E5) grew substantially better at low concentrations of FZ, as compared to growth without FZ.

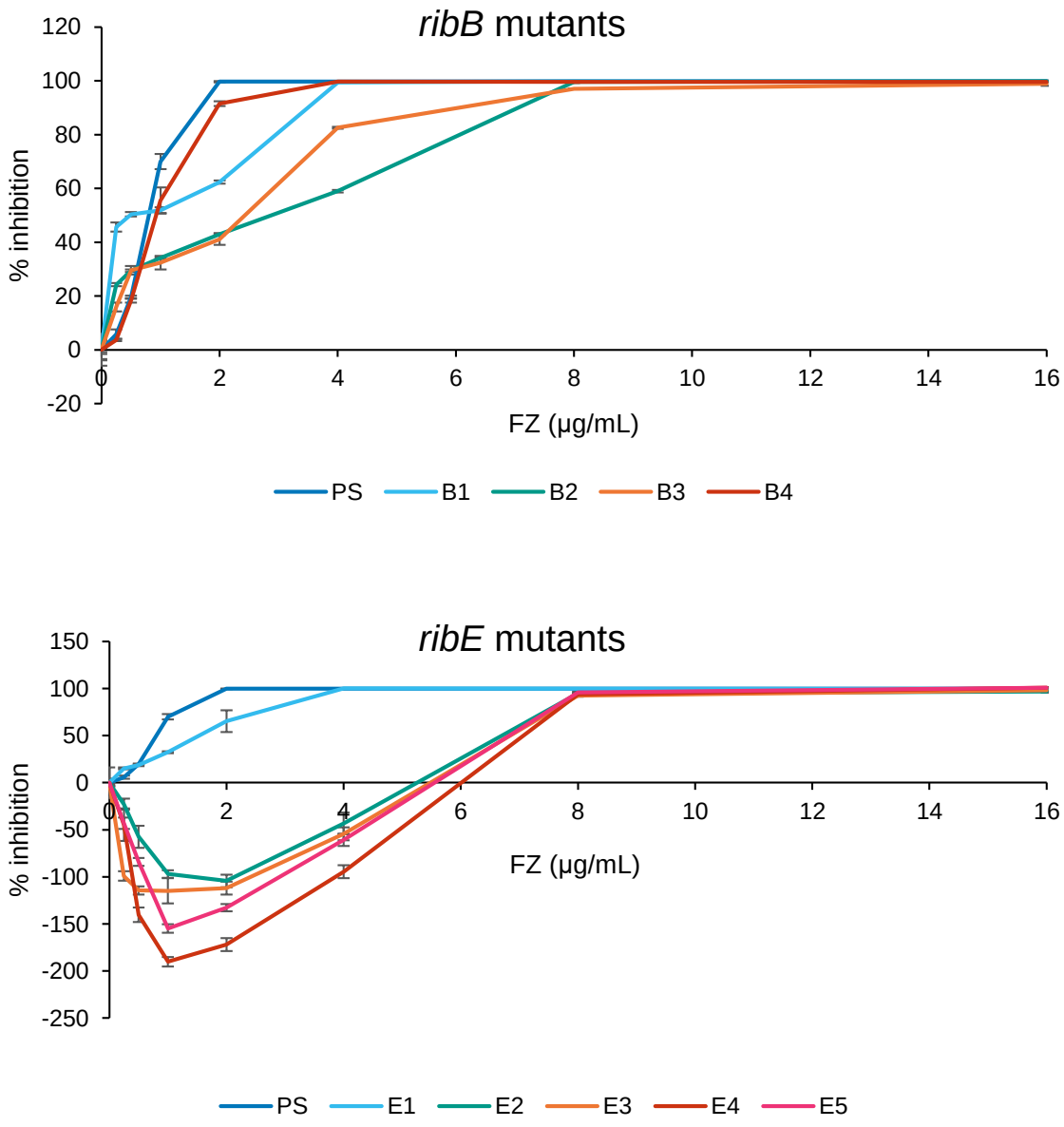

Figure 23: Dose response curves for the *ribB* and *ribE* mutants

Percent inhibition is shown at 18 hours growth. Zero percent inhibition is taken as the growth at zero FZ. Data shown is the mean of three technical replicates ± standard error of the mean.

Overall, these results show that a fitness cost is associated with all the *ribB* and *ribE* mutations, but especially with the *ribE* deletion mutants. Having a fitness cost is expected, due to both *ribB* and *ribE* being essential genes, however what is more surprising is that the *ribE* deletion mutants grow significantly better at low concentrations of FZ compared to no FZ. This means that subinhibitory concentrations of FZ partially reverse the fitness cost associated with the *ribE* deletion mutation. Interestingly, the *ribE* deletion mutants grew best at 1-2 μg/mL of FZ, and the selection concentration was 2 μg/mL FZ, meaning that the selection conditions were favourable for the growth of these strains.

4.2.2 Complementation with RibB or RibE

The *ribB/ribE* strains were tested to confirm that the *ribB* or *ribE* gene was responsible for the observed FZ resistance. This was done by complementing with the fully functional gene expressed from plasmids pCA24N::*ribB* or pCA24N::*ribE*. Expression of RibB/RibE was induced through the addition of 0.1 mM IPTG. Changes to VAN MIC were also investigated, as the strains were originally selected for as resistant to the FZ-VAN combination. MICs were determined *via* broth microdilution.

None of the strains had large changes in VAN MIC upon complementation (Table 14). This was as expected, as none of these strains had major VAN resistance to begin with, and the *ribB/ribE* mutations are expected to be causing FZ resistance only. All the complemented strains had a VAN MIC of 256 μg/mL, which corresponded to either no change or a 2-fold decrease.

The complemented *ribE* mutants all had an FZ MIC of 2 μg/mL, and the complemented *ribB* mutants and complemented parental strains had a FZ MIC of 1 μg/mL. This was a 2-fold decrease for the parental strains, as well as for the E1 mutant. All other strains had at least a 4-fold decrease. Therefore, all the mutants had a major decrease in MIC upon complementation with either functional *ribB* or *ribE* except for E1, which had only a 2-fold decrease along with both complemented parental strains. E1 was one of the mutants with only a 2-fold increase in MIC as compared to the parental strain, so the RibE in this strain may be more functional than in the other *ribE* mutants, and therefore the difference between the uncomplemented and complemented E1 mutant is smaller than in more severe mutants.

Table 14: MIC testing of complemented *ribB/ribE* mutants

Strain	FZ MIC* (µg/mL)	Decrease in FZ MIC	VAN MIC* (µg/mL)	Decrease in VAN MIC
E1 + *ribE*	2 (4)	2-fold	256 (512)	2-fold
E2 + *ribE*	2 (8)	4-fold	256 (512)	2-fold
E3 + *ribE*	2 (8)	4-fold	256 (256)	No change
E4 + *ribE*	2 (8)	4-fold	256 (512)	2-fold
E5 + *ribE*	2 (8)	4-fold	256 (512)	2-fold
PS + *ribE*	1 (2)	2-fold	256 (256)	No change
B1 + *ribB*	1 (4)	4-fold	256 (256)	No change
B2 + *ribB*	1 (8)	8-fold	256 (256)	No change
B3 + *ribB*	1 (8)	8-fold	256 (512)	2-fold
B4 + *ribB*	1 (4)	4-fold	256 (512)	2-fold
PS + *ribB*	1 (2)	2-fold	256 (256)	No change

*MICs for the corresponding untransformed strains are shown in brackets.

Complementation also significantly improved the growth of the E2, E3, E4, E5, and B3 mutants, while it increased growth in B1 and B2 in the early exponential phase (Figure 24). Growth was decreased in both the parental strain and E1. The decrease in growth of the parental strain was not unexpected due to the potentially demanding energy requirements to reproduce the plasmid and/or express the unneeded RibB or RibE. E1 is also predicted to have more functional RibE than the other *ribE* mutants due to its lower MIC for FZ, so the effort to express more RibE is potentially greater than the gain from more functional RibE.

Complementation with functional RibB or RibE caused a decrease in FZ MIC as well as improved the growth of the mutants. This confirms that the *ribB*/*ribE* mutations are responsible for the FZ resistance and slow growth in these mutants.

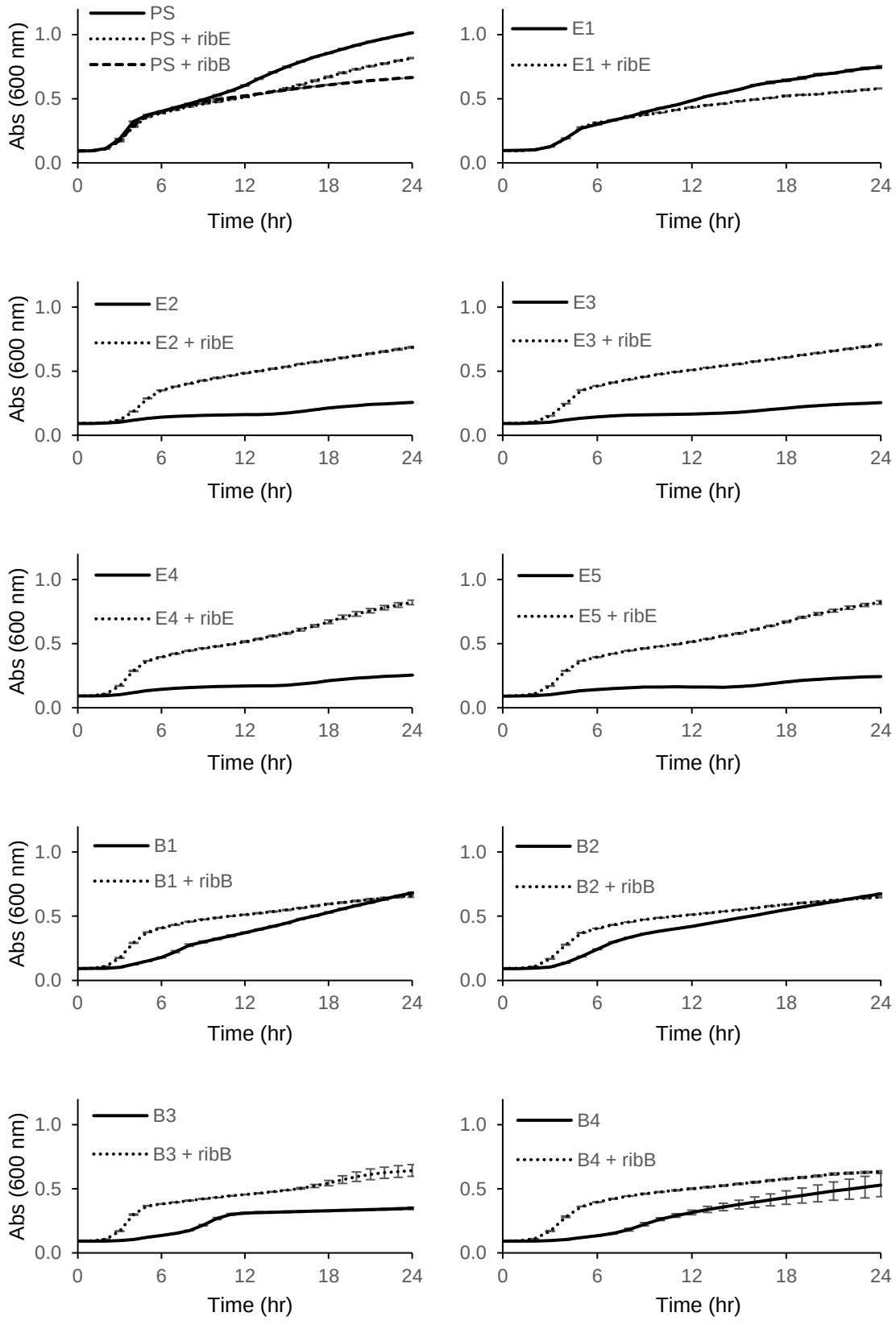

Figure 24: Growth curves for the complemented *ribB*/*ribE* mutants

Absorbance at 600 nm was measured every hour for 24 hr. Each graph shows the growth curve of the original and complemented strain. Data shown is the mean ± standard error of the mean of three technical replicates.

4.2.3 Nitroreductase assays

Four mutants were chosen for further investigations, two *ribE* and two *ribB*. Four of the five *ribE* mutants had identical deletion mutations. E4 was subsequently chosen for further investigations, as it was the only strain with a *ribE* deletion that did not contain any additional mutations. E1 had a different *ribE* mutation, an insertion, and so was chosen as the other *ribE* strain. In addition to E1 and E4, B2 and B3 were chosen from the *ribB* mutants as they had a larger resistance increase in MIC to FZ (four-fold), whereas B1 and B4 only had a two-fold increase.

Nitroreductase assays were conducted on the chosen mutants as well as their complemented strains. The nitroreductase assays were conducted to assess the nitroreductase ability by measuring the change in absorbance associated with FZ. The cells were lysed, and the cell lysate/cell-free extract (CFE) was combined with 0.1 mM FZ and 0.1 mM NADPH, in 50 mM Tris-HCl buffer (pH 7.4). Absorbance was measured at 400 nm every minute for 12 hrs. 400 nm is the maximum absorbance for furazolidone, and NADPH does not absorb at this wavelength.

Each experiment was carried out three times independently, and the rate of reaction (decrease in absorbance units (AU) per minute) was calculated for the first 10 minutes of each experiment. The mean and standard deviation of the three experiments is shown in Table 15. Representative graphs showing one of the three assays for each mutant type are shown in Figure 25.

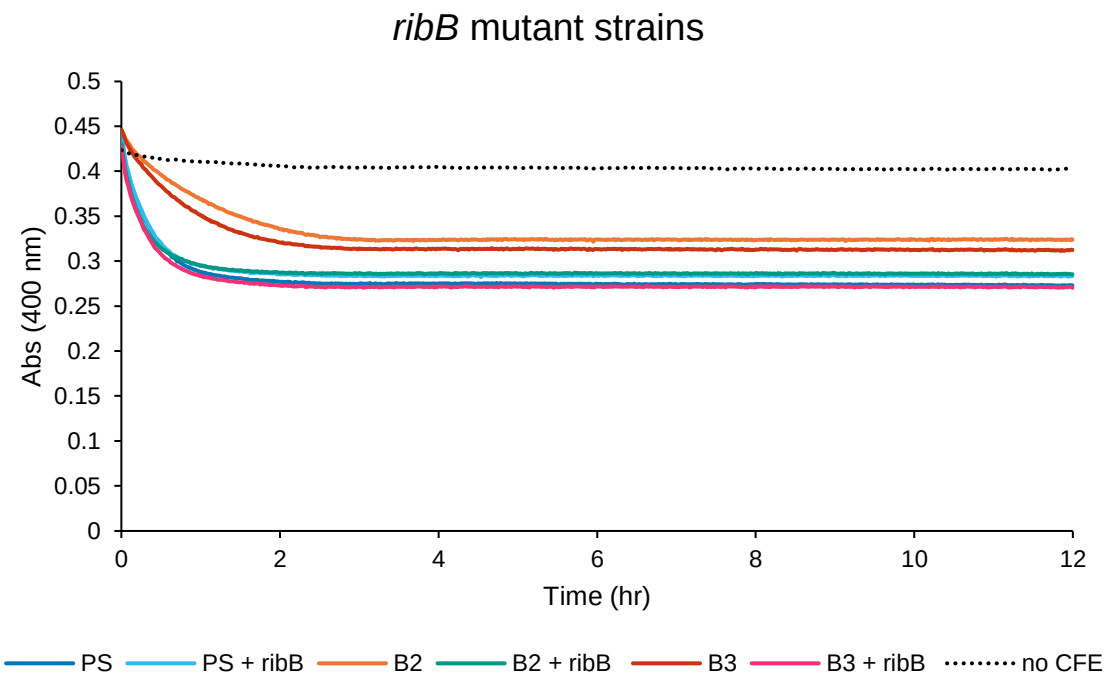

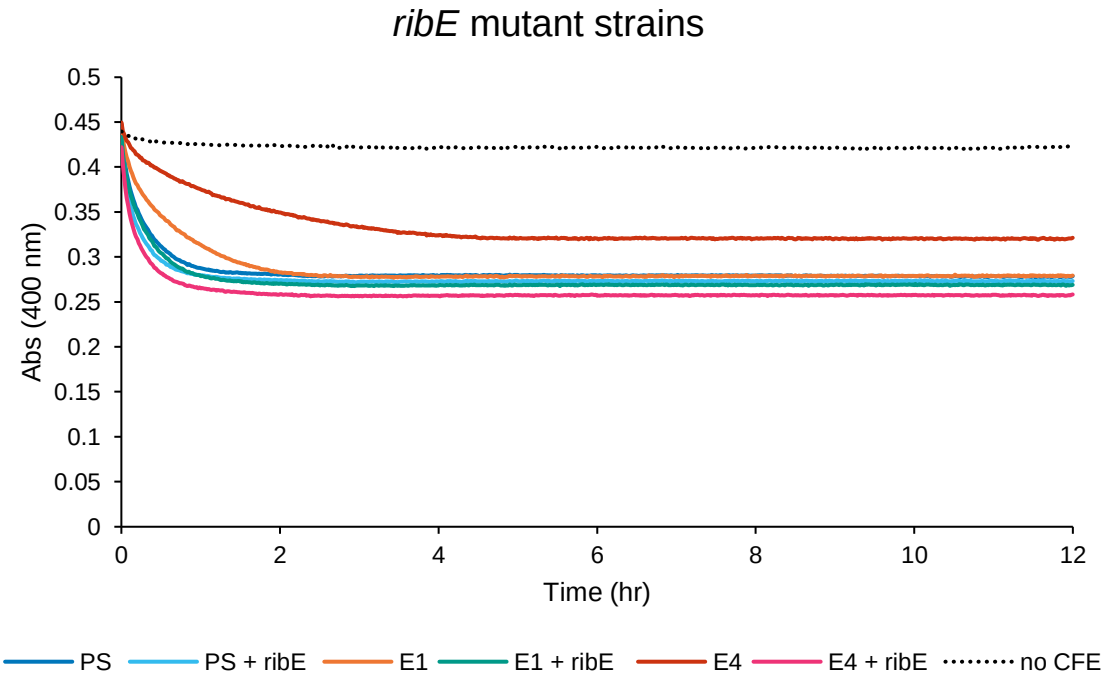

Figure 25: Nitroreductase assays for the *ribB* and *ribE* mutants

Absorbance was measured every minute for 12 hrs at 400 nm. Data is the mean of three technical replicates. CFE: cell-free extract.

Table 15: Nitroreductase activity

Strain	Slope (change in AU/min)
PS	-0.006 (± 0.002)
E1	-0.004 (± 0.001)
E4	-0.002 (± 0.001)
B2	-0.0021 (± 0.0005)
B3	-0.0028 (± 0.0007)
PS + ribE	-0.007 (± 0.003)
PS + ribB	-0.0060 (± 0.0006)
E1 + ribE	-0.006 (± 0.001)
E4 + ribE	-0.007 (± 0.002)
B2 + ribB	-0.0059 (± 0.0007)
B3 + ribB	-0.0057 (± 0.0007)
No CFE	-0.00003 (± 0.00005)

The nitroreductase assays show the decrease in absorbance associated with FZ, which shows how fast FZ is being reduced. NADPH is also used up by the nitroreductases in the reduction of FZ, however NADPH does not absorb at 400 nm. From Figure 25 and Table 15 the initial rate of reaction/decrease in FZ is higher for the parental strain as well as all transformed mutants [between -0.006 and -0.007 decrease in AU (absorbance units) per minute]. The nitroreductase activity in E1 is slightly lower (-0.004 AU/min), while the nitroreductase activities of E4, B2 and B3 were even lower, between -0.002 and -0.003 AU/min. The much lower nitroreductase activity in E4, B2 and B3 compared to the parental strain correlates with a larger increase in FZ MIC. Conversely, the E1 mutant has a relatively smaller decrease in nitroreductase activity, correlated with a smaller increase in FZ MIC. All the complemented strains showed similar nitroreductase activity as the parental strain, confirming that complementation with either fully functional RibB or RibE restores nitroreductase activity in the mutant strains tested.

4.2.4 Riboflavin supplementation

The E1, E4, B2 and B3 mutants were supplemented with 1 mM riboflavin. Riboflavin is downstream of the reactions catalysed by RibB and RibE and upstream of FMN and FAD in the riboflavin biosynthesis pathway. Supplementation with riboflavin is predicted to reverse the effects of the *ribB* and *ribE* mutations, improving the growth of the mutants and lowering the FZ MICs. From Figure 26, the growth curves over 24 hours show the addition of riboflavin improves growth of the mutants, while having no effect on the parental strain. When supplemented with riboflavin, all strains attained an OD_{600} of about 0.7 at 24 hours, matching the growth of the parental strain. This shows that the riboflavin supplementation improves growth to that of the parental strain.

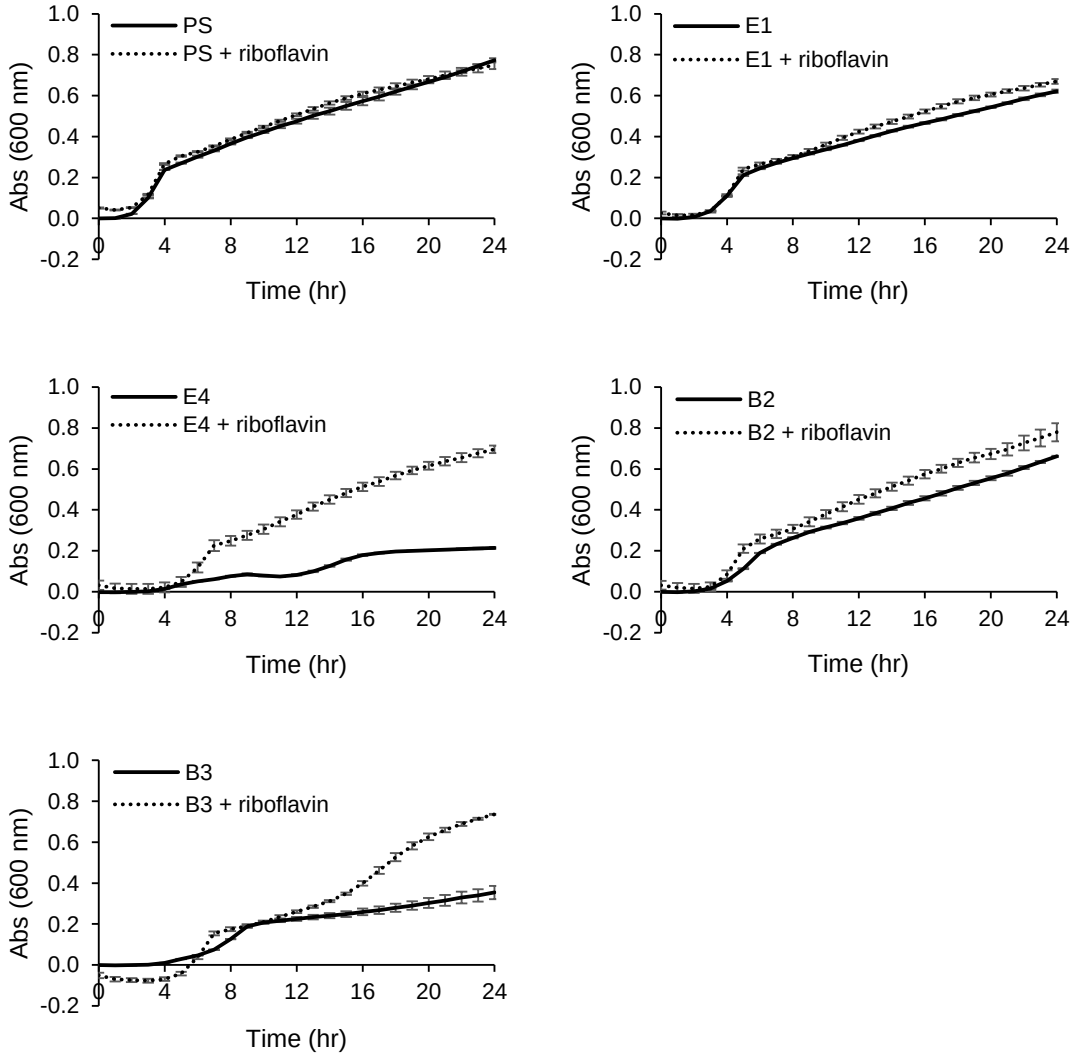

Figure 26: Growth curves upon riboflavin supplementation

Absorbance at 600 nm was measured every hour for 24 hours. Data shown is absorbance – absorbance (growth at time zero with or without riboflavin) to account for the absorbance of riboflavin. Data shown is the mean ± standard error of the mean for three technical replicates.

Next, the question was asked whether supplementation with riboflavin reduced the FZ MIC in the mutant strains. From the dose-response curves shown in Figure 27, the addition of riboflavin did increase growth inhibition at some subinhibitory FZ concentrations in strains E4, B2 and B3, especially strain E4, where the addition of riboflavin meant subinhibitory concentrations of FZ no longer improved growth. However, as can be seen from Table 16, the MICs were unchanged upon the addition of riboflavin.

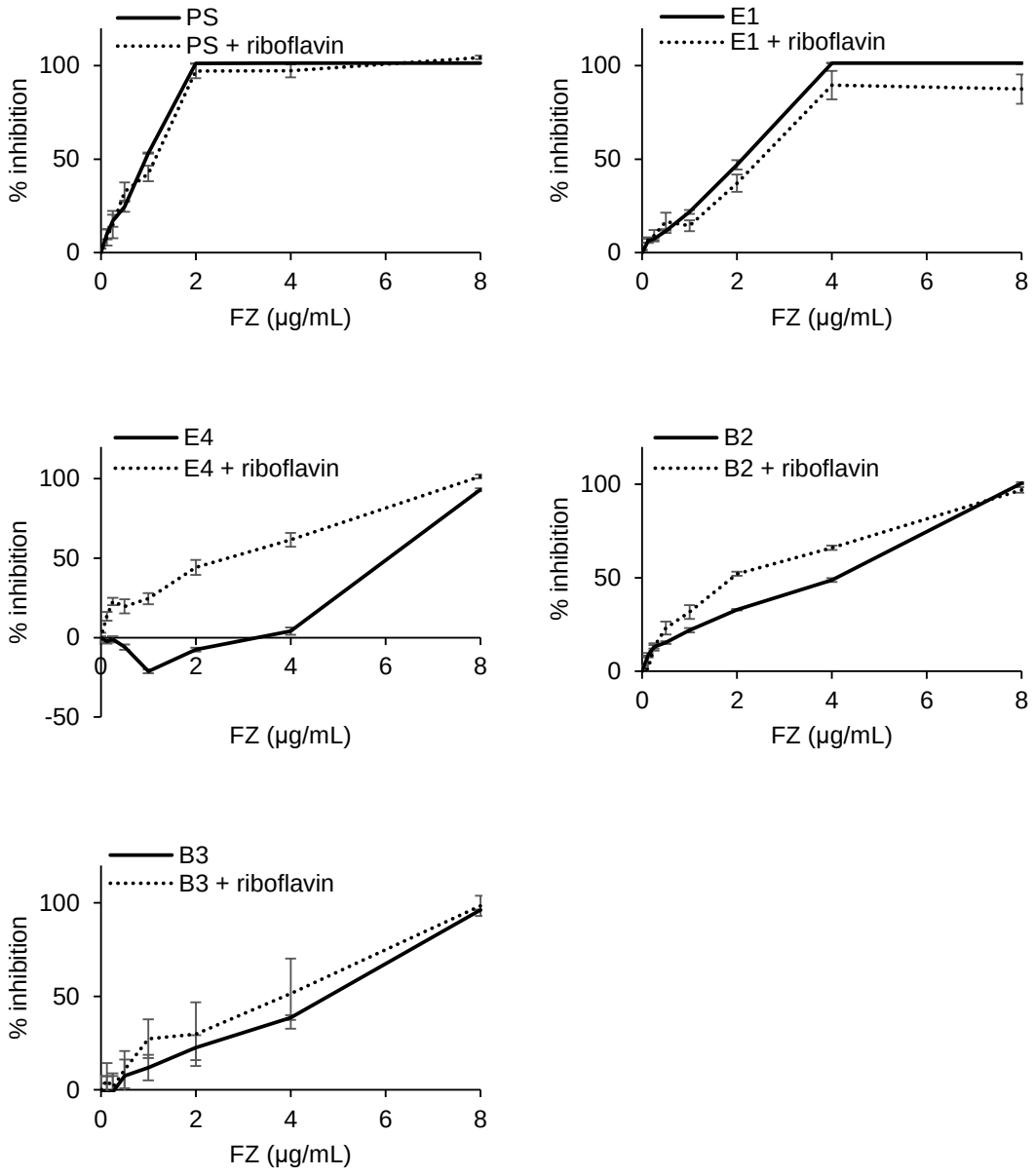

Figure 27: FZ dose-response curves upon riboflavin supplementation

Percent inhibition is shown at 18 hours growth. Zero percent inhibition is taken as the growth at zero FZ. Each graph shows the strain with and without the addition of 1 mM riboflavin. Data shown is the mean of three technical replicates ± standard error of the mean.

Table 16: FZ MICs upon addition of 1mM riboflavin

Strain	FZ MIC (μg/mL)	FZ MIC (1 mM riboflavin) (μg/mL)
PS	2	2
E1	4	4
E4	8	8
B2	8	8
B3	8	8

Overall, the addition of riboflavin reverts the slow growth of the mutants back to that of the parental strain and counteracts the fitness costs associated with the *ribB* and *ribE* mutations, but it does not make the mutants any less resistant to FZ. This is surprising because adding more riboflavin is expected to increase the amount of FMN and FAD present, which would be expected to restore the functioning of the nitroreductases NfsA and NfsB.

4.2.5 NfsA NfsB double knockouts

The *ribB* and *ribE* mutations affect the riboflavin biosynthesis pathway, where FMN and FAD are the ultimate products. FMN and FAD are essential cofactors of NfsA and NfsB, the key enzymes in *E. coli* that activate nitrofuran prodrugs including FZ. Decrease in the amount of functional RibB/RibE enzymes in the *ribB* and *ribE* mutants is expected to result in less FMN and FAD, diminishing the amount of functional NfsA and NfsB and in turn decreasing the activation of FZ. Given that, unexpectedly, supplementation of riboflavin did not restore FZ sensitivity in the *ribB* and *ribE* mutants, the question remained whether the riboflavin biosynthesis mutations increase resistance to FZ *via* NfsA and NfsB or not. To answer this question, *nfsA* and *nfsB* deletions were introduced into the *ribB* and *ribE* mutants. These double knockouts (Δ*nfsA* Δ*nfsB*) were constructed *via* stepwise P1 transduction of the Δ*nfsA::KAN*^{R} and Δ*nfsB::KAN*^{R} alleles into the *ribB* and *ribE* mutants using the corresponding Keio strains as donors (Baba *et al.*, 2006). The double knockout strains were confirmed by PCR amplification of regions containing the *nfsA* and *nfsB* genes as shown in Figure 28 and as described in section 2.10.

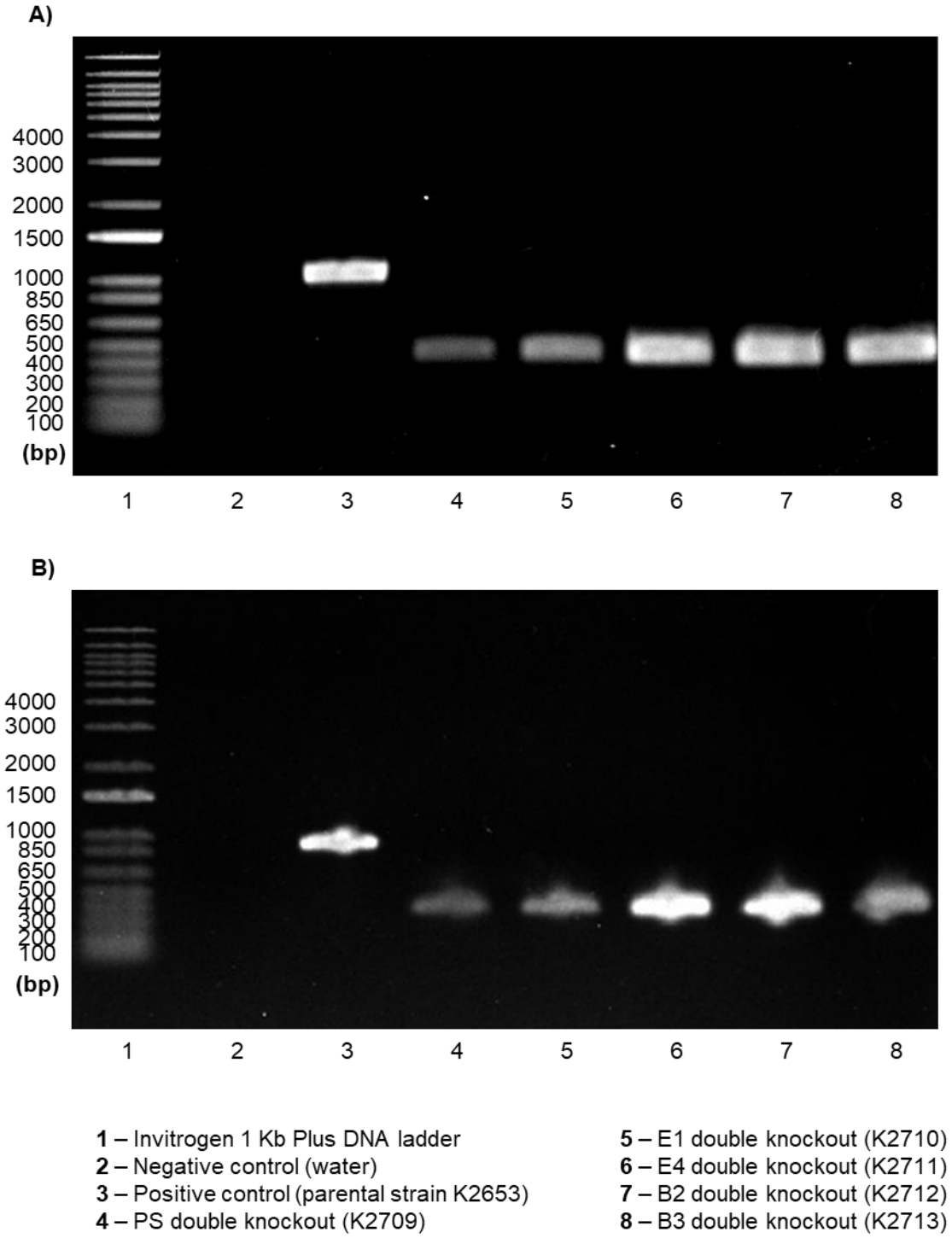

Figure 28: PCR confirmation of the A) *nfsA* and B) *nfsB* gene knockouts

Expected size of PCR products for ΔnfsA knockouts is 923 bp with the gene and 269 bp without the gene. Expected size of PCR products for ΔnfsB knockouts is 1051 bp with the gene and 328 bp without the gene. PCR analyses of all five knockout strains show successful removal of both *nfsA* and *nfsB*.

Removal of the NfsA and NfsB nitroreductases is expected to result in an increased MIC that is the same across all tested strains, due to the differences in FMN concentration from the *ribB/ribE* mutations no longer affecting nitroreductase function. The dose-response curves of the double knockout and original strains are shown in Figure 29.

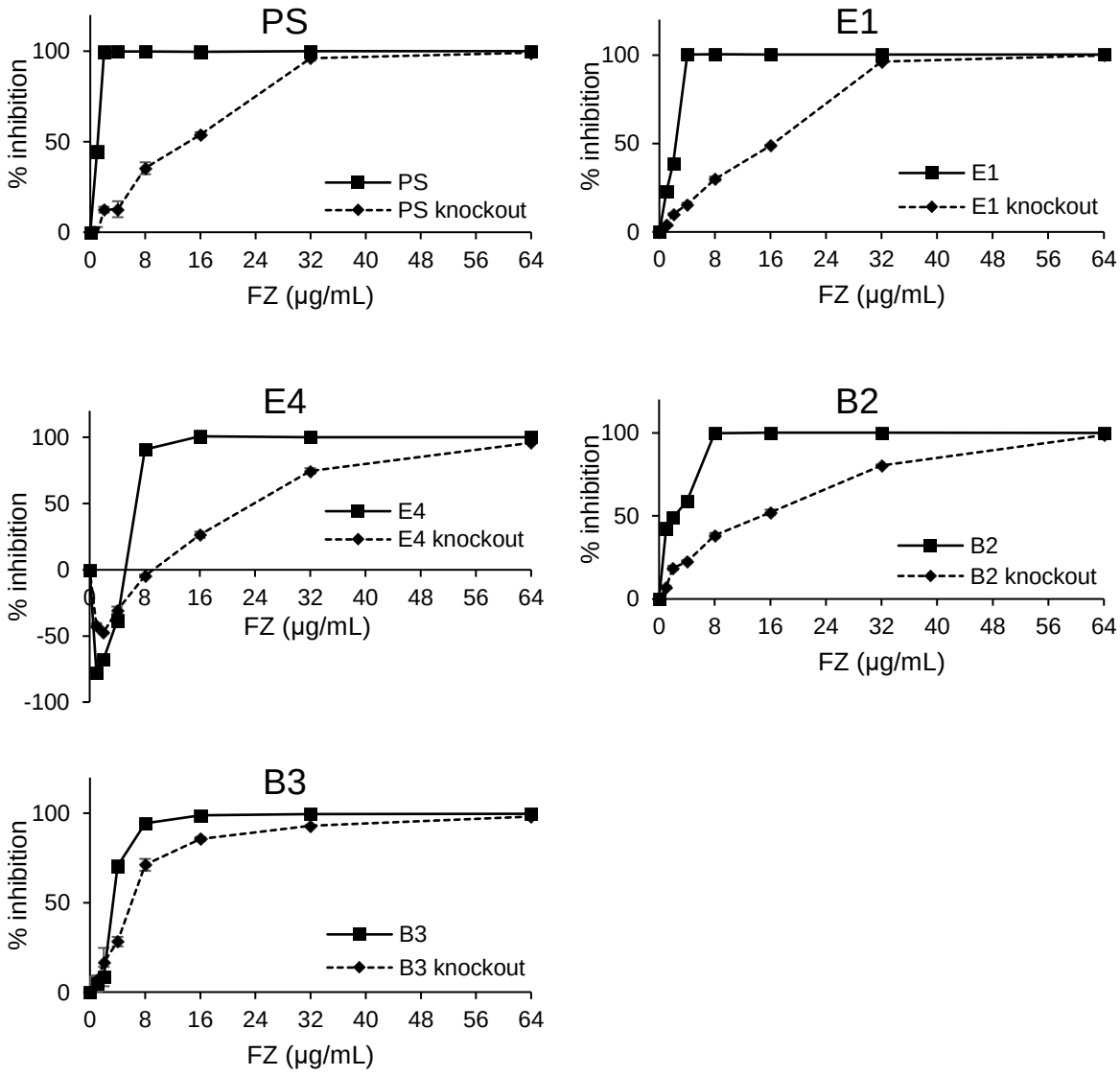

Figure 29: FZ dose-response curves for the Δ*nfsA* Δ*nfsB* double knockouts

Each graph shows the Δ*nfsA* Δ*nfsB* double knockout and original strain. Percent inhibition is shown at 18 hours growth. Zero percent inhibition is taken as the growth at zero FZ. Data shown is the mean ± standard error of the mean of three technical replicates.

In all cases, the double knockout was more resistant to FZ as expected. However, E4 and B2 both had some residual growth at 32 μg/mL FZ (75% and 80% growth inhibition respectively) unlike the parental strain (96% inhibition), E1 (96% inhibition) and B3 (93% inhibition). This means that the resistance cannot be entirely explained through NfsA and NfsB. One explanation is the presence of other proteins in *E. coli* that have nitroreductase activity. AhpF is an oxygen sensitive nitroreductase, that has been found in *E. coli* to activate nitrofurans, including FZ (Le *et al.*, 2019). AhpF mutations were found to correspond to a 1.25-fold increase in FZ MIC in a Δ*nfsA* Δ*nfsB* double knockout *E. coli* strain. Because AhpF requires FAD as a cofactor (Bieger & Essen, 2000; Dip *et al.*, 2014), and FAD is product of the riboflavin biosynthesis pathway, it is possible that the mutations affecting *ribB* in B2 and *ribE* in E4 are causing less FAD to be produced, reducing AhpF activity, and slightly increasing the FZ MIC above that of the parental strain. It was slightly surprising that B3, which had a four-fold increase in FZ MIC along with B2 and E4, did not show this.

4.2.6 Overexpression of NfsB

To investigate whether overexpression of the FZ-activating nitroreductases will affect the FZ resistance, strains overexpressing NfsB were constructed. The pCA24N::*nfsB* plasmid encoding NfsB was transformed into the PS, E1, E4, B2 and B3 strains. Expression was induced with 0.1 mM IPTG, and all strains were grown with and without 1 mM riboflavin. Expression of excess NfsB was expected to lower the MIC of the parental strain more than the mutant strains. The reason for this is that having more NfsB in the wild-type background means more FZ can be activated, creating more bactericidal intermediates. The *ribB* and *ribE* mutant strains are predicted to have limited FMN and FAD available, so adding more NfsB is not predicated to have as much of an effect. Where riboflavin is added, all strains are predicted to have a lower MIC, as more FMN and FAD is expected to be produced.

However, the MICs for all strains were unchanged. This means overexpression of NfsB did not significantly increase the nitroreductase activity. Addition of 1 mM riboflavin did not change the FZ MICs, however it did reduce the growth at some subinhibitory FZ concentrations in strains E4, B2, and B3 (Figure 30), which is no different to the effects of riboflavin on these strains when they were not overproducing NfsB (Figure 27).

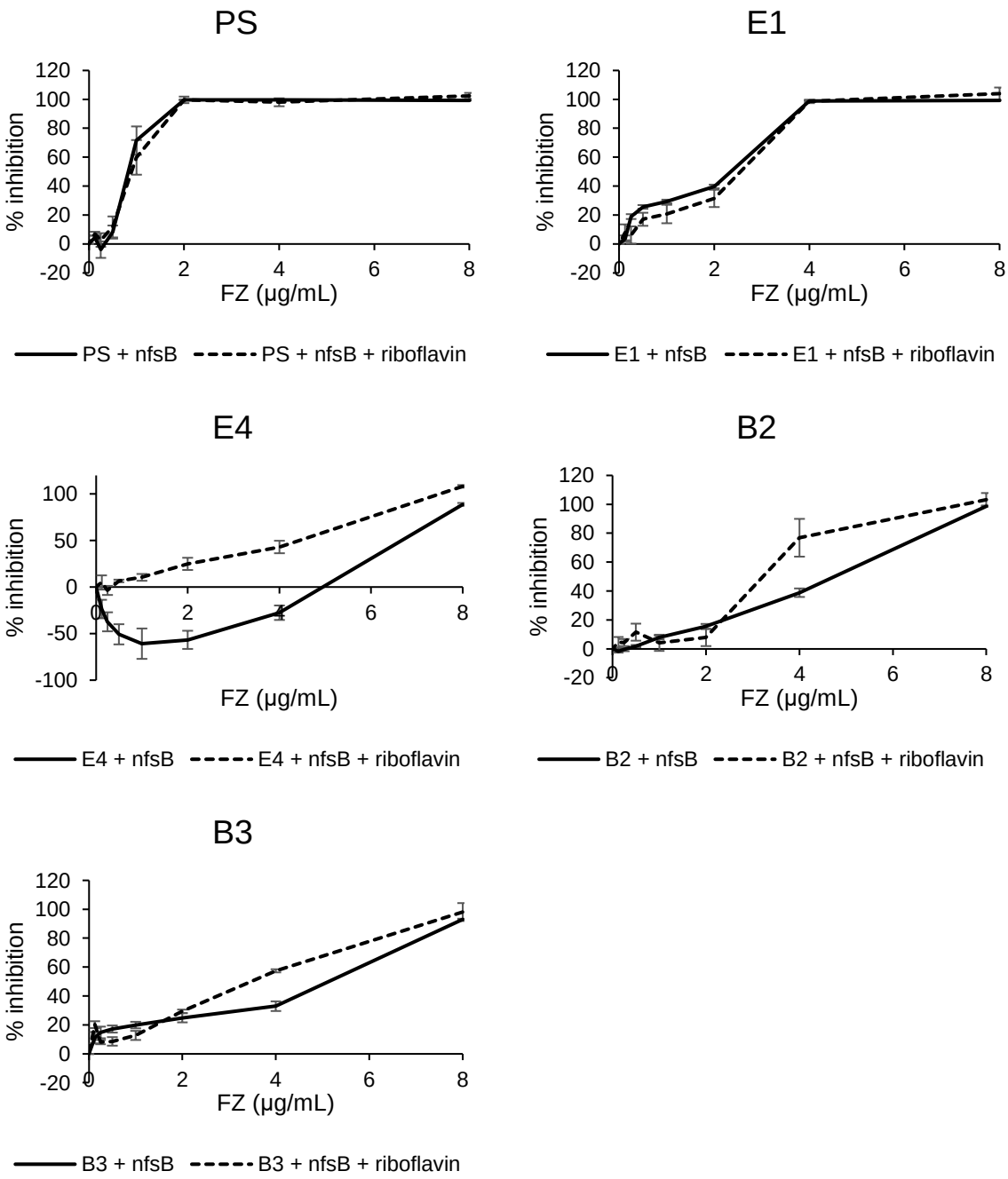

Figure 30: FZ dose-response curves for the NfsB transformed strains with and without the addition of 1 mM riboflavin

Percent inhibition of growth at increasing concentrations of FZ is shown and zero percent inhibition was taken as growth at zero FZ. The data is presented as the mean ± standard error of the mean of three independent colonies for each strain, each of which had three technical replicates.

4.3 Discussion

The *ribB* and *ribE* riboflavin biosynthesis pathway mutations were investigated to determine the mechanism of increased resistance to furazolidone.

Firstly, the effects of these mutations were examined. All the *ribB* and *ribE* mutations resulted in a fitness cost, as all strains grew slower than the parental strain. This was especially evident with the *ribE* deletion mutants (E2, E3, E4, and E5), which grew very poorly. Dose-response curves of the mutants revealed subinhibitory FZ concentrations substantially improved the growth of the *ribE* deletion strains. The reason for this is unclear, however the growth enhancing effect of subinhibitory FZ was only present in the *ribE* deletion mutants, which have the poorest growth. Therefore, this effect may only occur when the cell is very compromised. One link is that FZ induces oxidative stress and upregulates *soxS* (Olivera, Cox, *et al.*, 2021), and SoxS in turn upregulates GTP cyclohydrase II (RibA), which catalyses the first step in riboflavin biosynthesis (Koh *et al.*, 1996). However, overexpression of GTP cyclohydrase II does not correspond to an increase in flavins in *E. coli* (Koh *et al.*, 1996; Richter *et al.*, 1993). The predicted effect of the *ribB* and *ribE* mutations is a decrease in the amount of FMN and FAD present in the cell. This would affect the functioning of flavoproteins, which require FMN or FAD and have a large range of functions within the cell, especially in redox processes. It is possible that the effect on redox processes in the *ribE* deletion mutations is so severe that the presence of subinhibitory FZ improves the growth due to FZ acting as an electron donor and acceptor, improving redox processes within the cell.

Complementation with functional RibB or RibE showed the *ribB* and *ribE* mutations are responsible for the FZ resistance solely through inactivation of those two enzymes. This means that there are no polar effects of the mutations on other genes in the respective operons. The complemented strains showed improved growth up to the level of the parental strain, as well as greater susceptibility to FZ. Complementation was also shown to increase the nitroreductase activity of the mutant strains up to that of the parental strain. The nitroreductase assays also showed that nitroreductase activity corresponded to FZ resistance. Strains E4, B2, and B3 had the lowest nitroreductase activity, and have a four-fold increase in FZ MIC as compared to the parental strain. Strain E1 had a slightly lower nitroreductase activity, consistent with only a two-fold decrease in FZ MIC. The parental strain and all complemented strains had the highest nitroreductase activity, in agreement with their increased susceptibility to FZ.

Supplementation with 1 mM riboflavin improved the growth of the mutants up to that of the parental strain, reversing the fitness costs associated with the *ribB*/*ribE* mutations. However, riboflavin supplementation did not change the MICs for any of the strains, meaning that the addition of riboflavin did not result in significantly increased nitroreductase activity. Riboflavin supplementation did inhibit the growth rate at some of the sub-inhibitory concentrations of FZ in strains E4, B2 and B3, most notably the addition of riboflavin prevented the growth-enhancing effect of subinhibitory concentrations of FZ in strain E4. This supports the observation that subinhibitory concentrations of FZ only improve the growth when the cell is very compromised. The reason for riboflavin only reversing the fitness costs associated with the *ribB* and *ribE* mutations and not the FZ resistance is unclear. It could be said these mutations have two distinct effects, one that causes the FZ resistance, and one that results in poor growth. The addition of riboflavin only reverses the poor growth.

NfsA NfsB double knockouts were constructed in the parental strain, E1, E4, B2 and B3. The removal of these nitroreductases increased the FZ MIC of all the strains, but the FZ MIC was not the same in all strains, meaning effects on NfsA and NfsB were not the sole cause of the FZ resistance. The small difference can be reasonably explained by differences in additional nitroreductase activity due to the AhpF enzyme.

Overexpression of NfsB had no effect on FZ resistance in any of the strains.

5 General Discussion

5.1 General discussion

The increasing prevalence of antibiotic resistance is a growing threat to the ability to treat bacterial infections. As resistance continues to develop and become more widespread, existing antibiotics are becoming less and less effective. This is causing increased morbidity and mortality for patients, and is signalling a return to the pre-antibiotic era, where infections once easily treatable will once again become life-threatening. Particularly problematic are gram-negative pathogens, which dominate the WHO priority pathogen list for the research and development of new antibiotics. This is because gram-negative pathogens have an additional outer membrane which makes it more difficult for antibiotics to gain access to the cell, protecting gram-negative bacteria from many antibiotics effective against gram-positive bacteria. The current rate of development of new antibiotics is failing to keep up with the development and spread of bacterial resistance mechanisms, requiring additional approaches to combat antibiotic resistance. Combining existing drugs is one strategy that can have advantages such as reduced toxicity, increased efficacy, and reduced resistance development when compared to monotherapies (Foucquier & Guedj, 2015; Gómara & Ramón-García, 2019).

The furazolidone – vancomycin antibiotic combination was investigated in this thesis. The FZ – VAN combination is synergistic against gram-negative pathogens. Synergy lowers the dose required to be effective, reducing the side effects for the patient. Lowering the doses of this combination would reduce the nephrotoxicity side effects of vancomycin, and the toxicity and carcinogenic side effects of furazolidone. Also, VAN is only effective against gram-negative bacteria at concentrations that would be toxic to the patient. Combining VAN in a synergistic combination with FZ allows for the required dose to be lowered, repurposing VAN against gram-negative pathogens.

The aim of this thesis was to investigate the resistance development in *E. coli* against the FZ – VAN antibiotic combination. Investigating resistance development towards drugs or drug combinations is a crucial part of combating antibiotic resistance as well as assessing the clinical viability of a treatment. Investigating resistance can lead to the discovery of mechanisms of action of the drug, which in turn identifies bacterial drug targets that can be exploited in further drug development. In addition, identifying bacterial mechanisms of resistance can lead to the development of antibiotic adjuvants

designed to target this resistance, and render the bacteria susceptible to original drug once again.

There were seven main genes that were mutated in the resistant strains selected from the FZ – VAN combination plates. These included the essential genes *ribB*, *ribE*, *ftsH*, and *rpoC* which were mutated in 13 of the strains, and the non-essential genes *opgG*, *nlpI*, and *wecC*, which were mutated in three strains. In addition, the strain isolated from the VAN plate had a mutation in the non-essential *lpp* gene.

Strains with mutations in the riboflavin biosynthesis pathway, the *ribB* and *ribE* mutants, were chosen for further investigation into the mechanism by which they are causing the observed FZ resistance. Mutations in *ribE*, but not *ribB*, have been previously associated with nitrofuran resistance (Vervoort *et al.*, 2014). Confirming that mutations in *ribB*, specifically in the promoter and 5' UTR, are linked to increased nitrofuran resistance would allow for *ribB* to be included in genomic screening processes to predict antibiotic susceptibility and would allow for better resistance identification and improved selection of antibiotics for treatment.

The *ribB* and *ribE* mutations were found to result in a fitness cost, with all strains growing slower than the parental strain, with some entering a stationary phase at an OD_{600} as small as 0.2. Interestingly, sub-inhibitory concentrations of FZ caused substantially improved growth in the *ribE* deletion mutants, which had the slowest growth. Complementation with functional RibB or RibE showed these genes were solely responsible for the observed FZ resistance. Complemented strains showed a decrease in FZ MIC as well as improved growth and nitroreductase activity to match those of the parental strain. Nitroreductase activity was also found to directly correlate with FZ MIC. Supplementation with riboflavin improved the growth of all strains up to that of the parental strain, and increased growth inhibition at some sub-inhibitory concentrations of FZ, including preventing the growth-enhancing effect of sub-inhibitory FZ concentrations in the strains with a *ribE* deletion mutation. However, none of the FZ MICs were altered upon the addition of riboflavin. The mechanism of resistance was shown to predominantly act through the NfsA and NfsB nitroreductases, as knocking out both genes made the FZ MICs similar, and remaining differences can be reasonably attributed to the presence of oxygen-sensitive nitroreductases.

5.2 Conclusions

The high proportion of essential gene mutations indicates that resistance does not easily arise to the FZ – VAN combination, which is promising for its potential as a treatment option for gram-negative bacterial infections. In addition, combining VAN with FZ appeared to reduce the mutagenicity of FZ, with no mutations occurring in the *nfsA nfsB* genes, which are the most common cause of nitrofuran resistance.

The *ribB* and *ribE* gene mutations were linked to increased FZ resistance and reduced nitroreductase activity, which was found to be directly related to FZ MIC. The mechanism of resistance could be explained as acting on the nitroreductases NfsA and NfsB, however the effects on NfsA and NfsB were not the sole cause of the FZ resistance. The small difference may be due to the differences in nitroreductase activity level of the AhpF enzyme.

The mechanism of resistance is thought to be due to the *ribB* and *ribE* mutations causing less FMN and FAD to be produced, which are essential cofactors required for the nitroreductases NfsA and NfsB. This leads to less nitroreductase activity, which is required for the activation of FZ into bactericidal intermediates, leading to FZ resistance.

However, the addition of riboflavin, which is downstream of the reactions catalysed by RibB and RibE, and upstream of FMN and FAD in the riboflavin biosynthesis pathway, did not decrease the MICs, but did improve the growth up to that of the parental strain. Therefore, it is possible that the *ribB* and *ribE* mutations are affecting nitroreductase activity through mechanisms other than decreased FMN and FAD.

5.3 Future directions

For all the identified genes not chosen for further investigation, further investigation is required to confirm that the gene mutation is in fact responsible for the observed resistance, as well as investigation into the resistance mechanisms.

In addition, investigation into why sub-inhibitory concentrations of FZ can improve growth in selected *ribE* mutants is required, as well as why riboflavin supplementation reverts the fitness cost associated with the *ribB* and *ribE* mutations but does not lower the FZ MICs.

6 Bibliography

Abraham, E. P., & Chain, E. (1940). An enzyme from bacteria able to destroy penicillin. *Nature*, *146*(3713), 837-837.

Altschul, S. F., Madden, T. L., Schäffer, A. A., Zhang, J., Zhang, Z., Miller, W., & Lipman, D. J. (1997). Gapped BLAST and PSI-BLAST: a new generation of protein database search programs. *Nucleic Acids Research*, *25*(17), 3389-3402. https://doi.org/10.1093/nar/25.17.3389

Arthur, M., Depardieu, F., Snaith, H. A., Reynolds, P. E., & Courvalin, P. (1994). Contribution of VanY D,D-carboxypeptidase to glycopeptide resistance in *Enterococcus faecalis* by hydrolysis of peptidoglycan precursors. *Antimicrobial Agents and Chemotherapy*, *38*(9), 1899-1903. https://doi.org/10.1128/AAC.38.9.1899

Asmar, A. T., Ferreira, J. L., Cohen, E. J., Cho, S.-H., Beeby, M., Hughes, K. T., & Collet, J.-F. (2017). Communication across the bacterial cell envelope depends on the size of the periplasm. *PLoS Biology*, *15*(12), e2004303.

Averianova, L. A., Balabanova, L. A., Son, O. M., Podvolotskaya, A. B., & Tekutyeva, L. A. (2020). Production of vitamin B2 (riboflavin) by microorganisms: An overview. *Frontiers in Bioengineering and Biotechnology*, *8*. https://doi.org/10.3389/fbioe.2020.570828

Baba, T., Ara, T., Hasegawa, M., Takai, Y., Okumura, Y., Baba, M., Datsenko, K. A., Tomita, M., Wanner, B. L., & Mori, H. (2006). Construction of *Escherichia coli* K-12 in-frame, single-gene knockout mutants: the Keio collection. *Molecular systems biology*, *2*(1), 2006.0008.

Bakhit, M., Del Mar, C., Gibson, E., & Hoffmann, T. (2019). Exploring patients' understanding of antibiotic resistance and how this may influence attitudes towards antibiotic use for acute respiratory infections: a qualitative study in Australian general practice. *BMJ Open*, *9*(3), e026735. https://doi.org/10.1136/bmjopen-2018-026735

Bankevich, A., Nurk, S., Antipov, D., Gurevich, A. A., Dvorkin, M., Kulikov, A. S., Lesin, V. M., Nikolenko, S. I., Pham, S., & Prjibelski, A. D. (2012). SPAdes: a new genome assembly algorithm and its applications to single-cell sequencing. *Journal of computational biology*, *19*(5), 455-477.

Banzhaf, M., Yau, H. C., Verheul, J., Lodge, A., Kritikos, G., Mateus, A., Cordier, B., Hov, A. K., Stein, F., Wartel, M., Pazos, M., Solovyova, A. S., Breukink, E., van Teeffelen, S., Savitski, M. M., den Blaauwen, T., Typas, A., & Vollmer, W. (2020). Outer membrane lipoprotein NlpI scaffolds peptidoglycan hydrolases within multi-enzyme complexes in *Escherichia coli*. *Embo journal*, *39*(5), e102246. https://doi.org/10.15252/embj.2019102246

Barnich, N., Bringer, M.-A., Claret, L., & Darfeuille-Michaud, A. (2004). Involvement of lipoprotein NlpI in the virulence of adherent invasive *Escherichia coli* strain LF82 isolated from a patient with Crohn's Disease. *Infection and Immunity*, *72*(5), 2484-2493. https://doi.org/10.1128/IAI.72.5.2484-2493.2004

Bertenyi, K. K. A., & Lambert, I. B. (1996). The mutational specificity of furazolidone in the *lacI* gene of *Escherichia coli*. *Mutation Research/Fundamental and Molecular Mechanisms of Mutagenesis, 357*(1), 199-208. https://doi.org/10.1016/0027-5107(96)00102-9

Bieger, B., & Essen, L. O. (2000). Crystallization and preliminary X-ray analysis of the catalytic core of the alkylhydroperoxide reductase component AhpF from *Escherichia coli*. *Acta Crystallogr D Biol Crystallogr, 56*(Pt 1), 92-94. https://doi.org/10.1107/s0907444999014146

Bohin, J. P., & Lacroix, J. M. (2006). Osmoregulation in the periplasm. *The periplasm*, 325-341.

Bontemps-Gallo, S., Cogez, V., Robbe-Masselot, C., Quintard, K., Dondeyne, J., Madec, E., & Lacroix, J.-M. (2013). Biosynthesis of osmoregulated periplasmic glucans in *Escherichia coli*: The phosphoethanolamine transferase is encoded by *opgE*. *BioMed Research International, 2013*, 371429. https://doi.org/10.1155/2013/371429

Centers for Disease Control and Prevention. (2013). *Antibiotic Resistance Threats in the United States, 2013*. https://www.cdc.gov/drugresistance/pdf/ar-threats-2013-508.pdf

Chait, R., Craney, A., & Kishony, R. (2007). Antibiotic interactions that select against resistance. *Nature, 446*(7136), 668-671. https://doi.org/10.1038/nature05685

Chamberlain, R. E. (1976). Chemotherapeutic properties of prominent nitrofurans. *Journal of Antimicrobial Chemotherapy, 2*(4), 325-336. https://doi.org/10.1093/jac/2.4.325

Cherepanov, P. P., & Wackernagel, W. (1995). Gene disruption in *Escherichia coli*: TcR and KmR cassettes with the option of Flp-catalyzed excision of the antibiotic-resistance determinant. *Gene, 158*(1), 9-14. https://doi.org/10.1016/0378-1119(95)00193-A

Cingolani, P., Platts, A., Wang, L. L., Coon, M., Nguyen, T., Wang, L., Land, S. J., Lu, X., & Ruden, D. M. (2012). A program for annotating and predicting the effects of single nucleotide polymorphisms, SnpEff: SNPs in the genome of *Drosophila melanogaster* strain w1118; iso-2; iso-3. *Fly, 6*(2), 80-92.

Cockerill, F. R., Wikler, M. A., Alder, J., Dudley, M. N., Eliopoulos, G. M., Ferraro, M. J., Hardy, D. J., Hecht, D. W., Hindler, J. A., Patel, J. B., Powell, M., Swenson, J. M., Richard B. Thomson, J., Traczewski, M. M., Turnidge, J. D., Weinstein, M. P., & Zimmer, B. L. (2012). *Methods for Dilution Antimicrobial Susceptibility Tests for Bacteria That Grow Aerobically; Approved Standard—Ninth Edition*.

Consortium, T. U. (2020). UniProt: the universal protein knowledgebase in 2021. *Nucleic Acids Research, 49*(D1), D480-D489. https://doi.org/10.1093/nar/gkaa1100

Cooper, K. M., & Kennedy, D. G. (2007). Stability studies of the metabolites of nitrofuran antibiotics during storage and cooking. *Food Additives & Contaminants, 24*(9), 935-942. https://doi.org/10.1080/02652030701317301

Cox, G., & Wright, G. D. (2013). Intrinsic antibiotic resistance: Mechanisms, origins, challenges and solutions. *International Journal of Medical Microbiology, 303*(6), 287-292. https://doi.org/10.1016/j.ijmm.2013.02.009

Cox, M. P., Peterson, D. A., & Biggs, P. J. (2010). SolexaQA: At-a-glance quality assessment of Illumina second-generation sequencing data. *BMC bioinformatics, 11*(1), 1-6.

Coxeter, P. D., Mar, C. D., & Hoffmann, T. C. (2017). Parents' expectations and experiences of antibiotics for acute respiratory infections in primary care. *The Annals of Family Medicine, 15*(2), 149-154. https://doi.org/10.1370/afm.2040

D'Costa, V. M., McGrann, K. M., Hughes, D. W., & Wright, G. D. (2006). Sampling the antibiotic resistome. *Science, 311*(5759), 374-377. https://doi.org/10.1126/science.1120800

Datsenko, K. A., & Wanner, B. L. (2000). One-step inactivation of chromosomal genes in *Escherichia coli* K-12 using PCR products. *Proceedings of the National Academy of Sciences, 97*(12), 6640-6645.

Davies, J. (2006). Where have all the antibiotics gone? *The Canadian journal of infectious diseases & medical microbiology = Journal canadien des maladies infectieuses et de la microbiologie medicale, 17*(5), 287-290. https://doi.org/10.1155/2006/707296

Dip, P. V., Kamariah, N., Manimekalai, S., Nartey, W., Balakrishna, A. M., Eisenhaber, F., Eisenhaber, B., & Grüber, G. (2014). Structure, mechanism and ensemble formation of the alkylhydroperoxide reductase subunits AhpC and AhpF from *Escherichia coli*. *Acta Crystallographica Section D: Biological Crystallography, 70*(11), 2848-2862.

Ebel, W., Vaughn, G. J., Peters, H. K., & Trempy, J. E. (1997). Inactivation of *mdoH* leads to increased expression of colanic acid capsular polysaccharide in *Escherichia coli*. *Journal of Bacteriology, 179*(21), 6858-6861. https://doi.org/10.1128/jb.179.21.6858-6861.1997

Egan, A. J. F., Jean, N. L., Koumoutsi, A., Bougault, C. M., Biboy, J., Sassine, J., Solovyova, A. S., Breukink, E., Typas, A., Vollmer, W., & Simorre, J.-P. (2014). Outer-membrane lipoprotein LpoB spans the periplasm to stimulate the peptidoglycan synthase PBP1B. *Proceedings of the National Academy of Sciences, 111*(22), 8197-8202. https://doi.org/10.1073/pnas.1400376111

European Centre for Disease Prevention and Control. (2008). *Factsheet for experts - Antimicrobial resistance*. https://www.ecdc.europa.eu/en/antimicrobial-resistance/facts/factsheets/experts

Fiedler, W., & Rotering, H. (1988). Properties of *Escherichia coli* mutants lacking membrane-derived oligosaccharides. *Journal of Biological Chemistry, 263*(29), 14684-14689. https://doi.org/10.1016/S0021-9258(18)68091-3

Fleming, A. (1929). On the antibacterial action of cultures of a *Penicillium*, with special reference to their use in the isolation of *B. influenzæ*. *British journal of experimental pathology, 10*(3), 226-236. https://www.ncbi.nlm.nih.gov/pmc/articles/PMC2048009/

Foucquier, J., & Guedj, M. (2015). Analysis of drug combinations: current methodological landscape. *Pharmacology Research & Perspectives, 3*(3), e00149. https://doi.org/10.1002/prp2.149

Garrison, E., & Marth, G. (2012). Haplotype-based variant detection from short-read sequencing. *arXiv preprint arXiv:1207.3907*.

Goldberg, A., Fridman, O., Ronin, I., & Balaban, N. Q. (2014). Systematic identification and quantification of phase variation in commensal and pathogenic *Escherichia coli*. *Genome medicine, 6*(11), 112-112. https://doi.org/10.1186/s13073-014-0112-4

Gómara, M., & Ramón-García, S. (2019). The FICI paradigm: Correcting flaws in antimicrobial in vitro synergy screens at their inception. *Biochemical Pharmacology, 163*, 299-307. https://doi.org/10.1016/j.bcp.2019.03.001

Goodall, E. C., Isom, G. L., Rooke, J. L., Pullela, K., Icke, C., Yang, Z., Boelter, G., Jones, A., Warner, I., & Da Costa, R. (2021). Loss of YhcB results in dysregulation of coordinated peptidoglycan, LPS and phospholipid synthesis during *Escherichia coli* cell growth. *PLoS genetics, 17*(12), e1009586.

Grenier, F., Matteau, D., Baby, V., & Rodrigue, S. (2014). Complete genome sequence of *Escherichia coli* BW25113. *Genome Announcements, 2*(5). https://doi.org/10.1128/genomeA.01038-14

Hegreness, M., Shoresh, N., Damian, D., Hartl, D., & Kishony, R. (2008). Accelerated evolution of resistance in multidrug environments. *Proceedings of the National Academy of Sciences, 105*(37), 13977-13981. https://doi.org/10.1073/pnas.0805965105

Hemberger, S., Pedrolli, D. B., Stolz, J., Vogl, C., Lehmann, M., & Mack, M. (2011). RibM from *Streptomyces davawensis* is a riboflavin/roseoflavin transporter and may be useful for the optimization of riboflavin production strains. *BMC Biotechnology, 11*(1), 119. https://doi.org/10.1186/1472-6750-11-119

Houghton, L., Maher-Loughnan, G., Leslie, W., Perry, D. N. L., Beatty, D., & Sandiford, B. (1950). Treatment of pulmonary tuberculosis with streptomycin and para-amino-salicylic acid. *British Medical Journal*, *2*(4688), 1073-1085.

Huddleston, J. R. (2014). Horizontal gene transfer in the human gastrointestinal tract: potential spread of antibiotic resistance genes. *Infection and drug resistance*, *7*, 167.

Hutchings, M. I., Truman, A. W., & Wilkinson, B. (2019). Antibiotics: past, present and future. *Current Opinion in Microbiology*, *51*, 72-80. https://doi.org/10.1016/j.mib.2019.10.008

Huttner, B., Goossens, H., Verheij, T., & Harbarth, S. (2010). Characteristics and outcomes of public campaigns aimed at improving the use of antibiotics in outpatients in high-income countries. *The Lancet Infectious Diseases*, *10*(1), 17-31. https://doi.org/10.1016/S1473-3099(09)70305-6

Imamovic, L., & Sommer, M. O. A. (2013). Use of collateral sensitivity networks to design drug cycling protocols that avoid resistance development. *Science Translational Medicine*, *5*(204), 204ra132-204ra132. https://doi.org/10.1126/scitranslmed.3006609

Ito, K., & Akiyama, Y. (2005). Cellular functions, mechanism of action, and regulation of FtsH protease. *Annual Review of Microbiology*, *59*(1), 211-231. https://doi.org/10.1146/annurev.micro.59.030804.121316

Itou, J., Eguchi, Y., & Utsumi, R. (2009). Molecular mechanism of transcriptional cascade initiated by the EvgS/EvgA system in *Escherichia coli* K-12. *Bioscience, Biotechnology, and Biochemistry*, *73*(4), 870-878. https://doi.org/10.1271/bbb.80795

Jackson, B., Bohin, J., & Kennedy, E. (1984). Biosynthesis of membrane-derived oligosaccharides: characterization of *mdoB* mutants defective in phosphoglycerol transferase I activity. *Journal of Bacteriology*, *160*(3), 976-981.

Jiang, X. E., Tan, W. B., Shrivastava, R., Seow, D. C. S., Chen, S. L., Guan, X. L., & Chng, S.-S. (2020). Mutations in enterobacterial common antigen biosynthesis restore outer membrane barrier function in *Escherichia coli tol-pal* mutants. *Molecular Microbiology*, *114*(6), 991-1005. https://doi.org/10.1111/mmi.14590

Jordan, D. C. (1961). Effect of vancomycin on the synthesis of the cell wall mucopeptide of *Staphylococcus aureus*. *Biochemical and Biophysical Research Communications*, *6*(3), 167-170. https://doi.org/10.1016/0006-291X(61)90122-X

Kari, F. W., Huff, J. E., Leininger, J., Haseman, J. K., & Eustis, S. L. (1989). Toxicity and carcinogenicity of nitrofurazone in F344/N rats and B6C3F1 mice. *Food and Chemical Toxicology*, *27*(2), 129-137. https://doi.org/10.1016/0278-6915(89)90008-2

Kennedy, E. P. (1982). Osmotic regulation and the biosynthesis of membrane-derived oligosaccharides in *Escherichia coli*. *Proceedings of the National Academy of Sciences, 79*(4), 1092. https://doi.org/10.1073/pnas.79.4.1092

Kennedy, E. P., Rumley, M., Schulman, H., & Van Golde, L. (1976). Identification of sn-glycero-1-phosphate and phosphoethanolamine residues linked to the membrane-derived oligosaccharides of *Escherichia coli*. *Journal of Biological Chemistry, 251*(14), 4208-4213.

Kerantzas, C. A., Jacobs, W. R., Rubin, E. J., & Collier, R. J. (2017). Origins of combination therapy for tuberculosis: Lessons for future antimicrobial development and application. *mBio, 8*(2), e01586-01516. https://doi.org/10.1128/mBio.01586-16

Kitagawa, M., Ara, T., Arifuzzaman, M., Ioka-Nakamichi, T., Inamoto, E., Toyonaga, H., & Mori, H. (2005). Complete set of ORF clones of *Escherichia coli* ASKA library (A complete set of *E. coli* K-12 ORF archive): Unique resources for biological research. *DNA research, 12*(5), 291-299.

Koh, Y. S., Choih, J., Lee, J. H., & Roe, J. H. (1996). Regulation of the *ribA* gene encoding GTP cyclohydrolase II by the *soxRS* locus in *Escherichia coli*. *Molecular and General Genetics MGG, 251*(5), 591-598. https://doi.org/10.1007/BF02173649

Kouidmi, I., Levesque, R. C., & Paradis-Bleau, C. (2014). The biology of Mur ligases as an antibacterial target. *Molecular Microbiology, 94*(2), 242-253. https://doi.org/https://doi.org/10.1111/mmi.12758

Kovacs-Simon, A., Titball, R. W., & Michell, S. L. (2011). Lipoproteins of bacterial pathogens. *Infection and Immunity, 79*(2), 548-561. https://doi.org/10.1128/iai.00682-10

Kuhn, H.-M., Meier-Dieter, U., & Mayer, H. (1988). ECA, the enterobacterial common antigen. *FEMS microbiology Reviews, 4*(3), 195-222.

Lacroix, J.-M., Lanfroy, E., Cogez, V., Lequette, Y., Bohin, A., & Bohin, J.-P. (1999). The *mdoC* gene of *Escherichia coli* encodes a membrane protein that is required for succinylation of osmoregulated periplasmic glucans. *Journal of Bacteriology, 181*(12), 3626-3631.

Lacroix, J. M., Loubens, I., Tempete, M., Menichi, B., & Bohin, J. P. (1991). The *mdoA* locus of *Escherichia coli* consists of an operon under osmotic control. *Molecular Microbiology, 5*(7), 1745-1753.

Lanfroy, E., & Bohin, J. (1993). Physical map location of the *Escherichia coli* gene encoding phosphoglycerol transferase I. *Journal of Bacteriology, 175*(17), 5736-5737.

Langmead, B., & Salzberg, S. L. (2012). Fast gapped-read alignment with Bowtie 2. *Nature methods, 9*(4), 357-359.

Laubacher, M. E., & Ades, S. E. (2008). The Rcs phosphorelay is a cell envelope stress response activated by peptidoglycan stress and contributes to intrinsic antibiotic resistance. *Journal of Bacteriology, 190*(6), 2065-2074. https://doi.org/10.1128/JB.01740-07

Le, V. V. H., Davies, I. G., Moon, C. D., Wheeler, D., Biggs, P. J., & Rakonjac, J. (2019). Novel 5-nitrofuran-activating reductase in *Escherichia coli*. *Antimicrobial Agents and Chemotherapy, 63*(11), e00868-00819. https://doi.org/10.1128/aac.00868-19

Le, V. V. H., & Rakonjac, J. (2021). Nitrofurans: Revival of an “old” drug class in the fight against antibiotic resistance. *PLoS Pathogens, 17*(7), e1009663.

Leary, M., Heerboth, S., Lapinska, K., & Sarkar, S. (2018). Sensitization of drug resistant cancer cells: A matter of combination therapy. *Cancers, 10*(12), 483. https://www.mdpi.com/2072-6694/10/12/483

Levine, D. P. (2006). Vancomycin: A history. *Clinical Infectious Diseases, 42*(Supplement_1), S5-S12. https://doi.org/10.1086/491709

Li, H., Handsaker, B., Wysoker, A., Fennell, T., Ruan, J., Homer, N., Marth, G., Abecasis, G., & Durbin, R. (2009). The sequence alignment/map format and SAMtools. *Bioinformatics, 25*(16), 2078-2079.

Loubens, I., Debarbieux, L., Bohin, A., Lacroix, J.-M., & Bohin, J.-P. (1993). Homology between a genetic locus (*mdoA*) involved in the osmoregulated biosynthesis of periplasmic glucans in *Escherichia coli* and a genetic locus (*hrpM*) controlling pathogenicity of *Pseudomonas syringae*. *Molecular Microbiology, 10*(2), 329-340. https://doi.org/10.1111/j.1365-2958.1993.tb01959.x

Magnuson, K., Jackowski, S., Rock, C., & Cronan Jr, J. (1993). Regulation of fatty acid biosynthesis in *Escherichia coli*. *Microbiological reviews, 57*(3), 522-542.

Mai-Prochnow, A., Clauson, M., Hong, J., & Murphy, A. B. (2016). Gram positive and Gram negative bacteria differ in their sensitivity to cold plasma. *Scientific Reports, 6*, 38610-38610. https://doi.org/10.1038/srep38610

Mathelié-Guinlet, M., Asmar, A. T., Collet, J.-F., & Dufrêne, Y. F. (2020). Lipoprotein Lpp regulates the mechanical properties of the *E. coli* cell envelope. *Nature Communications, 11*(1), 1-11.

Matsuo, M., Hishinuma, T., Katayama, Y., & Hiramatsu, K. (2015). A mutation of RNA polymerase β' subunit (RpoC) converts heterogeneously vancomycin-intermediate *Staphylococcus aureus* (hVISA) into "slow VISA". *Antimicrobial Agents and Chemotherapy, 59*(7), 4215-4225. https://doi.org/10.1128/aac.00135-15

McCalla, D. R. (1979). Nitrofurans. In F. E. Hahn (Ed.), *Mechanism of Action of Antibacterial Agents* (pp. 176-213). Springer Berlin Heidelberg. https://doi.org/10.1007/978-3-642-46403-4_11

McCalla, D. R., Kaiser, C., & Green, M. H. L. (1978). Genetics of nitrofurazone resistance in *Escherichia coli*. *Journal of Bacteriology*, *133*(1), 10-16. https://jb.asm.org/content/jb/133/1/10.full.pdf

McCracken, R. J., & Kennedy, D. G. (2007). Detection, accumulation and distribution of nitrofuran residues in egg yolk, albumen and shell. *Food Additives & Contaminants*, *24*(1), 26-33. https://doi.org/10.1080/02652030600967214

Meier-Dieter, U., Starman, R., Barr, K., Mayer, H., & Rick, P. D. (1990). Biosynthesis of enterobacterial common antigen in *Escherichia coli*. Biochemical characterization of Tn10 insertion mutants defective in enterobacterial common antigen synthesis. *Journal of Biological Chemistry*, *265*(23), 13490-13497.

Michel, J.-B., Yeh, P. J., Chait, R., Moellering, R. C., & Kishony, R. (2008). Drug interactions modulate the potential for evolution of resistance. *Proceedings of the National Academy of Sciences*, *105*(39), 14918-14923. https://doi.org/10.1073/pnas.0800944105

Minato, Y., Dawadi, S., Kordus, S. L., Sivanandam, A., Aldrich, C. C., & Baughn, A. D. (2018). Mutual potentiation drives synergy between trimethoprim and sulfamethoxazole. *Nature Communications*, *9*(1), 1003. https://doi.org/10.1038/s41467-018-03447-x

Mitchell, A. M., Srikumar, T., Silhavy, T. J., & Hultgren, S. J. (2018). Cyclic enterobacterial common antigen maintains the outer membrane permeability barrier of *Escherichia coli* in a manner controlled by YhdP. *mBio*, *9*(4), e01321-01318. https://doi.org/10.1128/mBio.01321-18

Mokhtari, R. B., Homayouni, T. S., Baluch, N., Morgatskaya, E., Kumar, S., Das, B., & Yeger, H. (2017). Combination therapy in combating cancer. *Oncotarget*, *8*(23), 38022.

Murakami, K., Nasu, H., Fujiwara, T., Takatsu, N., Yoshida, N., Furuta, K., & Kaito, C. (2021). The absence of osmoregulated periplasmic glucan confers antimicrobial resistance and increases virulence in *Escherichia coli*. *Journal of Bacteriology*, *203*(12), e00515-00520.

Nieto, M., & Perkins, H. R. (1971). Modifications of the acyl-D-alanyl-D-alanine terminus affecting complex-formation with vancomycin. *Biochemical Journal*, *123*(5), 789-803.

O'Neill, J. (2015). *Securing new drugs for future generations: the pipeline of antibiotics*. Review on Antimicrobial Resistance.

O'Neill, J. (2014). AMR Review Paper-Tackling a crisis for the health and wealth of nations. *AMR Review Paper*.

Ocampo, P. S., Lázár, V., Papp, B., Arnoldini, M., Abel zur Wiesch, P., Busa-Fekete, R., Fekete, G., Pál, C., Ackermann, M., & Bonhoeffer, S. (2014). Antagonism between bacteriostatic and bactericidal antibiotics is prevalent. *Antimicrobial Agents and Chemotherapy, 58*(8), 4573-4582. https://doi.org/10.1128/aac.02463-14

Odds, F. C. (2003). Synergy, antagonism, and what the chequerboard puts between them. *Journal of Antimicrobial Chemotherapy, 52*(1), 1-1.

Ogura, T., Inoue, K., Tatsuta, T., Suzaki, T., Karata, K., Young, K., Su, L. H., Fierke, C. A., Jackman, J. E., & Raetz, C. R. (1999). Balanced biosynthesis of major membrane components through regulated degradation of the committed enzyme of lipid A biosynthesis by the AAA protease FtsH (HflB) in *Escherichia coli*. *Molecular Microbiology, 31*(3), 833-844.

Ogura, T., & Wilkinson, A. J. (2001). AAA+ superfamily ATPases: common structure–diverse function. *Genes to Cells, 6*(7), 575-597.

Ohara, M., Wu, H. C., Sankaran, K., & Rick, P. D. (1999). Identification and characterization of a new lipoprotein, NlpI, in *Escherichia coli* K-12. *Journal of Bacteriology, 181*(14), 4318-4325. https://doi.org/10.1128/JB.181.14.4318-4325.1999

Olivera, C., Cox, M. P., Rowlands, G. J., Rakonjac, J., & Bradford, P. A. (2021). Correlated transcriptional responses provide insights into the synergy mechanisms of the furazolidone, vancomycin, and sodium deoxycholate triple combination in *Escherichia coli*. *mSphere, 6*(5), e00627-00621. https://doi.org/10.1128/mSphere.00627-21

Olivera, C., Le, V. V. H., Davenport, C., & Rakonjac, J. (2021). In vitro synergy of 5-nitrofurans, vancomycin and sodium deoxycholate against Gram-negative pathogens. *Journal of Medical Microbiology, 70*(3).

Olivera, C. D. (2021). *Synergistic triple combination antibiotic therapy for Gram-negative bacterial infections: a thesis presented in partial fulfilment of the requirements for the degree of Doctor of Philosophy in Microbiology and Genetics at Massey University, Manawatu, New Zealand*

Ona, K. R., Courcelle, C. T., & Courcelle, J. (2009). Nucleotide excision repair is a predominant mechanism for processing nitrofurazone-induced DNA damage in *Escherichia coli*. *Journal of Bacteriology, 191*(15), 4959-4965. https://doi.org/10.1128/JB.00495-09

Ovchinnikov, Y. A., Monastyrskaya, G. S., Gubanov, V. V., Guryev, S. O., Salomatina, I. S., Shuvaeva, T. M., Lipkin, V. M., & Sverdlov, E. D. (1982). The primary structure ot *E. coli* RNA polymerase. Nucleotide sequence of the *rpoC* gene and amino acid sequence of the β′-subunit. *Nucleic Acids Research, 10*(13), 4035-4044. https://doi.org/10.1093/nar/10.13.4035

Palella Jr, F. J., Delaney, K. M., Moorman, A. C., Loveless, M. O., Fuhrer, J., Satten, G. A., Aschman, D. J., Holmberg, S. D., & Investigators, H. O. S. (1998). Declining morbidity and mortality among patients with advanced human immunodeficiency virus infection. *New England Journal of Medicine, 338*(13), 853-860.

Patel, S., Preuss, C.V., Bernice, F. (2021). *Vancomycin*. StatPearls Publishing. https://www.ncbi.nlm.nih.gov/books/NBK459263/

Pedrolli, D., Langer, S., Hobl, B., Schwarz, J., Hashimoto, M., & Mack, M. (2015). The *ribB* FMN riboswitch from *Escherichia coli* operates at the transcriptional and translational level and regulates riboflavin biosynthesis. *The FEBS journal, 282*(16), 3230-3242.

Perkins, H. R. (1969). Specificity of combination between mucopeptide precursors and vancomycin or ristocetin. *Biochemical Journal, 111*(2), 195-205.

Peterson, F. J., Mason, R. P., Hovsepian, J., & Holtzman, J. L. (1979). Oxygen-sensitive and-insensitive nitroreduction by *Escherichia coli* and rat hepatic microsomes. *Journal of Biological Chemistry, 254*(10), 4009-4014.

Pirrone, V., Thakkar, N., Jacobson, J. M., Wigdahl, B., & Krebs, F. C. (2011). Combinatorial approaches to the prevention and treatment of HIV-1 Infection. *Antimicrobial Agents and Chemotherapy, 55*(5), 1831-1842. https://doi.org/10.1128/aac.00976-10

Race, P. R., Lovering, A. L., Green, R. M., Ossor, A., White, S. A., Searle, P. F., Wrighton, C. J., & Hyde, E. I. (2005). Structural and mechanistic studies of *Escherichia coli* nitroreductase with the antibiotic nitrofurazone: reversed binding orientations in different redox states of the enzyme. *Journal of Biological Chemistry, 280*(14), 13256-13264.

Rai, A. K., Mitchell, A. M., & Garsin, D. A. (2020). Enterobacterial common antigen: synthesis and function of an enigmatic molecule. *mBio, 11*(4), e01914-01920. https://doi.org/10.1128/mBio.01914-20

Reygaert, W. C. (2018). An overview of the antimicrobial resistance mechanisms of bacteria. *AIMS microbiology, 4*(3), 482-501. https://doi.org/10.3934/microbiol.2018.3.482

Reynolds, P. E. (1961). Studies on the mode of action of vancomycin. *Biochimica et Biophysica Acta, 52*(2), 403-405. https://doi.org/10.1016/0006-3002(61)90698-9

Reynolds, P. E. (1989). Structure, biochemistry and mechanism of action of glycopeptide antibiotics. *European Journal of Clinical Microbiology and Infectious Diseases, 8*(11), 943-950. https://doi.org/10.1007/BF01967563

Reynolds, P. E., & Courvalin, P. (2005). Vancomycin resistance in *Enterococci* due to synthesis of precursors terminating in -d-Alanyl-d-Serine. *Antimicrobial Agents and Chemotherapy, 49*(1), 21-25. https://doi.org/10.1128/aac.49.1.21-25.2005

Reynolds, P. E., Depardieu, F., Dutka-Malen, S., Arthur, M., & Courvalin, P. (1994). Glycopeptide resistance mediated by enterococcal transposon Tn 1546 requires production of VanX for hydrolysis of D-alanyl-D-alanine. *Molecular Microbiology, 13*(6), 1065-1070.

Richter, G., Ritz, H., Katzenmeier, G., Volk, R., Kohnle, A., Lottspeich, F., Allendorf, D., & Bacher, A. (1993). Biosynthesis of riboflavin: cloning, sequencing, mapping, and expression of the gene coding for GTP cyclohydrolase II in *Escherichia coli*. *Journal of Bacteriology, 175*(13), 4045-4051.

Rumley, M. K., Therisod, H., Weissborn, A. C., & Kennedy, E. P. (1992). Mechanisms of regulation of the biosynthesis of membrane-derived oligosaccharides in *Escherichia coli*. *Journal of Biological Chemistry, 267*(17), 11806-11810.

Sailer, F. C., Meberg, B. M., & Young, K. D. (2003). β-Lactam induction of colanic acid gene expression in *Escherichia coli*. *FEMS Microbiology Letters, 226*(2), 245-249. https://doi.org/10.1016/s0378-1097(03)00616-5

Sanchez-Torres, V., Maeda, T., & Wood, T. K. (2010). Global regulator H-NS and lipoprotein NlpI influence production of extracellular DNA in *Escherichia coli*. *Biochemical and Biophysical Research Communications, 401*(2), 197-202. https://doi.org/10.1016/j.bbrc.2010.09.026

Schwechheimer, C., Rodriguez, D. L., & Kuehn, M. J. (2015). NlpI-mediated modulation of outer membrane vesicle production through peptidoglycan dynamics in *Escherichia coli*. *MicrobiologyOpen, 4*(3), 375-389. https://doi.org/10.1002/mbo3.244

Shibayama, K., Ohsuka, S., Sato, K., Yokoyama, K., Horii, T., & Ohta, M. (1999). Four critical aspartic acid residues potentially involved in the catalytic mechanism of *Escherichia coli* K-12 WaaR. *FEMS Microbiology Letters, 174*(1), 105-109. https://doi.org/10.1111/j.1574-6968.1999.tb13555.x

Singh, S. K., Parveen, S., SaiSree, L., & Reddy, M. (2015). Regulated proteolysis of a cross-link-specific peptidoglycan hydrolase contributes to bacterial morphogenesis. *Proceedings of the National Academy of Sciences of the United States of America, 112*(35), 10956-10961. https://doi.org/10.1073/pnas.1507760112

Sun, D., Jeannot, K., Xiao, Y., & Knapp, C. W. (2019). Editorial: Horizontal gene transfer mediated bacterial antibiotic resistance [Editorial]. *Frontiers in microbiology, 10*(1933). https://doi.org/10.3389/fmicb.2019.01933

Sun, W., Sanderson, P. E., & Zheng, W. (2016). Drug combination therapy increases successful drug repositioning. *Drug Discovery Today, 21*(7), 1189-1195. https://doi.org/10.1016/j.drudis.2016.05.015

Sutherland, C., Murakami, K. S., Lovett, S. T., & Hinton, D. (2018). An introduction to the structure and function of the catalytic core enzyme of *Escherichia coli* RNA

polymerase. *EcoSal Plus*, *8*(1). https://doi.org/10.1128/ecosalplus.ESP-0004-2018

Sutterlin, H. A., Zhang, S., & Silhavy, T. J. (2014). Accumulation of phosphatidic acid increases vancomycin resistance in *Escherichia coli*. *Journal of Bacteriology*, *196*(18), 3214-3220. https://doi.org/10.1128/JB.01876-14

Tao, J., Sang, Y., Teng, Q., Ni, J., Yang, Y., Tsui, S. K.-W., & Yao, Y.-F. (2015). Heat shock proteins IbpA and IbpB are required for NlpI-participated cell division in *Escherichia coli*. *Frontiers in microbiology*, *6*. https://doi.org/10.3389/fmicb.2015.00051

Thomas, C. M., & Nielsen, K. M. (2005). Mechanisms of, and barriers to, horizontal gene transfer between bacteria. *Nature Reviews Microbiology*, *3*(9), 711-721. https://doi.org/10.1038/nrmicro1234

Thomason, L., & Constantino, N. (2007). Court DL *E. coli* manipulation by P1 transduction. *Current Protocols in Molecular Biology*.

Tomoyasu, T., Yuki, T., Morimura, S., Mori, H., Yamanaka, K., Niki, H., Hiraga, S., & Ogura, T. (1993). The *Escherichia coli* FtsH protein is a prokaryotic member of a protein family of putative ATPases involved in membrane functions, cell cycle control, and gene expression. *Journal of Bacteriology*, *175*(5), 1344-1351.

Torella, J. P., Chait, R., & Kishony, R. (2010). Optimal drug synergy in antimicrobial treatments. *PLOS Computational Biology*, *6*(6), e1000796. https://doi.org/10.1371/journal.pcbi.1000796

Ventola, C. L. (2015). The antibiotic resistance crisis: part 1: causes and threats. *P & T : a peer-reviewed journal for formulary management*, *40*(4), 277-283. https://pubmed.ncbi.nlm.nih.gov/25859123

Vervoort, J., Xavier, B. B., Stewardson, A., Coenen, S., Godycki-Cwirko, M., Adriaenssens, N., Kowalczyk, A., Lammens, C., Harbarth, S., & Goossens, H. (2014). An *in vitro* deletion in *ribE* encoding lumazine synthase contributes to nitrofurantoin resistance in *Escherichia coli*. *Antimicrobial Agents and Chemotherapy*, *58*(12), 7225-7233.

Vogl, C., Grill, S., Schilling, O., Stülke, J. r., Mack, M., & Stolz, J. r. (2007). Characterization of riboflavin (vitamin B2) transport proteins from *Bacillus subtilis* and *Corynebacterium glutamicum*. *Journal of Bacteriology*, *189*(20), 7367-7375.

Vollmer, W., Blanot, D., & De Pedro, M. A. (2008). Peptidoglycan structure and architecture. *FEMS microbiology Reviews*, *32*(2), 149-167. https://doi.org/10.1111/j.1574-6976.2007.00094.x

von Wintersdorff, C. J. H., Penders, J., van Niekerk, J. M., Mills, N. D., Majumder, S., van Alphen, L. B., Savelkoul, P. H. M., & Wolffs, P. F. G. (2016). Dissemination of antimicrobial resistance in microbial ecosystems through

horizontal gene transfer. *Frontiers in microbiology*, *7*(173). https://doi.org/10.3389/fmicb.2016.00173

White, A. R., Kaye, C., Poupard, J., Pypstra, R., Woodnutt, G., & Wynne, B. (2004). Augmentin®(amoxicillin/clavulanate) in the treatment of community-acquired respiratory tract infection: a review of the continuing development of an innovative antimicrobial agent. *Journal of Antimicrobial Chemotherapy*, *53*(suppl_1), i3-i20.

Whiteway, J., Koziarz, P., Veall, J., Sandhu, N., Kumar, P., Hoecher, B., & Lambert, I. B. (1998). Oxygen-insensitive nitroreductases: analysis of the roles of *nfsA* and *nfsB* in development of resistance to 5-nitrofuran derivatives in *Escherichia coli*. *Journal of Bacteriology*, *180*(21), 5529-5539. https://doi.org/10.1128/jb.180.21.5529-5539.1998

World Health Organisation. (2017). *WHO Priority Pathogens List for R&D of New Antibiotics*. http://www.who.int/mediacentre/news/releases/2017/bacteria-antibiotics-needed/en/

World Health Organisation. (2020). *Antibiotic Resistance*. https://www.who.int/news-room/fact-sheets/detail/antibiotic-resistance

World Health Organization. (2018). *WHO report on surveillance of antibiotic consumption 2016–2018 early implementation* https://www.who.int/publications/i/item/9789241514880

Zenno, S., Koike, H., Kumar, A. N., Jayaraman, R., Tanokura, M., & Saigo, K. (1996). Biochemical characterization of NfsA, the *Escherichia coli* major nitroreductase exhibiting a high amino acid sequence homology to Frp, a *Vibrio harveyi* flavin oxidoreductase. *Journal of Bacteriology*, *178*(15), 4508-4514.

Zenno, S., Koike, H., Tanokura, M., & Saigo, K. (1996). Gene cloning, purification, and characterization of NfsB, a minor oxygen-insensitive nitroreductase from *Escherichia coli*, similar in biochemical properties to FRase I, the major flavin reductase in *Vibrio fischeri*. *The Journal of Biochemistry*, *120*(4), 736-744.

Zheng, W., Sun, W., & Simeonov, A. (2018). Drug repurposing screens and synergistic drug-combinations for infectious diseases. *British Journal of Pharmacology*, *175*(2), 181-191. https://doi.org/doi.org/10.1111/bph.13895

Zhou, A., Kang, T. M., Yuan, J., Beppler, C., Nguyen, C., Mao, Z., Nguyen, M. Q., Yeh, P., & Miller, J. H. (2015). Synergistic interactions of vancomycin with different antibiotics against *Escherichia coli*: trimethoprim and nitrofurantoin display strong synergies with vancomycin against wild-type *E. coli*. *Antimicrobial Agents and Chemotherapy*, *59*(1), 276-281. https://doi.org/10.1128/AAC.03502-14

Zhuge, L., Wang, Y., Wu, S., Zhao, R. L., Li, Z., & Xie, Y. (2018). Furazolidone treatment for *Helicobacter Pylori* infection: A systematic review and meta-analysis. *Helicobacter*, *23*(2), e12468.

Zimmerman, S. M., Lafontaine, A.-A. J., Herrera, C. M., Mclean, A. B., & Trent, M. S. (2020). A whole-cell screen identifies small bioactives that synergize with polymyxin and exhibit antimicrobial activities against multidrug-resistant bacteria. *Antimicrobial Agents and Chemotherapy, 64*(3), e01677-01619. https://doi.org/10.1128/aac.01677-19

Zückert, W. R. (2014). Secretion of bacterial lipoproteins: Through the cytoplasmic membrane, the periplasm and beyond. *Biochimica et Biophysica Acta (BBA) - Molecular Cell Research, 1843*(8), 1509-1516. https://doi.org/10.1016/j.bbamcr.2014.04.022

7 Supplementary Material

7.1 Sequencing reads

The raw sequencing reads are available from the NCBI Sequence Read Archive under BioProject accession PRJNA854676.

Sample name	Biosample Accession
K2653 (Parental strain)	SAMN29446158
K2654 FZ+VAN	SAMN29446159
K2655 FZ+VAN	SAMN29446160
K2657 FZ+VAN	SAMN29446161
K2658 FZ+VAN	SAMN29446162
K2659 FZ+VAN	SAMN29446163
K2660 FZ+VAN	SAMN29446164
K2661 FZ+VAN	SAMN29446165
K2662 (B1) FZ+VAN	SAMN29446166
K2663 (E1) FZ+VAN	SAMN29446167
K2664 FZ+VAN	SAMN29446168
K2665 (E2) FZ+VAN	SAMN29446169
K2666 (E3) FZ+VAN	SAMN29446170
K2667 (E4) FZ+VAN	SAMN29446171
K2668 (E5) FZ+VAN	SAMN29446172
K2669 (B2) FZ+VAN	SAMN29446173
K2670 (B3) FZ+VAN	SAMN29446174
K2671 (B4) FZ+VAN	SAMN29446175
K2673 VAN	SAMN29446176